National Transportation Safety Board

Office of Research and Engineering

Washington, DC 20594

ERA22FA318

AIRCRAFT PERFORMANCE & COCKPIT VISIBILITY STUDY

by John O'Callaghan

May 28, 2024

TABLE OF CONTENTS

A. ACCIDENT

Location: North Las Vegas, Nevada
Date: July 17, 2022
Time: 12:04 Pacific Daylight Time (PDT)
               19:04 Coordinated Universal Time (UTC)
Aircraft: Piper PA-46-350P JetProp DLX, N97CX
               Cessna 172N, registration N160RA

B. AIRCRAFT PERFORMANCE GROUP

Chairman: John O'Callaghan
                       National Transportation Safety Board (NTSB), RE-60
                       Washington, D.C.

Members: N/A

C. SUMMARY

On July 17, 2022, about 12:03 PDT[1], a Piper PA-46-350P JetProp DLX, N97CX (hereafter called "the Piper"), and a Cessna 172N, N160RA (hereafter called "the Cessna"), were destroyed in a mid-air collision while maneuvering to land at North Las Vegas Airport in North Las Vegas, Nevada (KVGT). The two pilots in the Piper, and the flight instructor and student pilot in the Cessna, were fatally injured. The Piper was operated as a Title 14 Code of Federal Regulations (CFR) Part 91 personal flight, and the Cessna was operated as a Title 14 CFR Part 91 instructional flight.

The Piper had been instructed by air traffic control (ATC) to fly left traffic for KVGT runway 30L and the Cessna had been instructed to fly right traffic for runway 30R. The airplanes collided about 0.17 nautical miles from the runway 30R displaced threshold. Figure 1 depicts the trajectories of the airplanes prior to the collision based on Automatic Dependent Surveillance – Broadcast (ADS-B) data provided by the Federal Aviation Administration (FAA).

The Piper was operating as an instrument flight rules (IFR) flight and had departed from Coeur d'Alene Airport - Pappy Boyington Field (KCOE), Coeur d'Alene, Idaho about 09:43, destined for KVGT. The Cessna was operating as a visual flight rules (VFR) training flight at KVGT.

The Cessna was in the VFR traffic pattern for runway 30R, flying a right-hand traffic pattern and communicating with the KVGT local controller. The Piper was inbound from the north on an IFR flight plan from KCOE.

---

[1] All times in this *Study* are in PDT unless otherwise noted.

At 11:56:08, the Nellis Radar Approach Control air traffic controller cleared the Piper for the visual approach and instructed the pilot to overfly KVGT at midfield for left traffic to runway 30L. Air traffic control responsibility for the flight was transferred from Nellis Radar Approach Control to KVGT at 11:58:26.

At 11:58:43, the Piper copilot contacted the KVGT local controller and reported "descending out of 7,600 feet msl for landing on three zero left and ah Nellis said to cross midfield." The KVGT local controller responded, "continue for three zero left." The copilot acknowledged and stated, "okay continue for runway three zero left nine seven charlie x-ray we will cross over midfield."

At 12:00:03, the Cessna pilot requested a "short approach." The VGT local controller transmitted "zero romeo alpha short approach approved runway three zero right cleared for the option," which was acknowledged by the Cessna pilot.

At 12:01:36, the KVGT local controller transmitted "november seven charlie x-ray runway three zero left cleared to land." The Piper copilot responded "three zero left cleared to land nine seven charlie x-ray."

At 12:01:57, the KVGT local controller transmitted "seven charlie x-ray I think I said it right runway three zero left seven charlie x-ray runway three zero left."

At 12:02:02 the Piper copilot transmitted "yeah affirmative runway three zero left that's what I heard nine seven charlie x-ray."

There were no further transmissions from either airplane.

Examination of the Piper wreckage revealed a series of crush impressions to the right wing leading edge about 2.5 ft outboard of the wing root. The impressions contained flakes of green primer, and cuts to the de-ice boot. The outboard leading edge was crushed up and aft. The right wingtip fairing and pitot tube were impact separated. Longitudinal scratches were visible along the right side of the fuselage. The wing flaps were found in the 36° (fully extended) position.

Examination of the Cessna wreckage revealed blue paint transfer on the lower surface of the separated outboard left wing and the lower surface of the left wing flap. Black de-ice boot material transfer was observed on the lower surface of the separated outboard left wing, the lower surface of the attached portion of the left wing at approximately Wing Station 100, and for an approximate 5 ft long distance outboard of the strut attach point, along the lower leading edge. The wing flap actuator indicated a flap position between 0° and 10°.

Both the Piper and Cessna were equipped with ADS-B "Out" equipment and transmitted ADS-B data during the accident flights. In addition, the Piper was equipped

with ADS-B "In" equipment that was capable of displaying air traffic information on a cockpit display. The Cessna was not equipped with ADS-B "In" equipment, and no portable ADS-B devices capable of displaying traffic information were found in the Cessna wreckage.

This *Aircraft Performance & Cockpit Visibility Study* presents the results of using recorded ADS-B data for both airplanes to calculate the position and orientation of each airplane in the minutes preceding the collision. This information is then used to estimate the approximate location of each airplane in the other airplane pilot's field of view (the "visibility study"), and to recreate the Cockpit Display of Traffic Information (CDTI) data that could have been presented to each pilot had both airplanes been equipped with ADS-B In capability (only the Piper was so equipped). As described further in section D.4, CDTI uses the ADS-B system to drive a traffic situation display in the cockpits of appropriately-equipped aircraft.

The sections that follow present the ADS-B data, weather data, and other information used in this *Study*, and describe the methods used to calculate aircraft speeds, orientation (pitch, yaw and roll angles), CDTI information, and cockpit visibility from this data. The results of these calculations are presented in the Figures and Tables described throughout the *Study*.

D. DETAILS OF THE INVESTIGATION

D.1.   The accident airplanes

D.1.1. The Piper PA-46-350P JetProp DLX

The PA 46-350 JetProp DLX is an aftermarket turbine engine conversion for the PA-46-350P Malibu Mirage offered by Rocket Engineering of Spokane, Washington. The conversion was certified in 1998 with a Pratt & Whitney PT6A-34 engine. N97CX, Piper serial number 4636128, was manufactured as a Malibu Mirage in 1997 with a Lycoming 350-SHP TIO-540-AE2A reciprocating engine. In April 2000, the airplane was converted to a JetProp DLX with the 560 SHP PT6A-34 turbine engine.

The baseline PA 46-350P Malibu Mirage is a single engine, low-wing, pressurized, retractable gear airplane with a maximum of six seats and a maximum takeoff weight of 4,300 lb. The JetProp DLX conversion does not affect the maximum takeoff weight.

Figure 2 depicts two pre-accident photographs of N97CX, and Figure 3 shows a 2-view diagram of the JetProp DLX, taken from the JetProp Pilot's Operating Handbook and FAA Approved Airplane Flight Manual (POH, Reference 1). Table 1 lists some dimensions of the airplane, as well as the weight of N97CX at the time of the accident (3,765 lb.) estimated by Piper based on the flight route from KCOE and assuming that the airplane departed KCOE at its maximum gross weight.

Item	Value
Reference dimensions (see Figure 3):	
Wing area	175 ft.^{2}
Wing span	43.0 ft.
Mass properties for N255BF:	
Gross weight at time of accident	**3,765 lb.** (estimate provided by Piper)

Table 1. Relevant geometry and gross weight for Piper N97CX.

The lift curve (C_L vs. α) of the PA-46-350P at flaps 36° was provided by Piper. This information is used with the wing area and weight shown in Table 1 to estimate the Piper's pitch and roll angles from ADS-B data (see section D.2.4).

An exemplar PropJet DLX made available to the NTSB by Mead Aircraft Services in Olathe, Kansas was surveyed with a laser scanner in support of the cockpit visibility study described in section D.3 and Appendix A.

D.1.2. The Cessna 172N Skyhawk

The C172N is a single-engine, four-seat high-wing airplane with a conventional tail, powered by a 160 BHP Lycoming O-320-H2AD reciprocating engine[2], with a maximum gross weight of 2,300 lb. Per FAA registration records, N160RA was manufactured in 1977. Figure 4 depicts two pre-accident photographs of N160RA, and Figure 5 shows a 3-view diagram of the C172N, taken from Reference 3. Table 2 lists some dimensions of the airplane, as well as the weight of N160RA at the time of the accident. Textron Aviation (Textron), that now owns the Type Certificates for Cessna aircraft, estimated that the accident weight was between 1,900 lb. and 1,950 lb. based on a nominal C172N empty weight, the weight of the crew, and a fuel weight based on estimates of the fuel burn in the traffic pattern. A weight of 1,930 lb. is assumed in this *Study*.

Item	Value
Reference dimensions (from References 3 & 4):	
Wing area	175.5 ft.^{2} (from Reference 4)
Wing span	36 ft. (see Figure 5)
Mass properties for N160RA:	
Gross weight at time of accident	**1,930 lb.** (estimate provided by Textron)

Table 2. Relevant geometry and gross weight for Cessna N160RA.

Aerodynamic information for the C172 (specifically, the lift coefficient (C_L) as a function of angle of attack (α)) was provided to the NTSB by Textron during a previous investigation. This information is used along with the wing area and weight shown in

---

[2] At the time of the accident, N160RA was equipped with a Lycoming O-360-A4M engine.

Table 2 to estimate the Cessna's pitch and roll angles from ADS-B data (see section D.2.4).

The geometry of an exemplar C172 owned by an NTSB employee was measured with a laser scanner in support of the cockpit visibility study described in section D.3 and Appendix A.

D.2.   Recorded ADS-B data for Piper N97CX and Cessna N160RA

Both airplanes involved in the midair collision were equipped with ADS-B equipment and transmitting ADS-B data at the time of the accident. "ADS-B Out" capability enables an aircraft to broadcast its three-dimensional position (latitude, longitude, and altitude) to other ADS-B equipped aircraft and to ADS-B ground stations. "ADS-B In" capability enables an aircraft to receive traffic messages from ADS-B Out equipped aircraft and from ADS-B ground stations. Traffic messages concerning non-ADS-B equipped aircraft within FAA radar coverage are broadcast to ADS-B equipped aircraft through an ADS-B function called Traffic Information Service – Broadcast (TIS-B). The ADS-B messages concerning the accident airplanes were used in the performance and cockpit visibility calculations presented in this *Study*.

Section D.4 of this *Study* presents recreations of the traffic information that could have been presented on CDTI displays in each aircraft. The symbology of the Garmin display that was installed in the Piper is recreated for that airplane, and the symbology of a nominal CDTI display is recreated for the Cessna, which was not equipped with either an installed or portable traffic display. Since CDTI is an application of the ADS-B system, to better understand the operation and benefit of CDTI, it is helpful to begin with a brief description of the ADS-B system itself.

D.2.1. Introduction to the ADS-B system

According to a 2007 "Fact Sheet" published by the FAA,[3] the "Next Generation Air Transportation System" (NextGen) program "is a wide ranging transformation of the entire national air transportation system - not just certain pieces of it - to meet future demands and avoid gridlock in the sky and in the airports. It moves away from legacy ground based technologies [such as radar] to a new and more dynamic satellite based technology." A key component of NextGen is the surveillance of aircraft by establishing their positions using Global Navigation Satellite System (GNSS) instead of by ground radar.[4] This GNSS-based surveillance is enabled through the "Automatic Dependent Surveillance – Broadcast" (ADS-B) system. As described in the FAA fact sheet,

---

[3] See: http://web.archive.org/web/20150403151639/http://www.faa.gov/news/fact_sheets/news_story.cfm?newsid=8145

[4] The GNSS system includes the Global Positioning System (GPS) constellation of satellites.

Automatic Dependent Surveillance Broadcast (ADS-B) is, quite simply, the future of air traffic control. As the backbone of the NextGen system, it uses GPS satellite signals to provide air traffic controllers and pilots with much more accurate information that will help keep aircraft safely separated in the sky and on runways. Aircraft transponders receive GPS signals and use them to determine the aircraft's precise position in the sky, which is combined with other data and broadcast out to other aircraft and air traffic control facilities. When properly equipped with ADS-B, both pilots and controllers will, for the first time, see the same real-time displays of air traffic, substantially improving safety.

Since January 1, 2020, ADS-B Out equipment (that broadcasts the airplane's position to ATC and other aircraft) is required to be installed on all aircraft in the National Airspace System (NAS) operating above 10,000 ft. and within or above Class B and C airspace, with certain exceptions (see 14 CFR 91.225).

The ADS-B capabilities that enhance a pilot's awareness of airborne traffic in his vicinity are described in Advisory Circular (AC) 20-172B, "Airworthiness Approval for ADS-B In Systems and Applications." Per the AC,

> ADS-B In refers to an appropriately equipped aircraft's ability to receive and display other aircraft's ADS-B information and ground station broadcast information, such as TIS-B and ADS-R [Automatic Dependent Surveillance – Rebroadcast]. The information can be received by an appropriately equipped aircraft on either or both of two radio frequency (RF) links: 1090 ES [Extended Squitter] or 978 MHz UAT [Universal Access Transceiver]. The received information is processed by onboard avionics and presented to the flight crew on a display.

ADS-B In avionics enable several aircraft surveillance applications. The applications most relevant to this accident are the enhanced visual acquisition (EVAcq) and ADS-B Traffic Advisory System (ATAS) applications. AC 20-172B describes these applications as follows:

> The enhanced visual acquisition application (EVAcq) … displays ADS-B traffic on a plan view (bird's eye view) relative to own-ship. This application is designed to support only the display and alerting of ADS-B traffic, including ADS-R, TIS-B, and TCAS [Traffic Collision Avoidance System] derived traffic. … The traffic information assists the flight crew in visually acquiring traffic out the window while airborne. EVAcq does not relieve the pilot of see and avoid responsibilities under 14 CFR 91.113b. This application is expected to improve both safety and efficiency by providing the flight crew enhanced traffic awareness. …
>
> ADS-B Traffic Advisory System (ATAS) is an Automatic Dependent Surveillance-Broadcast (ADS-B) In application intended to reduce the number of mid-air collisions and near mid-air collisions involving general aviation aircraft. Previously known as Traffic Situation Awareness with Alerts (TSAA), the name ATAS has been used in this AC as well as TSO-C195b to be more consistent with existing traffic advisory systems. ATAS provides voice annunciations to flight crews to draw attention to alerted traffic and also adds visual cues to the underlying basic traffic situation awareness application (e.g., Enhanced Visual Acquisition [EVAcq] or Basic Airborne Situation Awareness [AIRB]) in installations where a Traffic Display is available. The ATAS application uses ADS-B information, and where available Automatic Dependent Surveillance-Rebroadcast (ADS-R) and Traffic Information Service-Broadcast (TIS-B) information to provide the flight crew with indications of nearby aircraft in support of their see-and-avoid responsibility. ATAS is the only ADS-B application with an aural-only implementation (via an annunciator panel). All other

applications require a traffic display as defined by the CDTI [Cockpit Display of Traffic Information] requirements.

The cockpit display that presents traffic information to the pilot in a plan or "birds eye" view as stated in the EVAcq and ATAS application descriptions is the Cockpit Display of Traffic Information, or CDTI.

For this accident, recreations of the traffic information that *could* have been presented on the CDTI displays available to the Piper and the Cessna pilots were produced using recorded ADS-B traffic data provided by the FAA. Only the Piper pilot had an ADS-B In-based CDTI visual display available to him (described in section D.4). However, the information that could have been provided to the Cessna pilot if that airplane had been equipped with either an installed or portable CDTI is also presented, as a hypothetical scenario that serves to underscore the benefits of CDTI.

The CDTI recreations, and the traffic display and alerting capabilities of the equipment modeled in the recreations, are described further in section D.4.

D.2.2. Recorded ADS-B data provided by the FAA

The FAA provided the NTSB with recorded ADS-B data within a 10 nm radius of KVGT, and below 5,000 ft. above ground level (AGL), from 18:45 to 19:10 UTC (11:45 to 12:10 PDT). This information was used to determine the tracks of the Piper and Cessna prior to the accident, and to recreate the traffic that could have been presented on each airplane's CDTI display (these recreations are discussed in section D.4). The ADS-B data file provided by the FAA is available in the NTSB public docket for this accident.

The recorded ADS-B / TIS-B data includes the following parameters for all aircraft:

- UTC time of the report, in hours, minutes, and seconds. PDT = UTC – 7 hours.
- Aircraft identifying information (in a parameter called "ModeSId").
- GNSS-based latitude and longitude, to a resolution of 0.01 arc-seconds (≈1 ft.)
- Pressure altitude in feet, to the nearest 25 ft. (an uncertainty band of ± 12.5 ft.) for the Piper, and to the nearest 100 ft. (an uncertainty band of ± 50 ft.) for the Cessna.
- GNSS-based geometric altitude, to the nearest 25 ft. (an uncertainty band of ± 12.5 ft.) The GNSS altitude is the height above the WGS84 ellipsoid, which differs from MSL altitude by the height of the geoid.[5] At the accident site, MSL altitude is 91 ft. above GNSS altitude.[6]

---

[5] "The geoid … is the shape that the ocean surface would take under the influence of the gravity of Earth, including gravitational attraction and Earth's rotation, if other influences such as winds and tides were absent." (Wikipedia.org, accessed 10/10/2022.)

[6] Per https://geographiclib.sourceforge.io/cgi-bin/GeoidEval, the geoid at the accident site is about 27.8 m (91 ft.) below the surface of the WGS84 ellipsoid.

- North-south and east-west components of ground speed, to a resolution of 1 kt.
- Rate of climb based on pressure altitude, to a resolution of 1 ft./min.
- Numerous parameters documenting the source and quality of each reported GNSS position.

The sample rate of the GNSS-based ADS-B data is about 1 sample per second (1 Hz). The sample rates of the data for each aircraft can be gleaned from Figures 6 and 7.

D.2.3. Presentation of the ADS-B data

To calculate performance parameters (such as ground speed, track angle, pitch and roll angles, etc.) from the surveillance data, it is convenient to express the position of the airplane in rectangular Cartesian coordinates. The Cartesian coordinate system used in this *Study* is centered on the KVGT runway 30R displaced threshold, and its axes extend east, north, and up from the center of the Earth. The coordinates of the KVGT runway 30R displaced threshold are:

36° 12' 17.0803" N / 115° 11' 12.2029" W / 2,148.2 ft. MSL

The surveillance data from the Piper and Cessna are converted into this coordinate system using the WGS84 ellipsoid model of the Earth.

Figure 1 presents the ADS-B position data for the accident airplanes, plotted in terms of nautical miles north and east of the KVGT runway 30R displaced threshold, over a *Google Earth* satellite image background. Figure 7 presents the ADS-B altitude data.

Figures 1 and 7 also present cubic spline curve fits of the recorded airplane positions and altitudes that provide smooth time derivatives and reduce "noise" in the performance calculations resulting from uncertainty in the data, and that interpolate the data for both airplanes to common 1 Hz sample times (see "Estimates of airplane performance based on ADS-B data," below). In addition, the curve fit of the Piper ADS-B geometric altitude plotted in Figure 7 is lowered 18 ft. to match the Cessna geometric altitude at the time that the north and east coordinates of the airplanes coincide, in order to enforce a collision. (Lowering the Piper altitude, instead of raising the Cessna altitude, results in a better match of the barometric-based altitudes.)

Smooth trajectories can also be obtained by integrating the ADS-B recorded ground speed data. However, in this case, the resulting trajectories do not match the recorded ADS-B positions well enough to compute additional performance parameters with confidence (likely because both airplanes are maneuvering at the time of the collision, and the recorded ground speed components lag the true ground speeds).

The final trajectories used for the airplane performance calculations in this *Study* are depicted by the curves labeled "Piper curve fit" and "Cessna curve fit" in Figure 1

(hereafter referred to as the "smooth tracks"), and the curve fits of the ADS-B geometric altitudes plotted in Figure 7.

D.2.4. Estimates of airplane performance based on ADS-B data

ADS-B positions are GNSS-based and very accurate, but still contain some error or uncertainty. This uncertainty, combined with the relatively high sample rate of the data (1 Hz), results in spurious "noise," or unrealistic spikes and variations, in the computed ground speed. If not removed or otherwise corrected, the noise in the computed ground speed propagates into all the other performance calculations.

As noted above, the north-south and east-west components of ground speed, as computed by on-board avionics, are included in ADS-B messages. These speed components are very smooth and can be combined to produce a smooth total ground speed. In general, when the ground speed components recorded in ADS-B files are integrated over time, the resulting positions generally match the recorded ADS-B positions very well. However, in this case, the airplane positions obtained by integrating the ground speed components recorded in the ADS-B data do not match the recorded GNSS positions well enough to be used to compute additional parameters. Consequently, to obtain relatively smooth ground speeds that are more consistent with the ADS-B position data, the ADS-B east and north positions are curve-fitted with cubic splines, and the time derivatives of the curve fits are computed as the corresponding components of ground speed. A similar approach is used to smooth the ADS-B geometric altitudes and compute smooth rates of climb. The smoothed positions and altitude are used as the basis for ground speed and other performance calculations, as described below.

The Cockpit Visibility Study described in section D.3 requires that the Piper and Cessna track data be defined at common time points. Consequently, the curve fits of the ADS-B data are evaluated at common 1 Hz sample times.

Once the position (latitude, longitude, and altitude) of an airplane is known as a function of time, its orientation (i.e., the Euler angles: pitch, roll, and heading) can also be estimated as long as the following are true:

- The motion of the air mass relative to the Earth, i.e., the wind, is known;
- The lift coefficient of the airplane as a function of angle of attack is known;
- The gross weight of the airplane is known;
- The sideslip angle and lateral acceleration are negligible (i.e., the flight is coordinated).

In this *Study*, the weather reported in the 11:53 PDT Aviation Routine Weather Report (METAR) for KVGT is used: wind from 320° at 4 knots, visibility 10 statute miles, sky clear, temperature 38° C, dew point 12° C, altimeter 29.91 "Hg.

As noted above, this *Study* uses aerodynamic properties for the Piper and Cessna provided by Piper and Textron, respectively. Gross weights of 3,765 lb. and 1,930 lb. are assumed for the Piper and Cessna, respectively (see Tables 1 and 2). The flaps are assumed to be at 36° for the Piper and at 0° for the Cessna, consistent with the settings found in the wreckage. The flaps on the Piper likely transitioned from up (0°) to 36° as that airplane flew over the center of the airport and maneuvered toward runway 30R, but the analysis here assumes that the flaps are at 36° throughout. This assumption is valid for the moments before the collision, which are those of most interest.

The position of an airplane as a function of time defines its velocity and acceleration components. In coordinated flight, these components lie almost entirely in the plane defined by the airplane's longitudinal and vertical axes. Furthermore, any change in the *direction* of the velocity vector is produced by a change in the lift vector, either by increasing the magnitude of the lift (as in a pull-up), or by changing the direction of the lift (as in a banked turn). The lift vector also acts entirely in the aircraft's longitudinal-vertical plane, and is a function of the angle between the aircraft longitudinal axis and the velocity vector (the angle of attack, α). These facts allow the equations of motion to be simplified to the point that a solution for the airplane orientation can be found given the additional information about wind and the airplane lift curve (i.e., C_L vs. α). The results of the performance calculations for each airplane are presented below.

D.2.5. Estimated collision time, location, and geometry

The "curve fit" lines in Figures 1 and 7 depicting the flight tracks and altitudes of the Piper and Cessna are consistent with the ADS-B data for these airplanes. Figure 6 plots the east and north coordinates of the airplanes vs. time, and shows that these coincide at 12:02:51, which defines the time of the collision. The surveillance data for each airplane continue past this time for about 7 seconds.

The groundspeeds and track angles of the Piper and Cessna corresponding to the tracks shown in Figure 1 indicate that at the time of the collision, the velocity vector of the Piper *relative to the Cessna* was 38 kt. along a track of 344°. Since the Cessna's heading was about 307° at the time of collision, the Piper would have been moving at an angle of 344° - 307° = 37° relative to the Cessna's centerline, from aft left to forward right. Similarly, the velocity vector of the Cessna *relative to the Piper* was 38 kt. along a track of 164°. Since the Piper's heading was about 319° at the time of collision, the Cessna would have been moving at an angle of 164° - 319° = -155° relative to the Piper's centerline. The smaller angle between the centerline and a line drawn -155° to the centerline is -155° + 180° = 25°; the Cessna would have cut across the Piper's centerline from forward right to aft left at an angle 25° to the centerline.

The smooth Piper and Cessna tracks plotted in Figure 1 result in the following time and coordinates for the collision:

Time of collision = 12:02:51 PDT
Distance north of KVGT runway 30R displaced threshold = -0.1238 nm = -752 ft.
Distance east of KVGT runway 30R displaced threshold = 0.1225 nm = 744 ft.
Altitude = 2,258 ft. MSL = 113 ft. above KVGT runway 30R displaced threshold

The altitudes of the Piper and the Cessna are presented as a function of time in Figure 7. The barometric pressure altitudes recorded in the ADS-B data are presented, as well as the ADS-B geometric altitudes, the smoothed (curve fit) geometric altitudes, and the pressure altitude resulting from the integration of the recorded Cessna vertical speed over time. The performance calculations described below use the curve fit of the Piper ADS-B pressure altitude (depicted by the dashed black line) and the integrated Cessna vertical speed (depicted by the dashed blue line).

Figure 8 shows the true airspeed, calibrated airspeed, ground speed, and rate of climb calculated from the smooth trajectory and pressure altitude of the Piper. Figure 9 shows the corresponding calculations for the Cessna. In Figures 8 and 9 the computed ground speeds and rates of climb are compared to the values of these parameters recorded in the ADS-B data. The Figures indicate that at the time of the collision, the Piper's ground speed was about 111 knots, and the Cessna's groundspeed was about 78 knots. The gray circle symbols labeled "ADS-B recorded ground speed" are the ground speeds computed from the north and east velocity components recorded in the ADS-B data for each airplane. The black lines labeled "ground speed from curve fits" are the ground speeds computed from the curve fits of the ADS-B position data, and agree relatively well with the ADS-B recorded ground speeds, even though the integration of the recorded speed components results in the position errors that motivate using the curve fits. The true and calibrated airspeeds are computed based on the curve-fit ground speeds and the assumed wind (from 320° at 4 knots).

Figure 10 shows the separation distance between the two airplanes and the closure rate. The Figure indicates that the closure rate was about 38 knots at the time of the collision.

Figure 11 presents the pitch, flight path, roll, heading, and ground track angles calculated from the smooth tracks for the Piper and the Cessna. The Piper's track angle at the time of the collision was about 318°, and the Cessna's track angle was about 306°. Therefore, the collision angle (the smallest angle between the ground tracks of the aircraft at the time of impact)[7] is about 12° (318° - 306°), with the Piper approaching the Cessna from behind and to the left, and the Cessna approaching the Piper from ahead and to the right (see Figure 1).

---

[7] The collision angle is not to be confused with the angles the velocity vectors of the airplanes *relative to each other* make with each airplane's centerline, as discussed above. The relative velocity depends on the airplanes' groundspeeds, as well as their track angles; the collision angle as defined here only depends on the track angles.

Figures 1 and 6–11 indicate that the collision occurred as both airplanes were completing almost continuous turns from their downwind legs to a short final approach for KVGT runway 30R. The short final for the Cessna was consistent with the Cessna pilot's request for a "short approach," and during its right downwind-to-final turn the airplane leveled briefly on the right base leg for about 5 seconds, from about 12:02:17 to 12:02:22 (see Figure 11). The Piper, which had been cleared to land on runway 30L, overshot the centerline for that runway during its left downwind-to-final turn, and appeared to be lining up for runway 30R instead, even though the Piper copilot twice acknowledged the instruction to land on runway 30L.

Figures 1 and 11 show that after the Piper overflew the field near the middle of and perpendicular to runway 30L, it entered a continuous left turn at a roll angle that at one point reached 40°, remained in the turn from 12:02:00 until the collision at 12:02:51, and did not level out on either a left downwind or base leg. During this turn, the Piper's airspeed decreased from 123 kt. calibrated airspeed (KCAS) at 12:02:15 to about 106 KCAS at the collision. During the same period, the ground speed decreased from 138 kt. to 111 kt. Per the JetProp POH, the normal flaps down approach airspeed is 85 kt. indicated airspeed (KIAS). Consequently, during the final turn the Piper was flying 38 to 21 kt. faster than the nominal approach speed.

The Piper's excess speed might have contributed to the airplane's alignment with runway 30R instead of with runway 30L. The true heading of runway 30L is 314°, so the reciprocal heading (that would be flown on the downwind leg for that runway) is 134°. Figure 11 shows that the Piper turned through a heading of 134° at about 12:02:16. At that time, it was about 0.68 nm (4,132 ft.) to the left of the runway 30L centerline. Consequently, to have been aligned with the extended runway 30L centerline after having turned 180° left towards the runway heading, the radius of the turn would have had to have been 4,132 ft./2 = 2,066 ft. The turn radius is a function of the airplane's airspeed and roll angle:

$$r = \frac{V_T{}^2}{g \tan \phi}$$
[1]

Where r is the turn radius, V_T is the true airspeed, g is the acceleration due to gravity, and ϕ is the roll angle. The black line in Figure 12 shows the roll angle required to achieve a left turn radius of 2,066 ft. as a function of airspeed, as computed using Equation [1]. The multi-colored line in Figure 12 plots the combinations of roll angle and true airspeed computed from the Piper data. The color of the line indicates the corresponding ADS-B time, per the color scale shown on the plot, starting at 12:02:15 (points prior to this time are colored dark green). Figure 12 shows that during the turn the roll angle remained consistently below that required to achieve a turn radius of 2,066 ft. at the airspeeds the airplane was flying. The plot also shows that at the nominal approach speed of 85 kt., the required turn could have been accomplished with a roll angle less than 20°. At 100 kt., the required roll angle would have been only 23°. At the actual speeds flown, the required roll angle would have been between 32° and 37°.

D.3.   Cockpit visibility study

D.3.1. Azimuth and elevation visibility angles

Once the position and orientation of each airplane has been determined, its position in the body axis system of the other airplane can be calculated. These relative positions then determine where the "target" aircraft will appear in the field of view of the pilot of the "viewer" aircraft.

For this S*tudy*, the relative positions of the two airplanes (and the visibility of each from the other) were calculated at 1-second intervals up to the collision, beginning at 12:00:50 (about 2 minutes before the collision), when the Piper was about 2.7 nm north of the KVGT runway 30R displaced threshold, and the Cessna was turning onto the right downwind leg for runway 30R.

The "visibility angles" from the "viewer" airplane to the "target" airplane correspond to the angular coordinates of the line of sight between the airplanes, measured in a coordinate system fixed to the viewer airplane (the viewer's "body axis" system), and consist of the azimuth angle and elevation angle (see Figure 13). The azimuth angle is the angle between the x-axis and the projection of the line of sight onto the x-y plane. The elevation angle is the angle between the line of sight itself, and its projection onto the x-y plane. At 0° elevation, 0° azimuth is straight ahead, and positive azimuth angles are to the right. 90° azimuth would be out the right window parallel to the y axis of the airplane. At 0° azimuth, 0° elevation is straight ahead, and positive elevation angles are up. 90° elevation would be straight up parallel to the z axis. The azimuth and elevation angles depend on both the position (east, north, and altitude coordinates) of the viewer and target airplanes, and the orientation (yaw, pitch, and bank angles) of the viewer. The azimuth and elevation angles of points on the target away from its center of gravity (CG) also depend on the orientation of the target.

The position, altitude, and orientation of the Piper and the Cessna are based on smoothed ADS-B data, and so are sensitive to different ways of smoothing the data that all result in solutions within the uncertainty bounds of the data. Consequently, there is some uncertainty in the resulting visibility angles. The effects of these uncertainties on the visibility of each airplane from the other are considered below.

D.3.2. Azimuth and elevation angles of airplane structures from laser scans

The target airplane will be visible from the viewer airplane unless a non-transparent part of the viewer's structure lies in the line of sight between the two airplanes. To determine if this is the case, the azimuth and elevation coordinates of the boundaries of the viewer's transparent structures (windows) must be known, as well as the coordinates of the viewer's structure visible from the cockpit (such as the wings, nose, and wing struts). If the line of sight passes through a non-transparent structure (such as

the instrument panel, a window post, or a wing), then the target airplane will be obscured from the viewer.

For this *Study*, the azimuth and elevation angles of the windows and structures of the Piper and the Cessna were determined from the interior and exterior dimensions of exemplar airplanes, as measured using a laser scanner. The laser scanner produces a "point cloud" generated by the reflection of laser light off objects in the laser's path, as the scanner sweeps through 360° of azimuth and approximately 150° of elevation. The 3-dimensional coordinates of each point in the cloud are known, and the coordinates of points from multiple scans (resulting from placing the scanner in different positions) are "merged" by the scanner software[8] into a common coordinate system. By placing the scanner in enough locations so that the scanner can "see" every part of the airplane, the complete exterior and interior geometry of the airplane can be defined.

For this *Study*, the scanner was placed in several locations to scan the exterior of the airplanes, and in the pilot seats to scan the interior of the airplanes. The scanner software was then used to identify the points defining the outline of the cockpit windows (from the interior scans) and exterior structures visible from the cockpit (from the exterior scans). The coordinates were transformed into the airplane's body axis system and, ultimately, into azimuth and elevation angles from the pilot's eye position. The transformation method is described in Appendix A.

The azimuth and elevation angles of the viewer airplane's windows and other structures are very sensitive to the pilot's eye location in the cockpit. If the pilot moves his head forward or aft, or from a position centered over his seat to one close to a window surface, the view out the window (and the azimuth and elevation angles of all the airplane's structures) change significantly. This potential variability in the pilot's eye position, and the consequent variability in the location of the window edges and airplane structures in the pilot's field of view, is by far the greatest source of uncertainty as to whether the target aircraft is obscured or not at a given time.

To evaluate the effect of varying eye position on the visibility of the target airplane, the azimuth and elevation angles of the cockpit windows and other airplane structures were computed for a matrix of eye positions displaced from the nominal eye positions,

---

[8] FARO SCENE software: see https://www.faro.com/en/Products/Software/SCENE-Software.

as described below. The pilots' "nominal" eye positions were identified by scanning an individual seated in the cockpit of each airplane.[9]

In addition to the calculation of the visibility angles, this *Study* presents recreations of possible views from the pilots' seats (including simulation-based depictions of the outside world) constructed assuming the nominal eye positions as defined above.

D.3.3. Results: azimuth and elevation angle calculations

The azimuth and elevation angles from the "viewer" airplanes to the "target" airplanes are shown as a function of time in Figure 14. In the top plot, the Piper is the "viewer" and the Cessna is the "target," and in the bottom plot, the Cessna is the "viewer" and the Piper is the "target." Figure 14 also plots the azimuth and elevation angles to the sun from each airplane.

Plots of the "target" airplane elevation angle vs. azimuth angle for the two minutes preceding the collision are shown in Figures 15 and 16, along with the azimuth and elevation coordinates of the "viewer" airplane cockpit windows and other structures, as computed for the nominal pilot eye position from the pilots' seats. Figure 15a presents the view from the pilot's (left) seat of the Piper, and Figure 15b presents the view from the copilot's (right) seat of the Piper. The trajectory of the Cessna in these views is depicted by the solid multicolored line. Figure 16 presents the view from the pilot's seat of the Cessna to the Piper. The view from the copilot's seat of the Cessna is not depicted, since the view of the Piper from that seat would have been almost entirely obscured by the pilot in the left seat and the pilot's seatback and headrest.

In Figures 15 and 16, the window edges are outlined with a black line, the cockpit structures are colored gray, and the windows are colored white. The trajectory of the "target" airplane over time is depicted by the multicolored line, where the color of the line at any point indicates the time corresponding to that point, per the color scale in the Figures. The coloring starts at time 12:02:10; before that time, the line is simply dark gray. If the multicolored line passes through a shaded area of the plot, the "target" airplane is obscured from view by the "viewer" airplane structure.

To further clarify the cockpit geometry and scan points depicted in Figures 15 and 16, scanner images of the cockpits are presented in Figures 17 and 18. Figure 17a is an

---

[9] The individual in the scans is 68" tall. Per their flight physical records, the pilot in the left seat of the Piper was 74" tall, the pilot-rated passenger (copilot) in the right seat of the Piper was 62" tall, the pilot in the left seat of the Cessna was 75" tall, and the instructor in the right seat of the Cessna was 74" tall. The differences in height between the individual in the scans and the different occupants of the airplanes can introduce differences between their eye positions and affect the visibility from the cockpit, though the exact differences are hard to determine because the cockpit seats are adjustable vertically as well as horizontally. The effects of possible differences in "nominal" eye positions can be evaluated from the visibility matrix described below.

image of the full 360° scan from the pilot's seat of the exemplar Piper. Figure 17b is a similar image from the copilot's seat of the exemplar Piper. Figure 18 is an image from the pilot's seat of the exemplar Cessna. The red rectangles in these Figures highlight the cockpit areas depicted in Figures 15 and 16.

The azimuth and elevation angles of the sun are also of interest, because sun glare can affect a pilot's ability to see other aircraft. The azimuth (relative to true north) and altitude angles of the sun at the time and location of the accident were 144.62° and 72.10°, respectively.[10] To compute the location (azimuth and elevation angles) of the sun in the Piper and Cessna pilots' fields of view, the coordinates of the sun in earth coordinates were computed (using the sun angles and an assumed very large distance to the sun), and then transformed into the airplane body axis coordinates using the Euler angles shown in Figure 11. The azimuth and elevation angles of the sun were then computed from its body axis coordinates. The results are presented in Figure 14.

The results of these calculations indicate that in both the Piper and Cessna pilots' fields of view, the sun would have appeared sufficiently high in the sky so as to be always shielded by the cockpit structure above the windows. Hence, it is not likely that sun glare would have affected either pilot's ability to see the other airplane.

Figure 15a indicates that cockpit structure would have obscured the Cessna from the Piper pilot's field of view except between 12:02:28 and 12:02:43 (a period of 15 seconds), when the Cessna would have crossed the pilot's windshield from the upper left to the lower right as the Piper was in a left turn to align with the runway heading. At 12:02:43, eight seconds before the collision, the Cessna might have again become obscured by the Piper's instrument panel and center windshield post. Figure 15b indicates that the situation would have been much the same for the pilot-rated passenger in the Piper's copilot seat (copilot), except that the Cessna might have been in view in the copilot's windshield for 6 seconds longer (until 12:02:49, two seconds before the collision). If both the pilot and the copilot were concentrating on the airplane's turn and alignment with runway 30R, with their eyes focused on the runway, they might not have noticed the Cessna even when it was visible in the windshield.

Figure 16 indicates that the Piper would have been visible in the Cessna's windshield from 12:02:06 to 12:02:37 (a period of 31 seconds), crossing the windshield from the upper right to the middle left as the Cessna was in a right turn to align with the runway heading. The Piper might have been obscured for about 3 seconds (from 12:02:20 to 12:02:23) behind the whiskey compass on the Cessna's instrument panel. During another 3 seconds (between 12:02:37 and 12:02:40), the Piper would have been obscured behind the Cessna's left window post before reappearing in the Cessna's left door window. The Piper would have passed behind the Cessna pilot's left shoulder (through an azimuth angle of -90°) at 12:02:44.5, 6.5 seconds before the collision. As

---

[10] As computed using https://www.susdesign.com/sunangle/.

with the Piper pilot, if the Cessna pilot was concentrating on the airplane's turn and alignment with runway 30R, with his eyes focused on the runway, he might not have noticed the Piper even when it was visible through the windows.

As noted above, the azimuth and elevation angles of the window and cockpit structures are sensitive to the position of the pilot's eyes in the cockpit. To determine how these angles change as the pilot's eye position changes (e.g., by leaning in different directions, or by a seat height adjustment), plots similar to Figures 15 and 16 were generated for the 27 different eye positions shown in Table 3. The positions are expressed as displacements from the nominal eye position along the three airplane body axes ($\{\Delta x_b, \Delta y_b, \Delta z_b\}$[11]).

Case name	Δx_b from nominal, in. (+ forward, - aft)	Δy_b from nominal, in. (+ right, - left)	Δz_b from nominal, in. (+ down, - up)
CCD	0	0	+1.5
FCD	+3	0	+1.5
ACD	-3	0	+1.5
FLD	+3	-3	+1.5
CLD	0	-3	+1.5
ALD	-3	-3	+1.5
FRD	+3	+3	+1.5
CRD	0	+3	+1.5
ARD	-3	+3	+1.5
CCC (nominal)	0	0	0
FCC	+3	0	0
ACC	-3	0	0
FLC	+3	-3	0
CLC	0	-3	0
ALC	-3	-3	0
FRC	+3	+3	0
CRC	0	+3	0
ARC	-3	+3	0
CCU	0	0	-1.5
FCU	+3	0	-1.5
ACU	-3	0	-1.5
FLU	+3	-3	-1.5
CLU	0	-3	-1.5
ALU	-3	-3	-1.5
FRU	+3	+3	-1.5
CRU	0	+3	-1.5
ARU	-3	+3	-1.5

Table 3. Matrix of eye positions for cockpit structure azimuth and elevation angle calculations.

The results of the calculations are presented in Figure 19 for the Piper pilot's field of view, in Figure 20 for the Piper copilot's field of view, and in Figure 21 for the Cessna

---

[11] The body axis system is illustrated in Figure 13.

pilot's field of view. The trajectory of each "target" airplane in these Figures is depicted by the solid red line.

As shown in Figures 19-21, a variation in the pilot's eye position from the nominal position changes where the target airplane appears in the viewer's field of view, and how and when the target airplane might become obscured by the viewer airplane's structure. For example, Figure 21 shows that the brief obscuration of the Piper by the whiskey compass on the top of the Cessna's instrument panel is sensitive to movements of the Cessna pilot's eye position. In contrast, Figures 19a-c show that even though the position of the Cessna in the Piper's windshield changes with the Piper pilot's eye position, during the final seconds before the collision the Cessna always becomes obscured for a time by the Piper instrument panel and center windshield post.

Figures 19-21 indicate that the visibility of one aircraft from the other can be very sensitive to the position of the pilots' eyes relative to the window structures. This observation underscores the fact that scanning for traffic visually can be more effective if pilots move their heads as well as redirect their eyes, since head movements may bring otherwise obscured aircraft into view.

D.3.4. Simulated views from the Piper and Cessna cockpits

While Figures 15, 16, and 19-21 depict where the "target" airplanes could have appeared in the "viewer" airplanes' windows, they do not provide a sense of the background against which the targets would appear, and against which the pilot of each airplane would have to see the target. To provide a rough approximation of these backgrounds and of how the view from each cockpit evolved over time, the views from the cockpits were recreated in the *Microsoft Flight Simulator X* (*FSX*) simulation program, using airplane, sky, and terrain graphics inherent in *FSX*.

The cockpit structures at the nominal pilots' eye points (based on the laser scans) were constructed in *FSX* as semi-transparent panels that "mask" the view from each cockpit (see Appendix B); the cockpit geometries built into the airplane models in the simulation were not used. Airplane models were only used to represent the exterior "target" airplane geometry in the recreated views. The position (latitude, longitude, and altitude) and attitude (heading, pitch, and roll) of each airplane were recreated in *FSX* using the *FS Recorder* program developed by Matthias Neusinger,[12] based on the position and attitude data used for the performance calculations for each airplane.

FSX contains inherent options to customize the time, date, and weather depiction in the simulation. The time and date were set to those of the accident (12:03 PDT on July 17, 2022), which results in the correct placement of the sun in the sky. The weather

---

[12] This program used to be available at http://www.fs-recorder.net/, but the website is no longer operational.

option was set to "clear skies" with "maximum visibility" and no clouds. This option was selected to compensate for the limited resolution of the computer display (for which the size of distant but theoretically visible objects can be smaller than a pixel), in order to display pixels representing the target airplanes as soon as possible. The resulting weather is generally consistent with the KVGT 11:53 METAR.

The view depicted by *FSX* depends on the program's "camera" settings. In this *Study*, the *FSX* camera is equivalent to the pilot's eyes: the view from the cockpit depends on the camera's position, orientation (where it's pointed), and its "field of view" (i.e., the range of azimuth and elevation angles that can be "seen" by the camera). The widest field of view available in *FSX* is 90° horizontally and about 62° vertically. [13] Consequently, if the camera is pointed straight ahead (0° azimuth), then only azimuth angles between -45° and +45° will be visible in that view. If objects of interest (e.g., the target airplane) are beyond this range, then to "see" them the camera will have to be rotated away from 0° azimuth toward the object. However, in this case, a portion of the view straight-ahead will be lost, which may be unsatisfactory for the purpose of giving the viewer a good sense of the airplane's direction of travel and general situation relative to the outside world.

To see objects beyond ±45° of azimuth while at the same time preserving a field of view of at least ±45° of azimuth about the direction of travel, the view from two co-located cameras can be joined side-by-side: the first camera pointed away from 0° azimuth to capture the object, and the second camera pointed in such a way that the boundaries of the fields of view of the cameras coincide at a particular azimuth angle. For example, if one camera is rotated to -45° azimuth, the left boundary of its field of view will be at -45° - 45° = -90°, and the right boundary will be at -45° + 45° = 0°. If the second camera is rotated to +45° azimuth, its left boundary will be at +45° - 45° =0° (coinciding with the right boundary of the first camera), and its right boundary will be at +45° + 45° = +90°. Setting the views from the cameras side-by-side, a continuous field of view from -90° to +90° is obtained.

However, discontinuities (kinks) in straight lines may appear at the boundary of these views when they are viewed side-by-side on a flat surface (such as a computer screen), because the viewer will be viewing both from the same angle, whereas the view on the left is intended to be viewed at an angle rotated 90° from that on the right. The discontinuities can be removed if each view is presented on a separate surface (monitor), and then the surfaces are joined at a 90° angle. However, this solution may be impractical (and is impossible for presenting screenshots of these views in a single document), and so the line discontinuities at the boundaries of the views may simply need to be tolerated. At non-zero roll angles, the slope of the horizon line is discontinuous at the boundary between the views, but there is no break in the horizon line itself.

---

[13] These values are for an *FSX* window with an aspect ratio of 1.6, at a "zoom" setting of 0.3.

As shown in Figure 14, because both the Piper and Cessna completed 180° turns while maneuvering towards runway 30R, the azimuth angle of the other airplane in the pilots' fields of view spanned over 180°. Consequently, for this *Study* two cameras are used to recreate the views from both cockpits. For the Piper, the cameras are pointed along azimuth angles of -45° and +45°, providing a total field of view from -90° to +90°. For the Cessna, the cameras are pointed along azimuth angles of -90° and 0°, providing a total field of view from -135° to +45°.

Screenshots of the Piper cockpit recreation are presented in Figures 22a-g, along with simulated Cockpit Display of Traffic Information (CDTI) screens depicting the traffic information that the Garmin device installed in the Piper might have provided (the CDTI screens are discussed in section D.4). The times of the screenshots correspond to the events listed in Table 4. The locations of the Cessna in Figures 22a-g are highlighted by the yellow circles, though the airplane itself may be too small to be seen in some of the *FSX* images.

Screenshots of the Cessna cockpit recreation are presented in Figures 23a-g, along with simulated CDTI screens depicting the traffic information that a CDTI display meeting RTCA document DO-317B standards (described below) might have provided, had the Cessna been equipped with such a device. The locations of the Piper in Figures 23a-g are highlighted by the yellow circles, though the airplane itself may be too small to be seen in some of the *FSX* images.

Time (PDT)	Letter ID in Figures 22 & 23	Time before collision (seconds)	Horizontal separation (nm)	Horizontal separation (ft)	Vertical separation (ft)	Closure rate (kt)
12:02:15	a	36	1.4784	8,983	10	102
12:02:21	b	30	1.2704	7,719	40	145
12:02:29	c	22	0.8877	5,394	25	196
12:02:34	d	17	0.6145	3,734	36	193
12:02:39	e	12	0.3592	2,182	14	173
12:02:44	f	7	0.1498	910	18	121
12:02:49	g	2	0.0271	165	10	56

Table 4. Times corresponding to recreated cockpit views and CDTI displays in Figures 22 and 23.

A measure of the size of the "target" airplane in the field of view of the "viewer" is the difference in azimuth and elevation angles between different points on the "target." For this *Study*, the azimuth and elevation angles of the nose, tail, center, and left and right wingtips of the targets were computed (the angles plotted in Figures 14-16 correspond to the center of the targets). The difference in azimuth and elevation angles between the nose and the tail of the targets are presented as a function of time in Figure 24 as the lines labeled "Δ azimuth, fuselage" and "Δ elevation, fuselage." The difference in angles between the left and right wingtips are presented as the lines labeled "Δ azimuth, wings" and "Δ elevation, wings." In these calculations, the nose, tail,

and wingtips are assumed to lie in a plane, and so the airplanes in this representation have zero thickness. Hence, the information in Figure 24 does not represent the size of the *area* of the target presented to the viewer (which is what makes the target visible), but only the extent of a subset of dimensions that contribute to the area. Nonetheless, Figure 24 does provide a measure of the target size, and of the very sudden increase in size (called the "blossom" effect) within a few seconds of the collision. Reference 5 describes the minimum object size required for an object to be seen and recognized by a person:

> Visual acuity is the ability to see high levels of detail in an image. Distant acuity is commonly measured using a Snellen eye chart containing static, high contrast letters positioned 20 feet from an observer [see Reference 6]. The ability to resolve a detail (a line or a space) as small as 1 minute of arc [0.0167°] is considered normal acuity. This permits a person to recognize a simple shape (such as a test letter such as "E") that subtends 5 minutes of arc (0.083 degrees).

However, the actual visual detection threshold depends on many factors, including viewer age, contrast, illumination, color, and the viewer's focus. Reference 5 notes that unfamiliar objects can be harder to recognize, and emphasizes the importance of visual contrast:

> Research indicates that the minimum subtended angle required for recognizing an uncommon shape in a field of distractor items is 0.20 degrees [Reference 7].
> …
> Visual contrast is another consideration for estimating recognition time …. The minimum subtended angle for recognizing complex, low contrast targets is about 0.40 to 0.60 degrees [Reference 8].

Given these uncertainties, Figure 24 should not be used to determine a specific time at which the pilots "should" have been able to see the other airplane.

The yellow highlighted areas Figure 24 indicate the time periods during which, with the pilots' eyes at their nominal positions, the center of the "target" airplanes would have been obscured from the "viewer" pilots' views by airplane structure, consistent with Figures 15 and 16. At all other times, the target airplanes would not have been obscured from the viewer pilots' views.

Consistent with Figure 15, Figure 24 indicates that the Cessna would have been in the Piper pilot's field of view for only 15 seconds (between 12:02:28 and 12:02:43). During most of this time, the Cessna would have appeared as a small object (spanning less than 1° of azimuth and elevation) in the Piper's windshield. Critically, the Cessna would have been obscured behind the Piper's center window post during the last 8 seconds before the collision, as it grew in size in the field of view. In addition, Figures 22 a-g indicate that the Cessna would have appeared on or slightly below the horizon and against a complex background, which would have made it more difficult to identify.

Figure 24 indicates that the Piper would have been visible in the Cessna pilot's field of view from 12:02:06 until the collision, except for the two 3-second periods from 12:02:20 - 12:02:23 and 12:02:37 – 12:02:40. Figures 23 a-g indicate that the Piper would have appeared on or slightly below the horizon and against a complex background, which would have made it more difficult to identify. As noted earlier, the Piper would have passed behind the Cessna pilot's left shoulder at 12:02:44.5, 6.5 seconds before the collision. It seems unlikely that the Cessna pilot would have looked over his left shoulder to scan for traffic while maneuvering onto the final approach to the runway, and so would have likely remained unaware of the Piper approaching from his left aft quarter.

D.4. Cockpit Display of Traffic Information (CDTI) study

D.4.1. Recreation and simulation of CDTI displays

The Automatic Dependent Surveillance – Broadcast (ADS-B) system, and the enhanced visual acquisition (EVAcq) and ADS-B Traffic Advisory System (ATAS) applications of the ADS-B system, were introduced above in section D.2.1. As mentioned there, the cockpit display that presents traffic information to the pilot in a plan or "birds eye" view per the EVAcq and ATAS application descriptions is the Cockpit Display of Traffic Information, or CDTI. As noted in Section D.2.1, the Piper had an ADS-B In-based CDTI visual display installed, but the Cessna did not have such an display installed, and no portable display device was found in the Cessna wreckage.

The Garmin CDTI device installed in the Piper (a Garmin G500 Avionics Display System) implements similar but different traffic alerting criteria than those prescribed by the ATAS ADS-B In function described in AC 20-172B (the ATAS standards are defined in RTCA document DO-317B, "Minimum Operational Performance Standards (MOPS) for Aircraft Surveillance Applications (ASA) System"). For this investigation, simulated CDTI displays for both the Piper and the Cessna were generated based on the recorded ADS-B information[14] for the area and time of the accident, using the Garmin G500 conventions and criteria for the Piper, and the DO-317B criteria for the Cessna (for a hypothetical scenario in which the Cessna would have been equipped with CDTI). These simulations depict the traffic information that *could* have been presented to the pilots of both airplanes.

The DO-317B and Garmin G500 traffic display and alerting conventions are described below.

---

[14] As noted above, the FAA provided the NTSB with recorded ADS-B a data within a 10 nm radius of KVGT, and below 5,000 ft. above ground level (AGL), from 18:45 to 19:10 UTC (11:45 to 12:10 PDT). The data file provided by the FAA is included in the public docket for this accident.

D.4.2. DO-317B graphical conventions and alert criteria

AC 20-172B describes the graphical conventions (symbol requirements) for the CDTI, which are more completely defined in RTCA document DO-317B. These requirements specify that, among other things,

- The position of the ownship symbol should allow the display of traffic in all directions around the ownship, and indicate the direction of travel of the ownship.
- If the directionality of the traffic target is known, the traffic symbol should be an arrowhead pointing in the direction of travel.
- Traffic symbols that are not proximate (i.e., not within 6 nm and ±1,200 ft. of the ownship) should be cyan-colored or white and open (not filled).
- Traffic symbols that are proximate should be cyan or white and filled.
- Traffic that generates an ATAS alert should be displayed with yellow symbols enclosed in a circle.

DO-317B also specifies the aural annunciations that should accompany an ATAS traffic alert. The components of the annunciation include the alert "Traffic," followed by the relative traffic bearing expressed as a clock position (e.g., "two o'clock"), the relative altitude ("high," "low," or "same altitude"), the range to the target in nautical miles, and optionally, the vertical tendency[15] (e.g., "descending"). The example of a complete annunciation given in DO-317B is "Traffic, two o'clock, high, two miles, descending." The aural annunciation is provided both when a traffic target first generates an ATAS alert (by the algorithm predicting that the ownship will penetrate a "protected airspace zone" (PAZ) around the target), and again when the algorithm predicts that the ownship will penetrate a smaller, "collision airspace zone" (CAZ) around the target.[16]

As noted above, the Cessna was not equipped with any installed CDTI display, and no portable display was found in the Cessna wreckage. It is therefore likely that the Cessna pilot did not have any CDTI available to assist him in seeing and avoiding other traffic. To assess the traffic information and alerts that a CDTI *could* have provided to the Cessna pilot during the accident flight had one been available, the symbology and alerting criteria of a DO-317B compliant CDTI were simulated using the ADS-B data for the time and area of the accident. Images of the resulting traffic displays are shown in Figure 23. Note that the actual scale of the display (and in many applications, the map background as well) are selectable by the pilot; for clarity, the simulated images use a simple black background with the outer range ring set to 5 nm. The NTSB DO-317B simulation reproduces the aural alerts that accompany PAZ and CAZ alerts; in this case,

---

[15] The vertical tendency will only be annunciated when the computed rate of climb or descent is at least 500 ft./min.

[16] Per DO-317B, the size of the PAZ depends on the closure rate between the aircraft, increasing as the closure rate increases. The size of the CAZ is constant at a 500 ft. radius and a height of ±200 ft.

the simulation produced the following PAZ alert concerning the Piper at 12:02:21 (30 seconds before the collision): "Traffic, 1 o'clock, same altitude, one mile" (see Figure 23b). The simulation did not produce a second (CAZ) alert, likely because the maneuvering of both airplanes in the seconds before the collision precluded the alert algorithm from predicting a penetration of the relatively small CAZ (the prediction algorithm projects the positions of each airplane forward in time assuming constant speeds and headings, and in this case the headings of both airplanes were changing as they maneuvered onto the final approach for runway 30R).

D.4.3. Piper equipment: Garmin 500 / GDL 88 symbology and alert criteria

As noted above, the Piper was equipped with a Garmin G500 Avionics Display System paired with a Garmin GDL 88 ADS-B Transceiver for displaying ADS-B traffic information.[17] The traffic information that could have been presented on the G500 screen will be considered here (the resulting images are shown in Figure 22).

The Garmin *G500 Cockpit Reference Guide* (Reference 9) defines the graphical conventions for traffic information displayed on the G500. Under the heading of "ADS-B Traffic (Optional)" Reference 9 states:

> The ADS-B traffic page provides an enhanced display of traffic from a compatible ADS-B In system. Available ADS-B traffic features may include individual target selection and other details, such as type, direction, groundspeed, and motion.

Figure 25 presents images from Reference 9 that illustrate the ADS-B traffic presentation and symbology on the G500. Note that the "Directional Alerted Traffic" symbol is a black-filled arrowhead over a yellow circle. The conditions required for a traffic target to be classified as a Traffic Alert (TA) are defined in the Garmin *GDL 88 ADS-B Transceiver Pilot's Guide* (Reference 10). Section 4.2.4 of Reference 10, titled "Conflict Situational Awareness (CSA)," states:

> Conflict Situational Awareness is an alerting algorithm that provides TCAS-like Traffic Alerts on ADS-B, ADS-R, and TIS-B targets to enhance situational awareness.
>
> The GDL 88 issues an aural alert when a Conflict Situational Awareness (CSA) alert is displayed: "Traffic-<X> O'Clock, <Y>, <Z>" spoken once, (where <X> is the clock position of the intruder, <Y> is the relative position (Above, Below), and <Z> is the range in nautical miles).
>
> As in some TCAS I TA implementations, altitude above terrain is used to adjust the sensitivity of the CSA algorithm to minimize nuisance alerts. Radar Altitude (if available), Height Above Terrain (as provided by a GNS or GTN navigator with a terrain database), and Geodetic Altitude are used to adjust the sensitivity of the CSA algorithm.

Up to 1,000 ft. Radar Altitude or Height Above Terrain (the situation of the accident flights), the GDL 88 is in Sensitivity Level 2, which means the CSA algorithm generates

---

[17] Per a maintenance record of equipment installed on N97CX on 11/04/2015.

a TA when the closure rate of a target provides less than 20 seconds of separation from the ownship, or when a target comes within 0.2 nm and 850 vertical feet of the ownship.

The symbology and alerting criteria for the Garmin 500 / GDL 88 combination described above were simulated using the ADS-B data for the time and area of the accident. Images of the resulting traffic displays are shown in Figure 22. Note that the actual scale and map background of the display are selectable by the pilot; for clarity, the simulated images use a simple black background with the outer range ring set to 5 nm. The actual settings used on the accident flight are unknown. As shown in Figure 22c, the simulation generated a TA concerning the Cessna at 12:02:29, 22 seconds before the collision. The aural alert associated with this TA would have been "Traffic, 11 o'clock, same altitude, less than one mile."

A TA and associated aural alert received while in an airport's traffic pattern might not provoke a pilot's concern, since proximate aircraft are to be expected in such an environment. Nonetheless, traffic displays and alerts can be useful even in this situation by helping pilots to become aware of the presence and location of other aircraft and helping them to judge whether any of these merit additional monitoring.

E. CONCLUSIONS

The circumstances of this accident underscore the difficultly in seeing airborne traffic (the foundation of the "see and avoid" concept in visual meteorological conditions), even when pilots might be alerted to traffic in the vicinity by equipment such as CDTI. While CDTI with aural alerts can help to make pilots aware of surrounding traffic, and prompt them to look in the right direction for conflicting traffic, in this accident the benefits of CDTI might have been defeated by (1) the probability that the Cessna pilot did not have a CDTI display available to him; and (2) even though the Piper was equipped with CDTI, a TA and associated aural alert received while in an airport's traffic pattern might not have provoked concern, since proximate aircraft are to be expected in such an environment. An NTSB simulation indicates that if a DO-317B compliant CDTI had been available on the Cessna, it might have generated a PAZ visual and aural alert concerning the Piper about 30 seconds before the collision. An NTSB simulation of the Garmin 500 / GDL 88 combination installed on the Piper indicates that this system would have generated a visual and aural TA alert concerning the Cessna about 22 seconds before the collision.

Even though traffic alerts from a CDTI while in the traffic pattern at an airport might not be as concerning as alerts received in other flight regimes, they can still be useful by helping pilots to become aware of the presence and location of other aircraft and helping them to judge whether any of these merit additional monitoring.

Regarding the pilots' opportunities to see the other airplane through the cockpit windows, Section D.3 presents the results of using the recorded surveillance data to

estimate the location of each airplane in the other airplane's windows during the minute prior to the collision. The results are shown in Figures 14-16 and 19-24.

The visibility of one airplane from another is sensitive to the position of the pilot's eyes relative to the cockpit windows. This sensitivity is illustrated in Figures 19 - 21, which underscore the fact that looking for traffic can be more effective if pilots move their heads as well as redirect their eyes, since head movements may bring otherwise obscured aircraft into view. The descriptions of visibility that follow correspond to the pilots' eyes in their nominal positions, with the understanding that the views out the windows change if the pilots move their heads.

During the minute prior to the collision the Cessna would have been in the Piper pilot's field of view for only 15 seconds (between 12:02:28 and 12:02:43). During most of this time, the Cessna would have appeared as a small object (spanning less than 1° of azimuth and elevation) in the Piper's windshield. Critically, the Cessna would have been obscured behind the Piper's center window post during the last 8 seconds before the collision, as it grew in size in the field of view. In addition, the Cessna (when visible) would have appeared on or slightly below the horizon and against a complex background, which would have made it more difficult to identify.

During the same minute, the Piper would have been visible in the Cessna pilot's field of view from 12:02:06 until the collision, except for the two 3-second periods from 12:02:20 - 12:02:23 and 12:02:37 – 12:02:40. The Piper would have appeared on or slightly below the horizon and against a complex background, which would have made it more difficult to identify. The Piper would have passed behind the Cessna pilot's left shoulder at 12:02:44.5, 6.5 seconds before the collision, making it less likely that the Cessna pilot would have become aware of the Piper approaching from his left aft quarter as both airplanes maneuvered onto the final approach for runway 30R.

Calculations of the position of the sun at the time of the accident indicate that in both the Piper and Cessna pilots' fields of view, the sun would have appeared sufficiently high in the sky so as to be always shielded by the cockpit structure above the windows. Hence, it is not likely that sun glare would have affected either pilot's ability to see the other airplane.

On two occasions prior to the collision, the Piper copilot received and acknowledged ATC instructions to land on runway 30L. However, instead of maneuvering onto the final approach for runway 30L, the Piper maneuvered onto the final approach for runway 30R, onto which the Cessna had been cleared for "the option" to either land or execute a touch-and-go. Both airplanes flew "short" approaches (meaning that the length of the final approach segment while aligned with the runway heading was shorter than usual). The Cessna pilot requested and was cleared for such a "short" approach.

After overflying the field from northeast to southwest, the Piper entered a continuous left turn through the downwind and base legs of the traffic pattern, through the extended centerline of runway 30L, and onto the extended centerline of runway 30R (see Figure 1). During this turn, the Piper was flying 38 to 21 kt. faster than the nominal approach speed. This excess speed might have contributed to the airplane's alignment with runway 30R instead of with runway 30L. Even though the Piper achieved a roll angle as high as 40° during the left turn, on average the roll angle remained consistently below that required to align with runway 30L at the airspeeds the airplane was flying.

At the nominal approach speed of 85 kt., the required turn could have been accomplished with a roll angle less than 20°. At 100 kt., the required roll angle would have been only 23°. At the actual speeds flown, the required roll angle would have been between 32° and 37°.

Submitted by: John O'Callaghan
National Resource Specialist – Aircraft Performance

F. REFERENCES

1. JetProp LLC, *JetProp DLX Pilot's Operating Handbook and FAA Approved Airplane Flight Manual*, document # 560.1002, Change 17, original FAA approval date July 30, 1998.

2. Piper Aircraft Inc., *Malibu Mirage PA-46-350P SN 4636021 and up Pilot's Operating Handbook and FAA Approved Airplane Flight Manual*, report # VB-1602, Rev. 8, revision date 10/22/2013.

3. Cessna Aircraft Company, *1979 Cessna Skyhawk Model 172N Information Manual*, document D1138-13-RPC-2500-5/90, dated 07/01/1978.

4. Textron Aviation, *Cessna Model 172M Basic Data*, report no. S-172M-0(73), dated April 3, 1972 (Textron proprietary document).

5. National Transportation Safety Board, Office of Aviation Safety, *Human Performance Specialist's Factual Report: Cessna 208B / Dudek Paragliders Solo 21, Fulshear, Texas, December 21, 2021* (NTSB accident number CEN22FA081). October 12, 2023. (Available through the NTSB CAROL search tool at https://data.ntsb.gov/carol-main-public/landing-page).

6. Gibb, R., Gray, R., and Scharff, L. (2010). *Aviation visual perception: Research, misperception and mishaps*. London: Routledge.

7. Steedman, W.C., Baker, C.A. (1960). *Target size and recognition*. Human Factors, 2(3), 120-127.

8. Van Cott, H.P, Kinkade, R.G. (1972). *Human Engineering Guide to Equipment Design (Revised Edition)*. U.S. Government Printing Office, Washington, DC.

9. Garmin, *G500/G600 Cockpit Reference Guide*, document 190-00601-03 Rev J, August 2018.

10. Garmin *GDL 88 ADS-B Transceiver Pilot's Guide*, document 190-01122-03 Rev. A, October 2012.

G. GLOSSARY

G.1. Acronyms

AC	Advisory Circular
ADS-B	Automatic Dependent Surveillance - Broadcast
ADS-R	Automatic Dependent Surveillance - Rebroadcast
AFM	Airplane Flight Manual
AGL	Above ground level
ATAS	ADS-B Traffic Advisory System
ATC	Air Traffic Control
CDTI	Cockpit Display of Traffic Information
CFR	Code of Federal Regulations
CG	Center of Gravity
FAA	Federal Aviation Administration
GNSS	Global Navigation Satellite System
GPS	Global Positioning System
IFR	Instrument Flight Rules
PDT	Mountain Daylight Time
METAR	Meteorological Terminal Air Report (Aviation Routine Weather Report)
MSL	Mean Sea Level
NAS	National Airspace System
KCOE	Coeur d'Alene Airport - Pappy Boyington Field, Coeur d'Alene, Idaho

KVGT	North Las Vegas Airport in North Las Vegas, Nevada
NTSB	National Transportation Safety Board
POH	Pilot's Operating Handbook
TA	Traffic Advisory (Garmin 500 system)
TCAS	Traffic Collision Avoidance System
TIS-B	Traffic Information Service - Broadcast
UTC	Universal Coordinated Time
VFR	Visual Flight Rules

G.2. English symbols

C_L Lift coefficient

G.3. Greek symbols

α	Angle of attack
γ	Flight path angle
θ	Pitch angle
ϕ	Roll angle
ψ_H	True heading angle
ψ_T	True track angle

FIGURES

ERA22FA318: Midair collision, Piper PA46-350P N97CX / Cessna 172N N160RA
North Las Vegas, NV, 07/17/2022
Plan view of Piper and Cessna ADS-B data

Figure 1.

Photo credit: FlightAware

Photo credit: Chris Kennedy
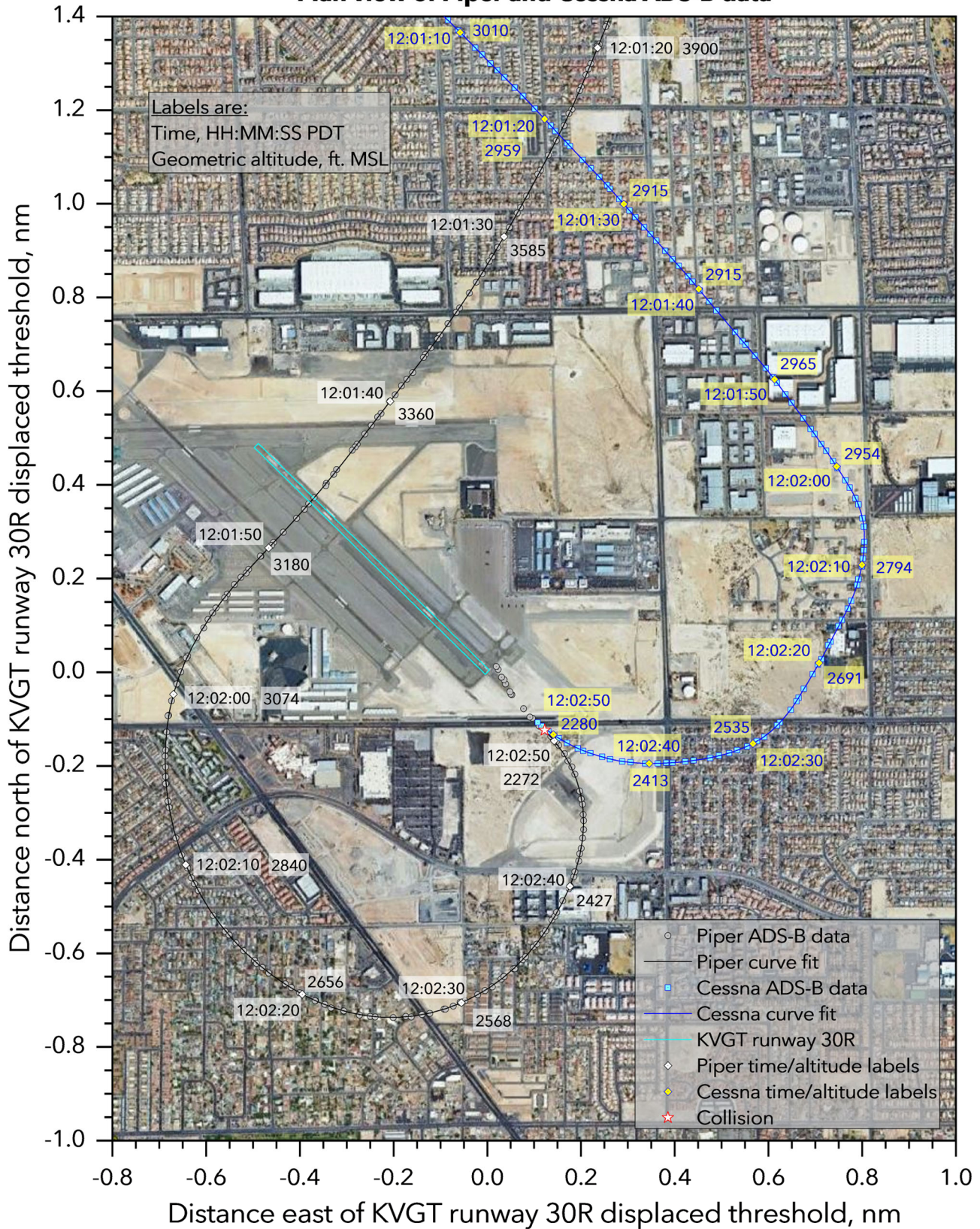
Figure 2. Pre-accident photographs of PA-46-350P PropJet DLX N97CX.
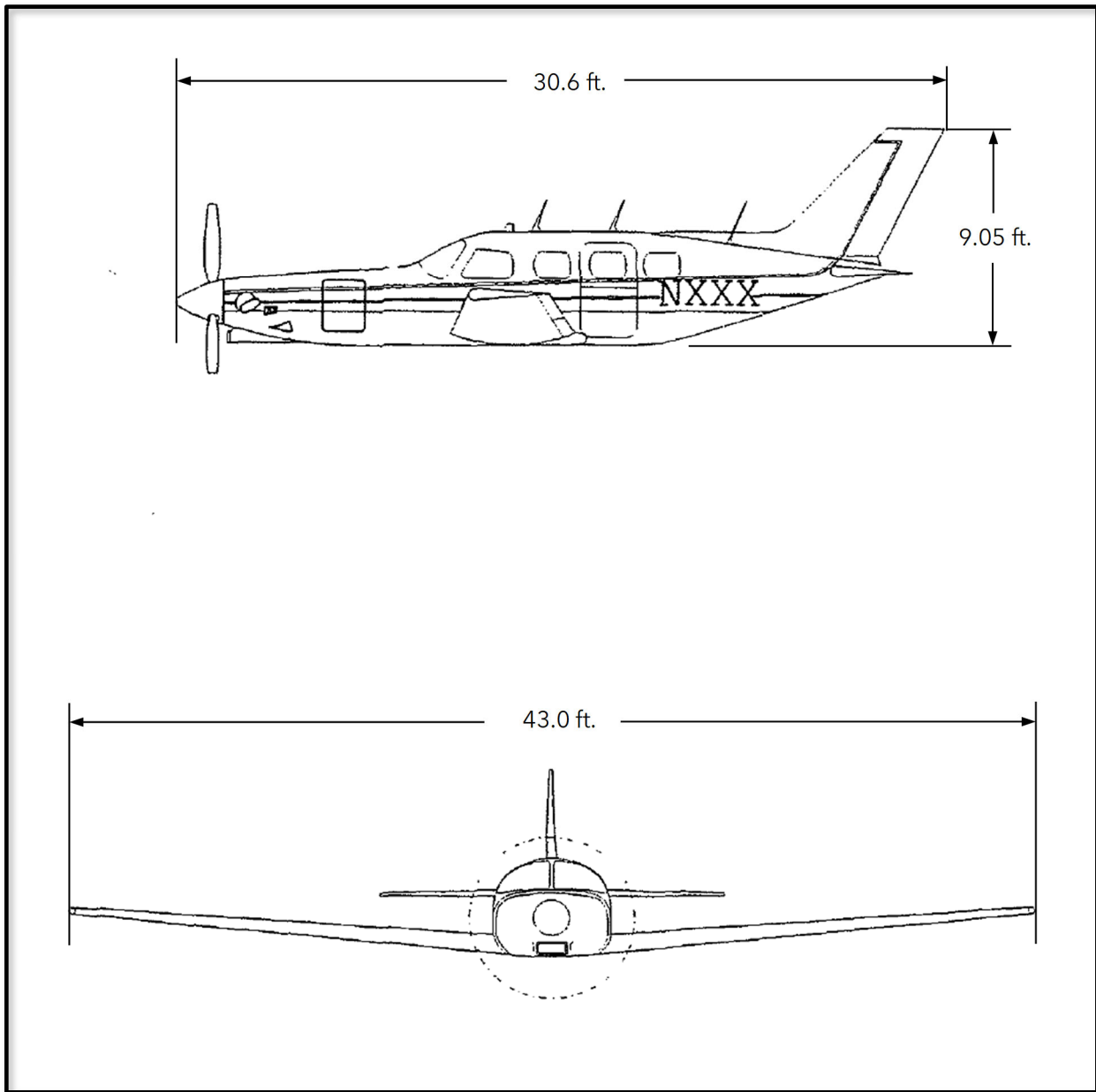
Figure 3.   2-view of the PA-46-350P PropJet DLX, from Reference 1. Fuselage length determined from laser scans; other dimensions taken from Reference 2.

Figure 4. Pre-accident photographs of Cessna 172N N160RA.
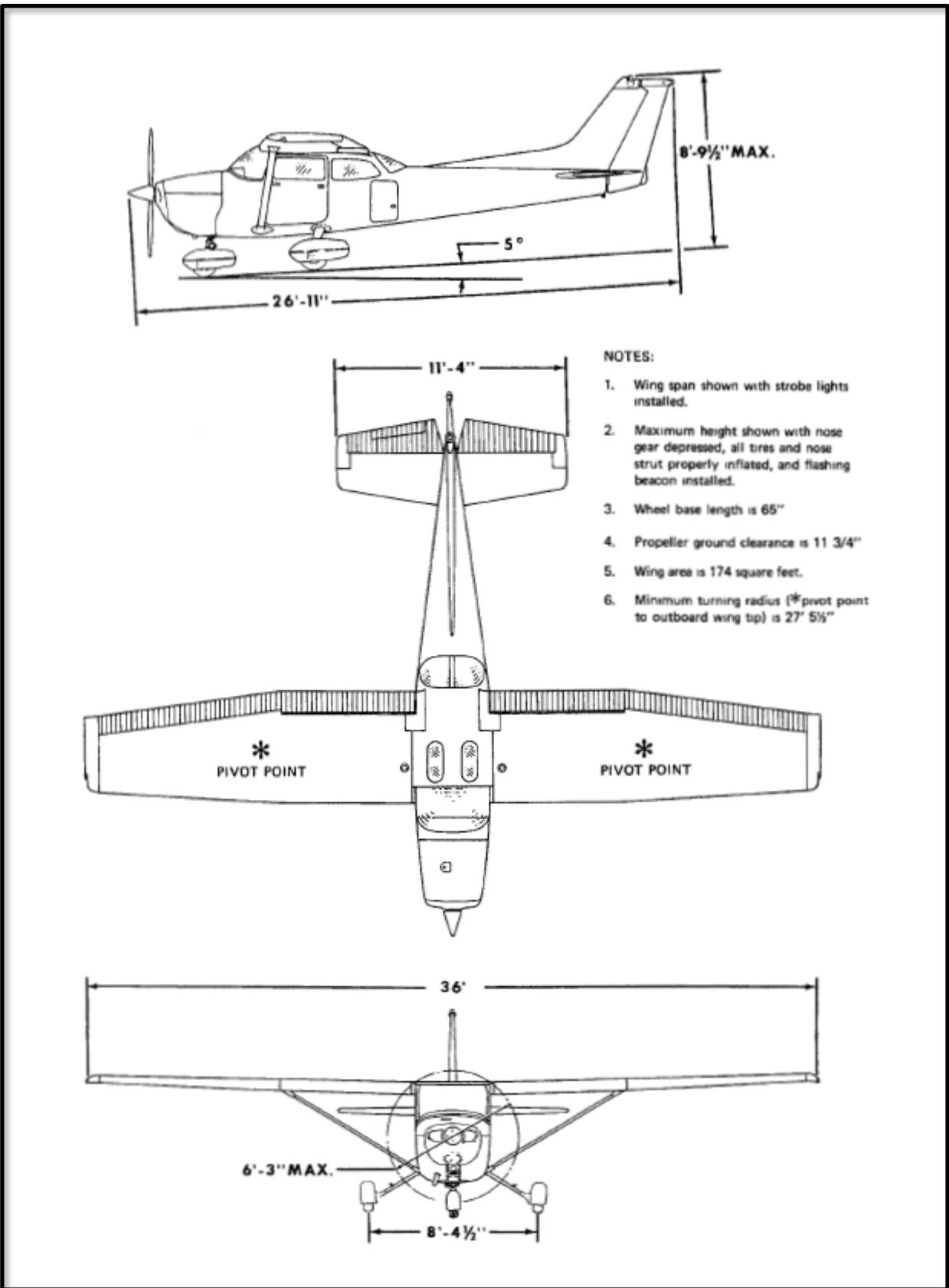
Figure 5. 3-view of the Cessna 172 Skyhawk, from Reference 3.

ERA22FA318: Midair collision, Piper PA46-350P N97CX / Cessna 172N N160RA
North Las Vegas, NV, 07/17/2022
Piper and Cessna north and east coordinates vs. time
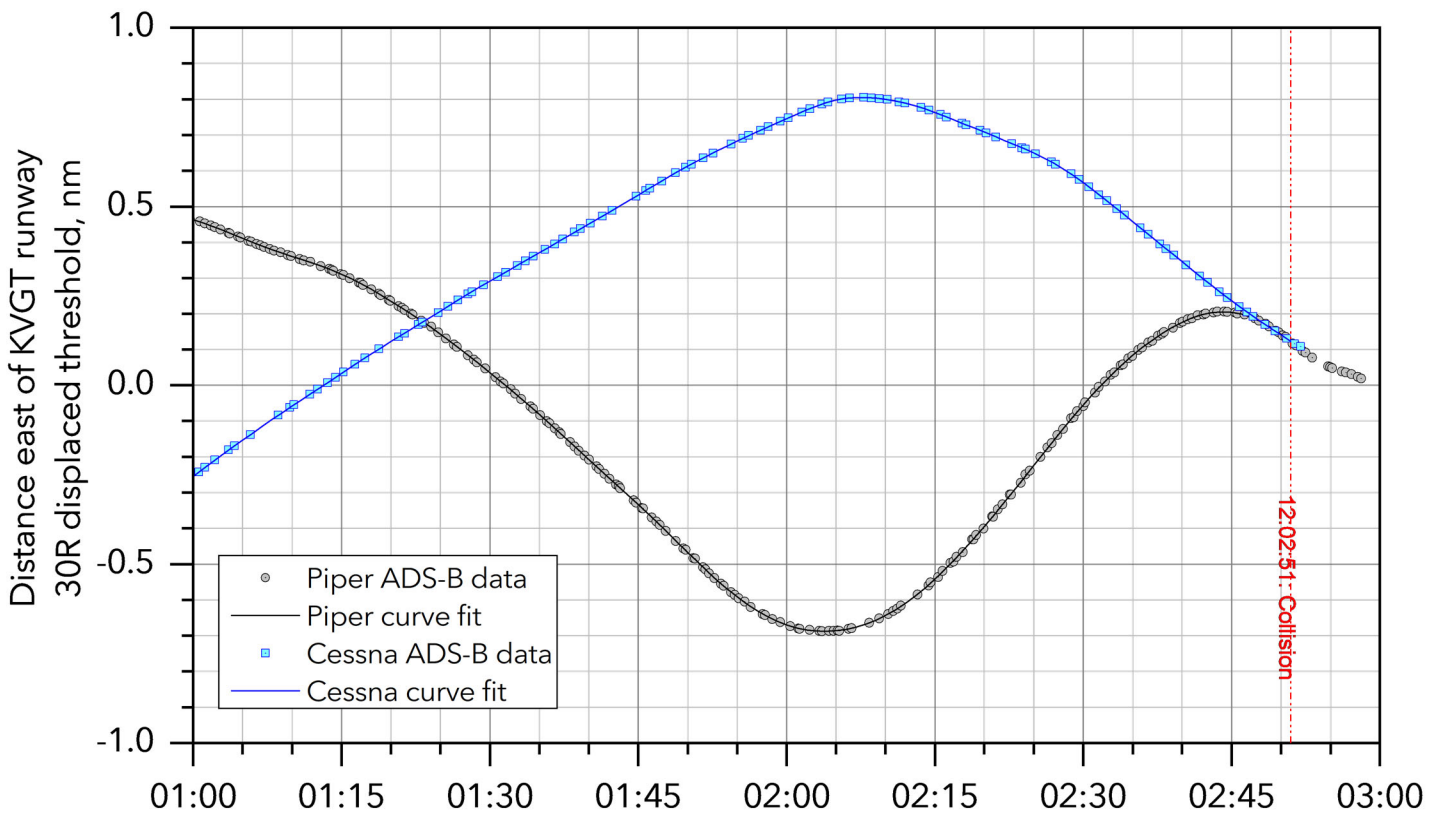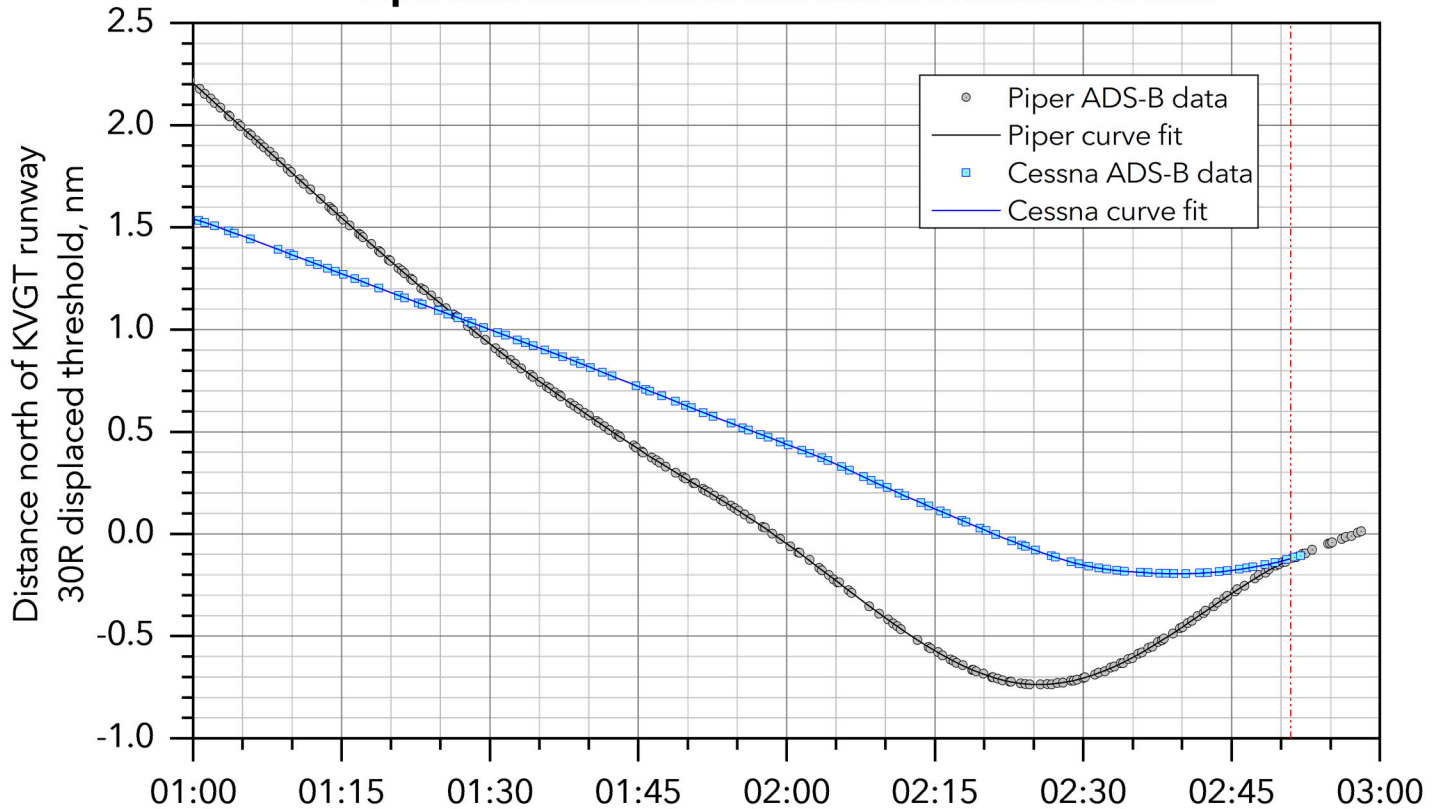
Figure 6.

**ERA22FA318: Midair collision, Piper PA46-350P N97CX / Cessna 172N N160RA
North Las Vegas, NV, 07/17/2022
Piper and Cessna altitude vs. time**

Legend:
- Piper ADS-B geometric altitude
- Curve fit of Piper ADS-B geometric altitude
- Piper ADS-B pressure altitude
- Curve fit of Piper ADS-B pressure altitude
- Cessna ADS-B geometric altitude
- Curve fit of Cessna ADS-B geometric altitude
- Cessna ADS-B pressure altitude
- Integrated Cessna ADS-B vertical speed

12:02:51: Collision

KVGT RUNWAY 30R THRESHOLD ELEVATION = 2148 FT.

Altitude, feet MSL

ADS-B time, MM:SS after 12:00:00 PDT

Figure 7.

AIRCRAFT PERFORMANCE & COCKPIT VISIBILITY STUDY

ERA22FA318: Midair collision, Piper PA46-350P N97CX / Cessna 172N N160RA
North Las Vegas, NV, 07/17/2022
Piper speeds and rate of climb vs. time
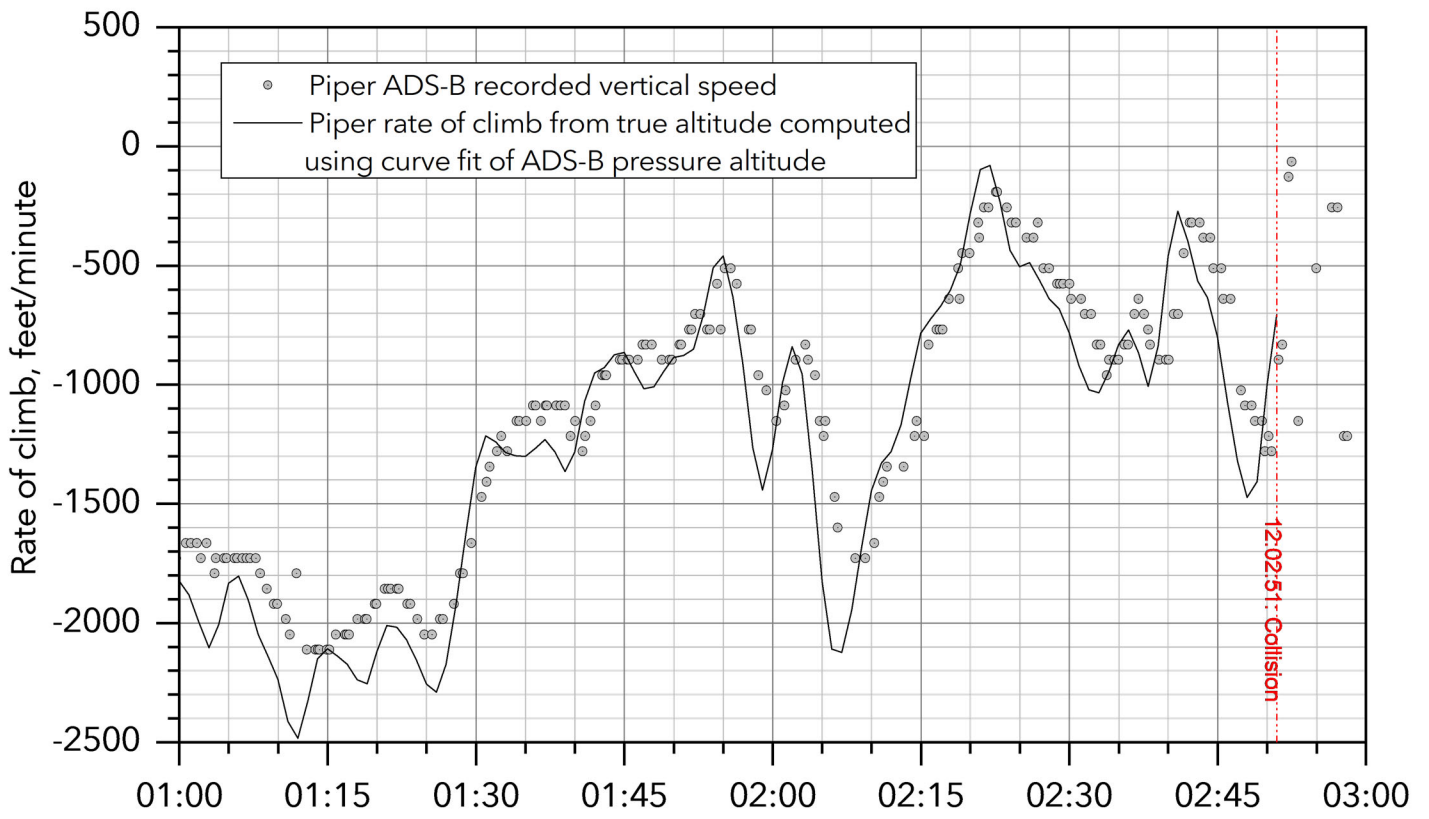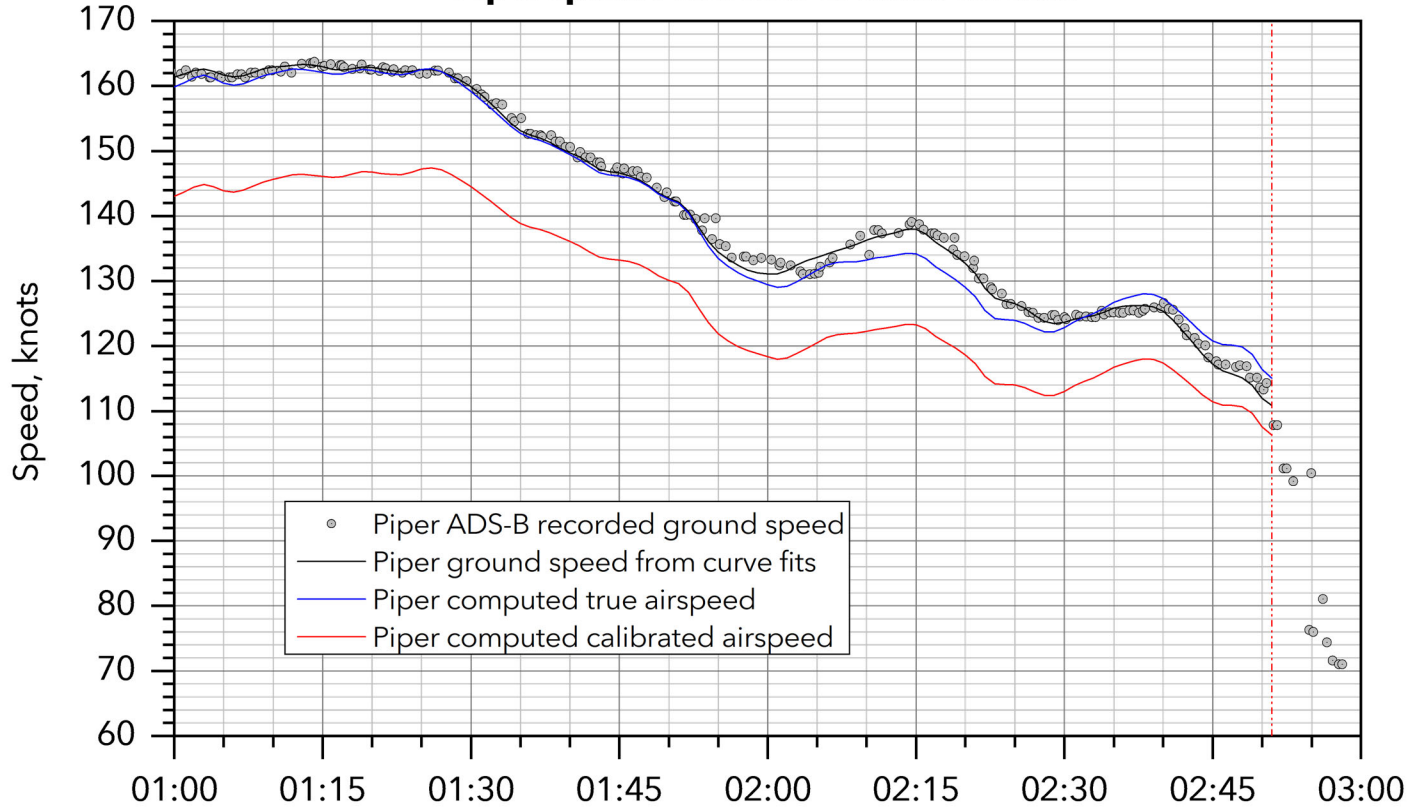
Figure 8.

AIRCRAFT PERFORMANCE & COCKPIT VISIBILITY STUDY

ERA22FA318
PG 40 OF 77

ERA22FA318: Midair collision, Piper PA46-350P N97CX / Cessna 172N N160RA
North Las Vegas, NV, 07/17/2022
Cessna speeds and rate of climb vs. time
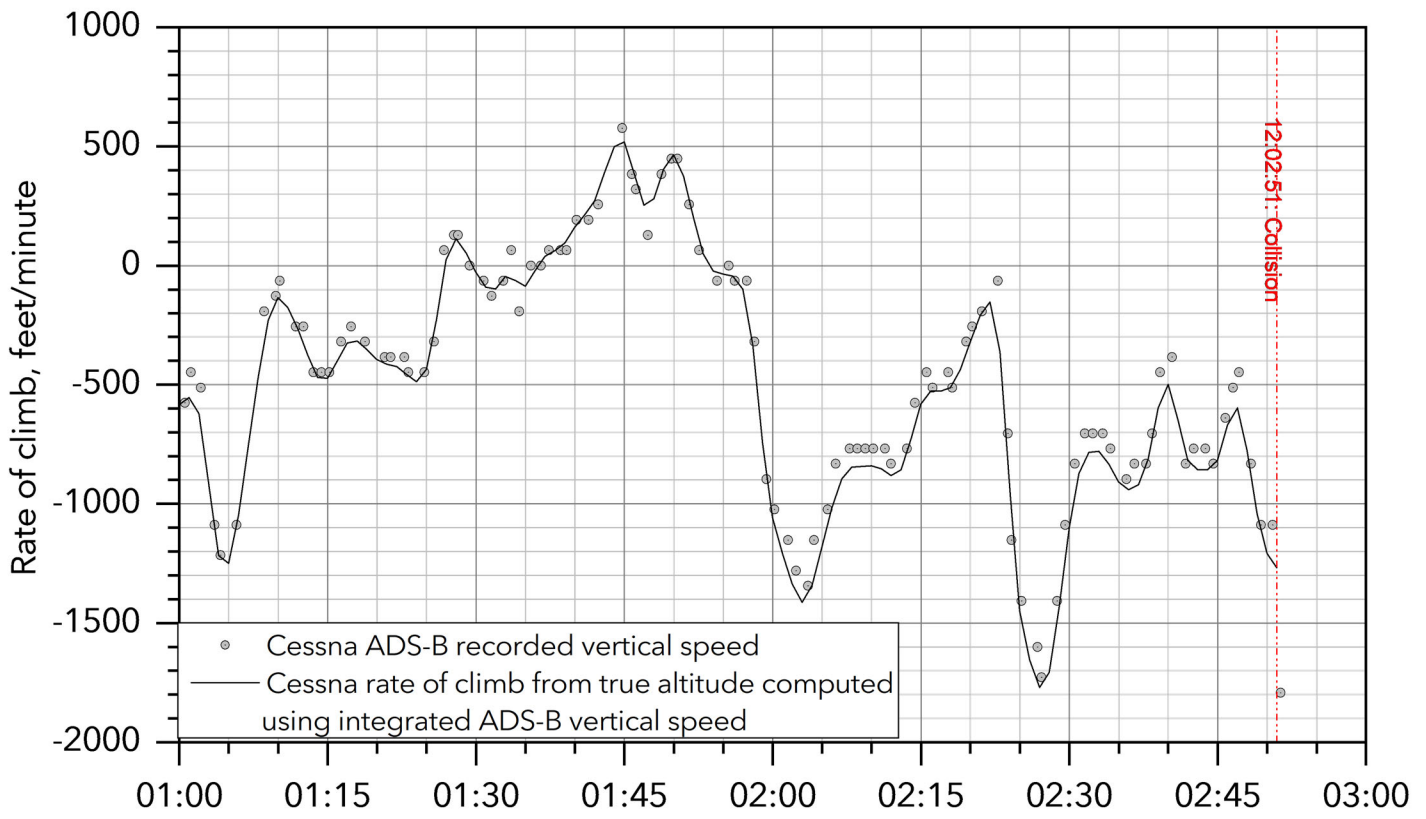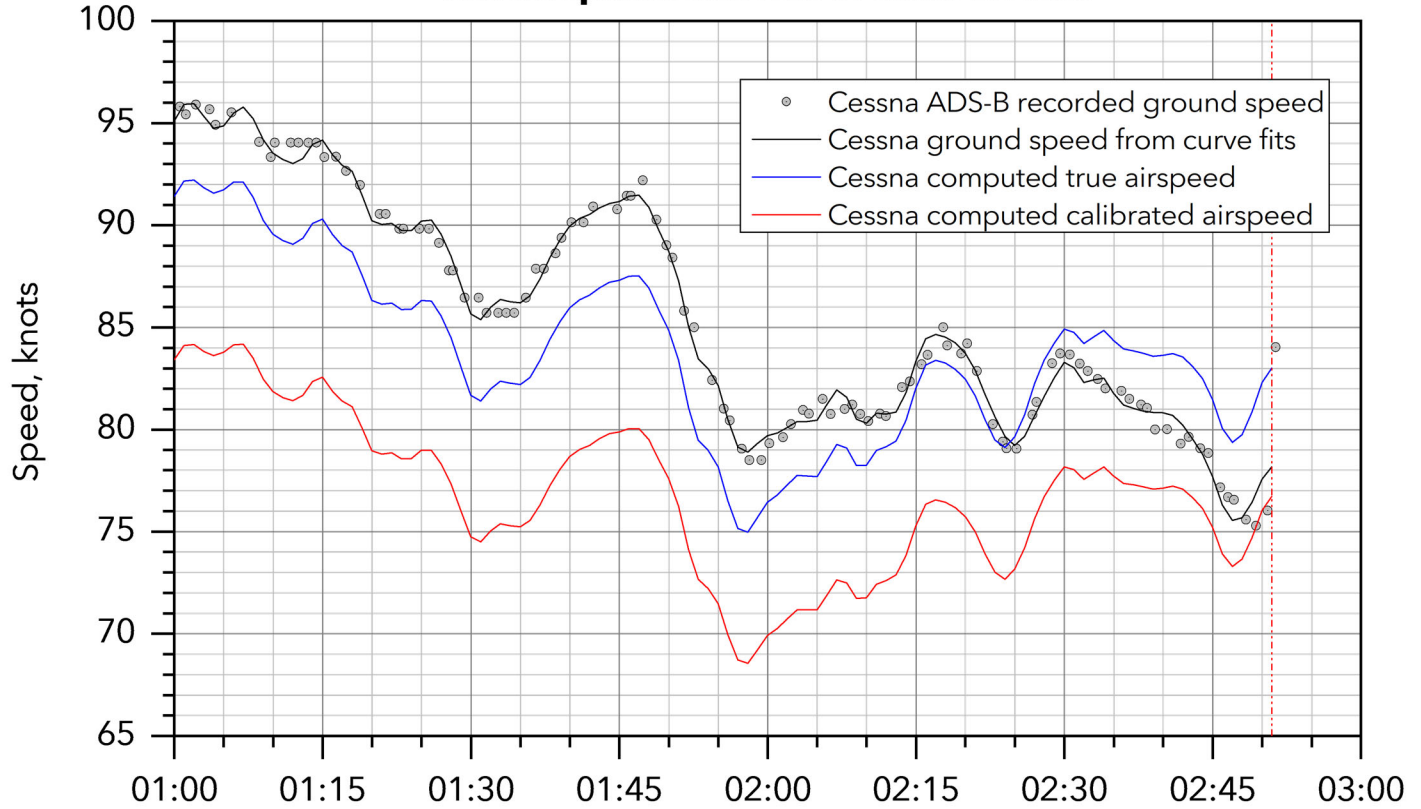
Figure 9.

**ERA22FA318: Midair collision, Piper PA46-350P N97CX / Cessna 172N N160RA
North Las Vegas, NV, 07/17/2022
Piper and Cessna separation and closure**
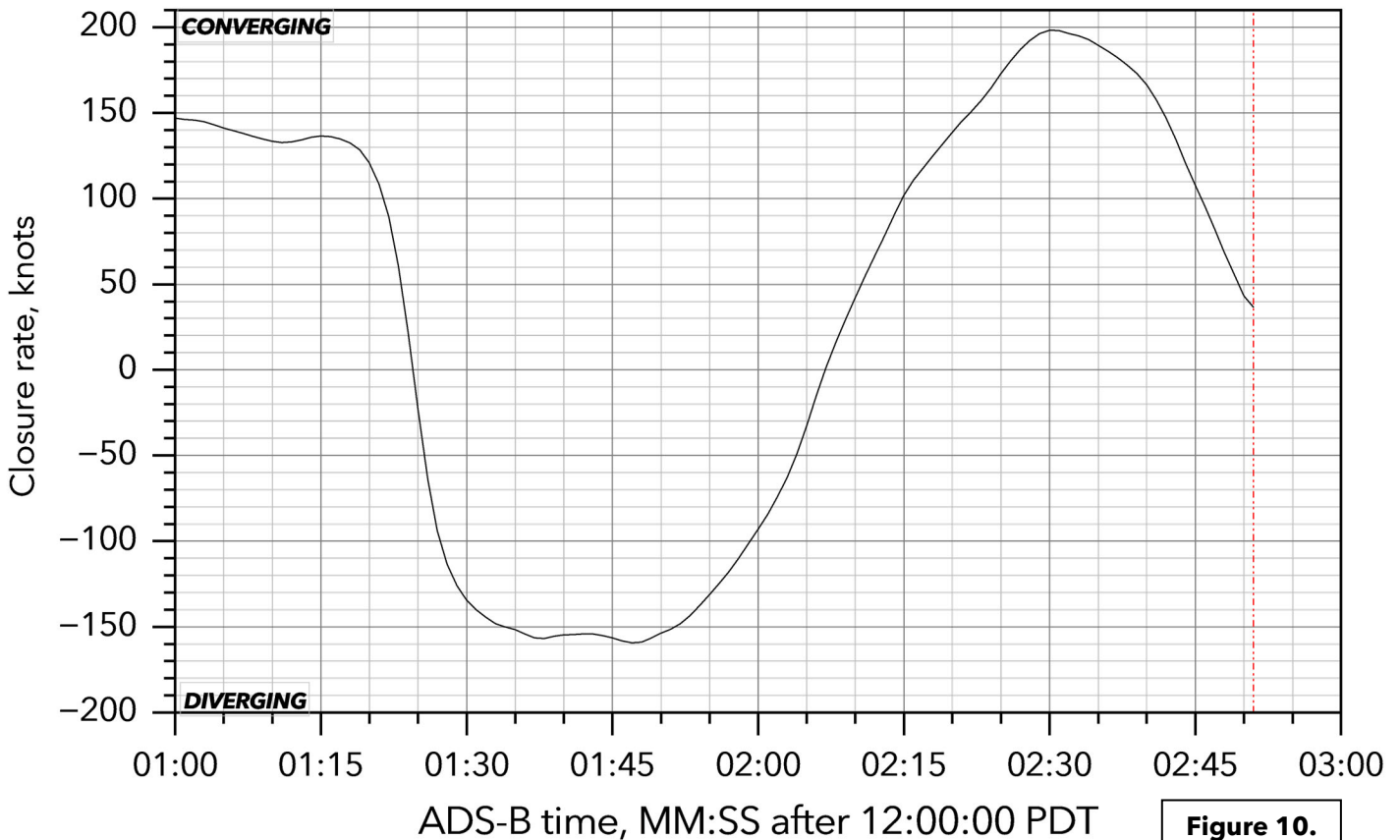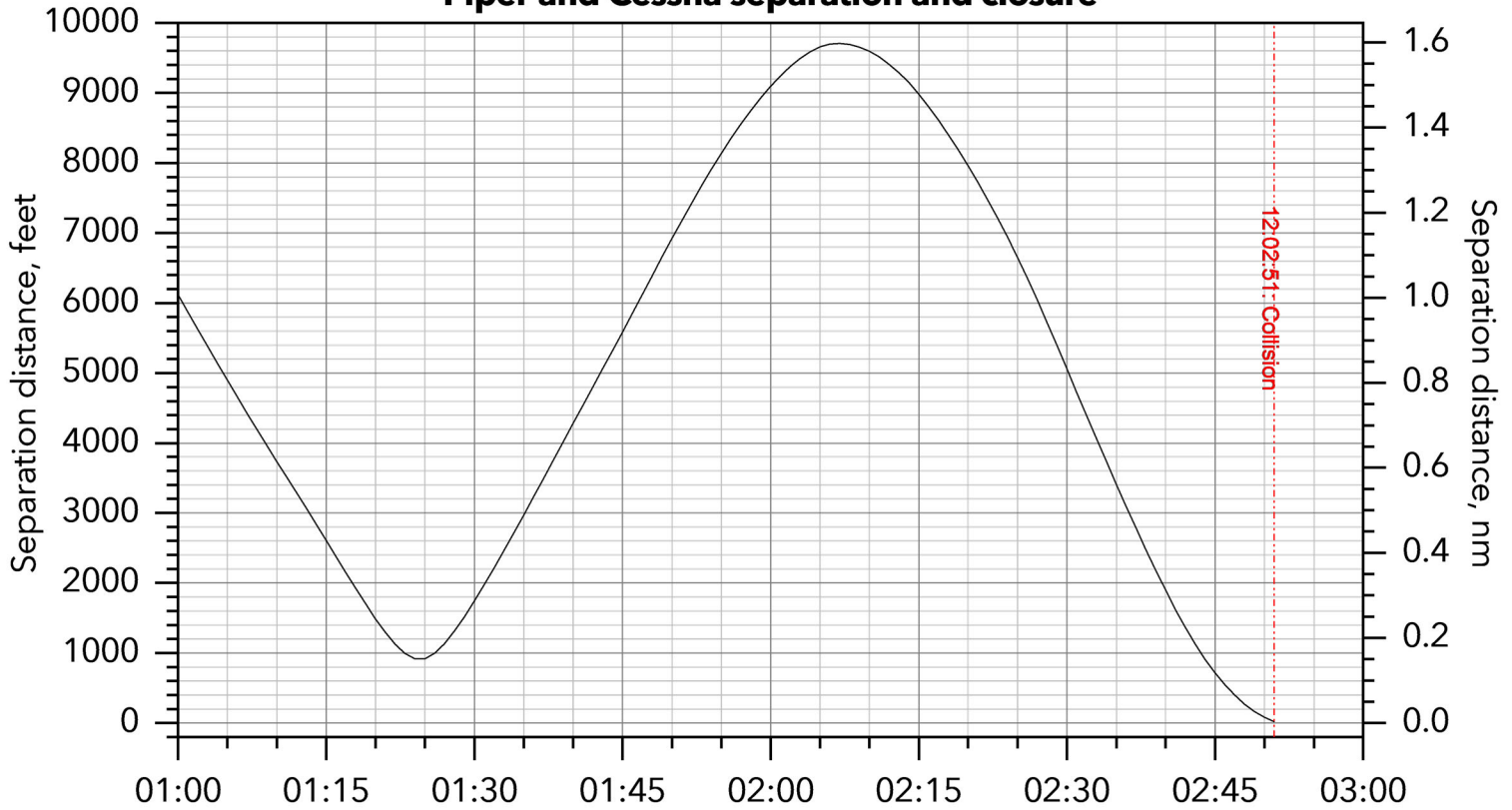
Figure 10.

AIRCRAFT PERFORMANCE & COCKPIT VISIBILITY STUDY

ERA22FA318: Midair collision, Piper PA46-350P N97CX / Cessna 172N N160RA North Las Vegas, NV, 07/17/2022
Piper and Cessna Euler angles
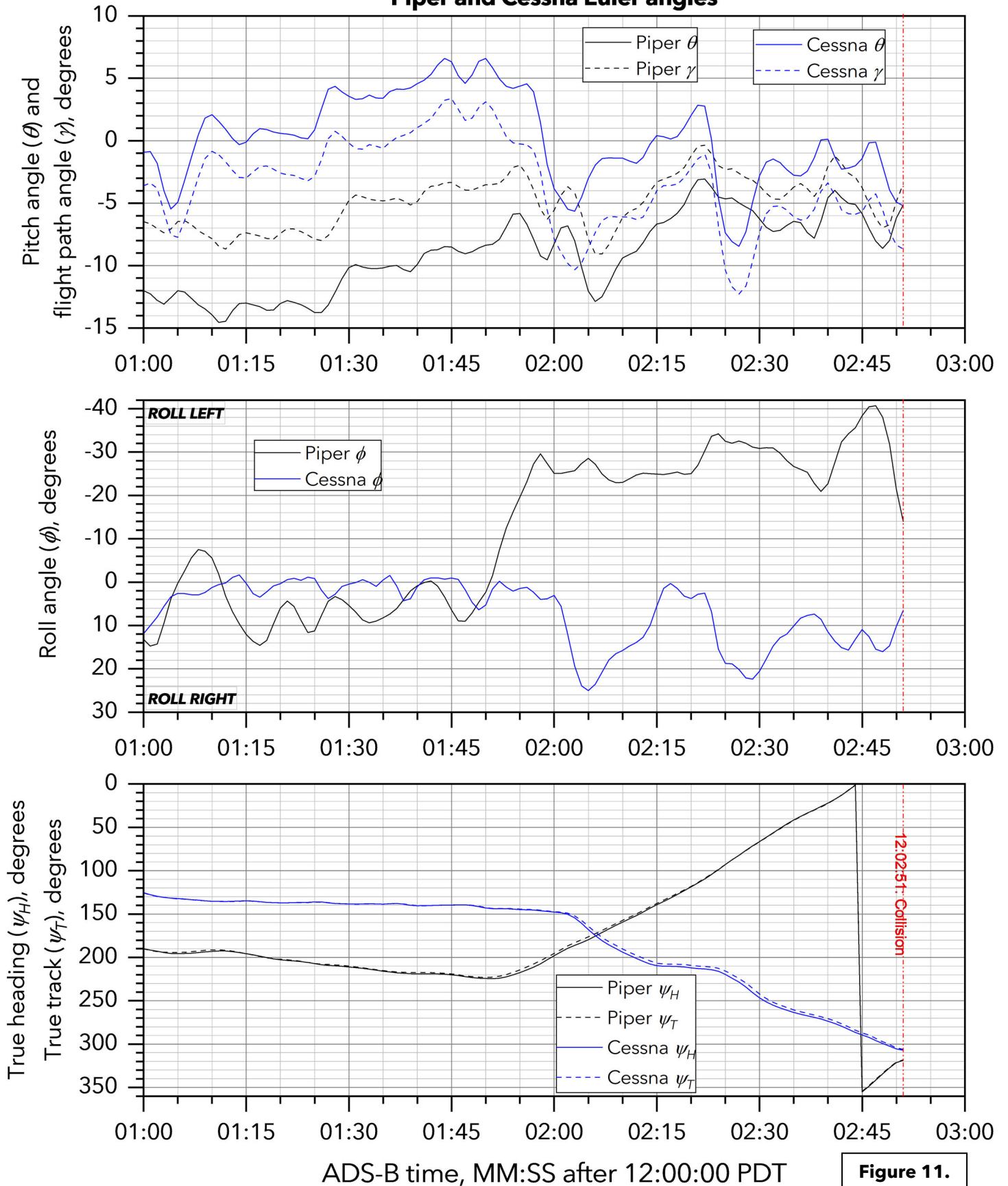
Figure 11.
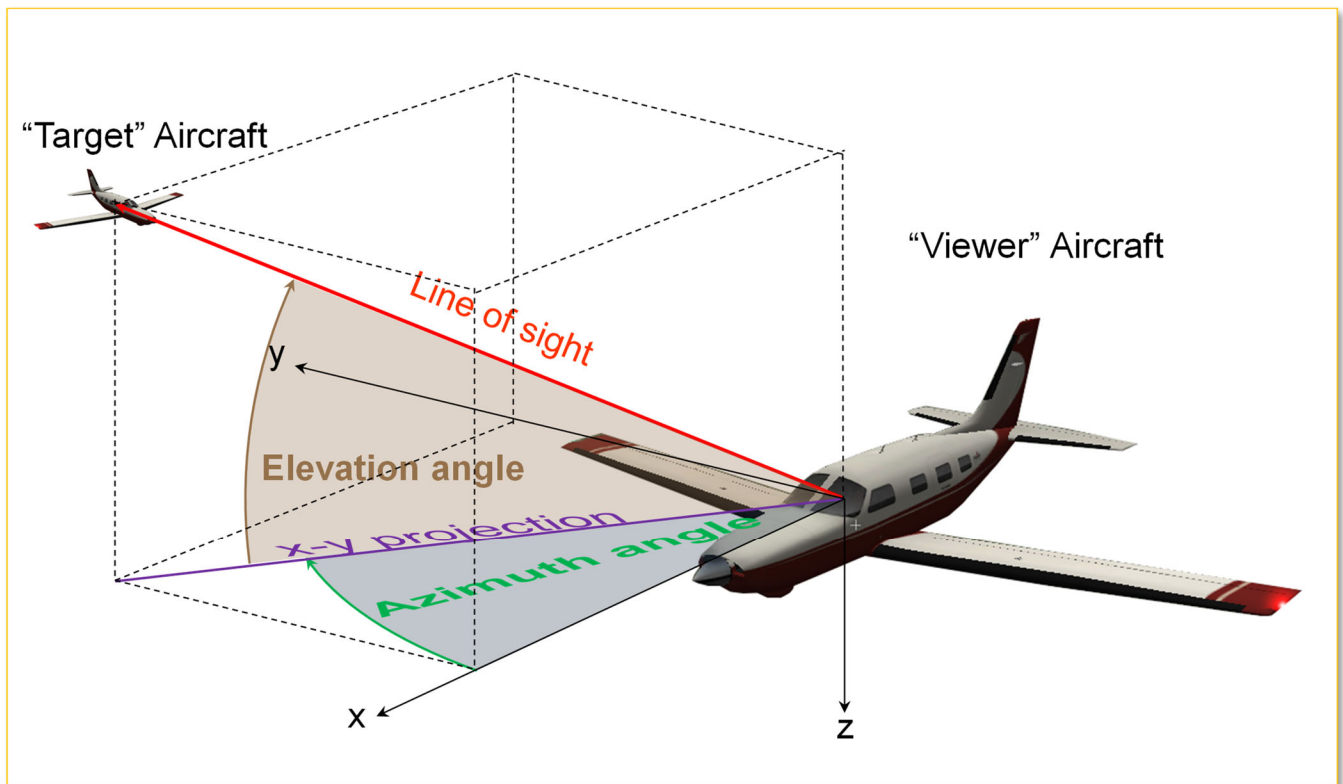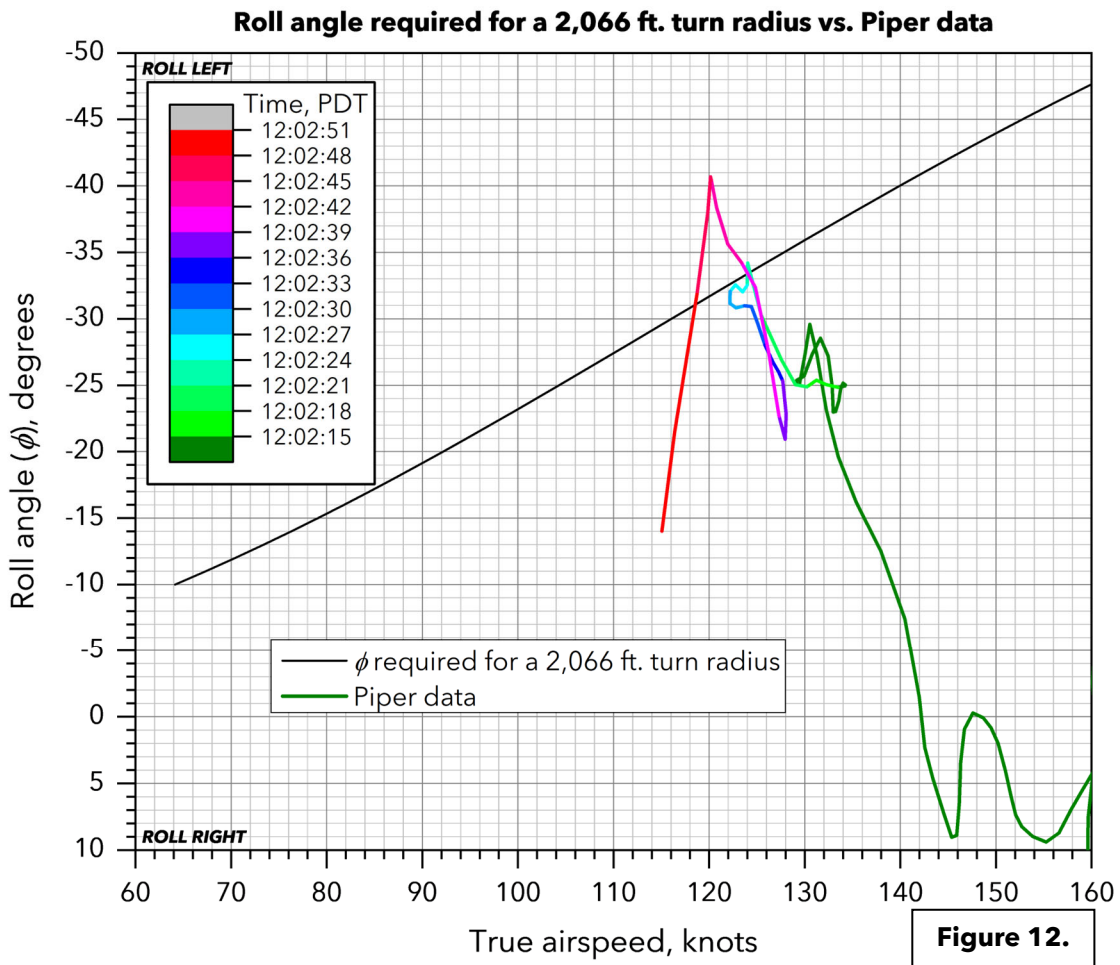
Figure 12.

Figure 13. Azimuth and elevation angles from "viewer" airplane to "target" airplane.

Piper and Cessna azimuth and elevation angles vs. time
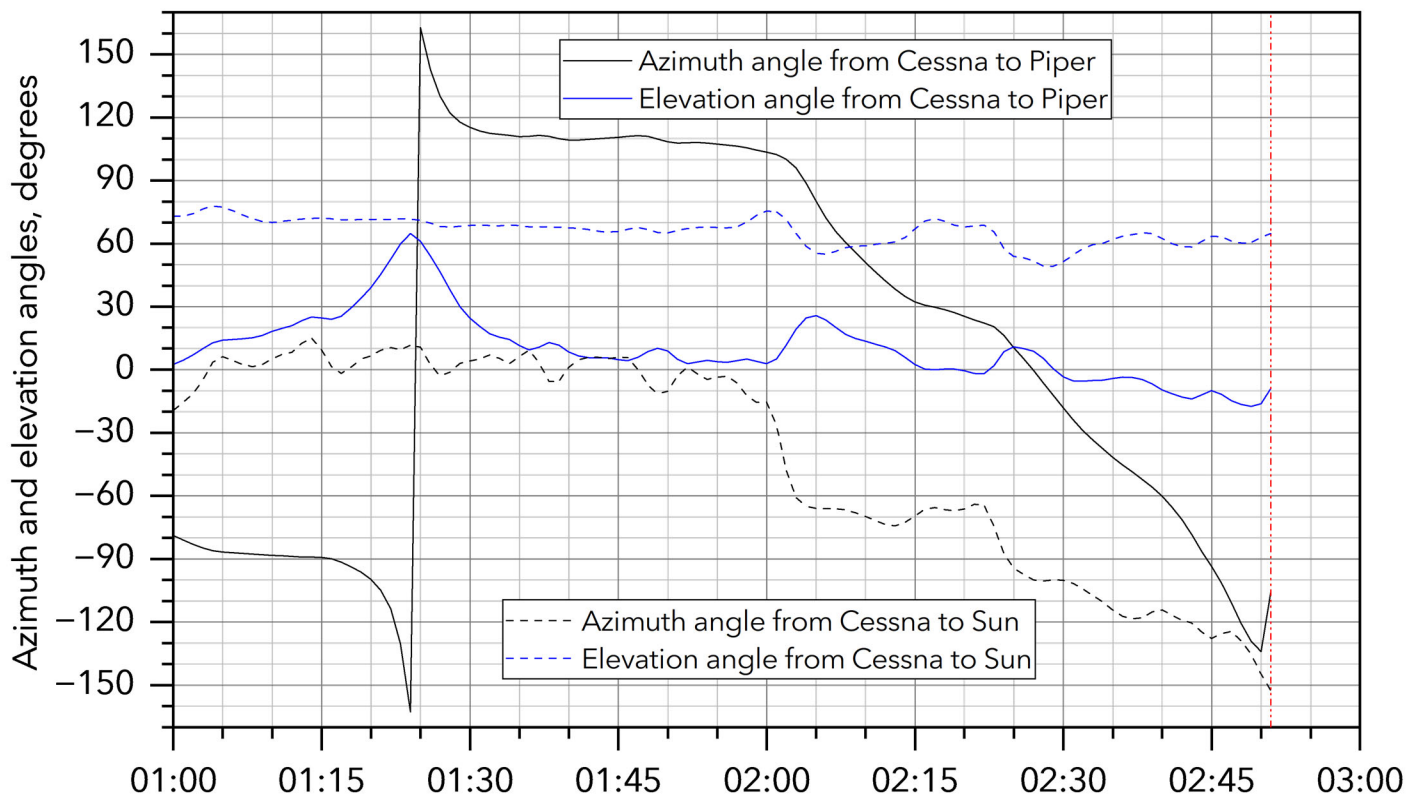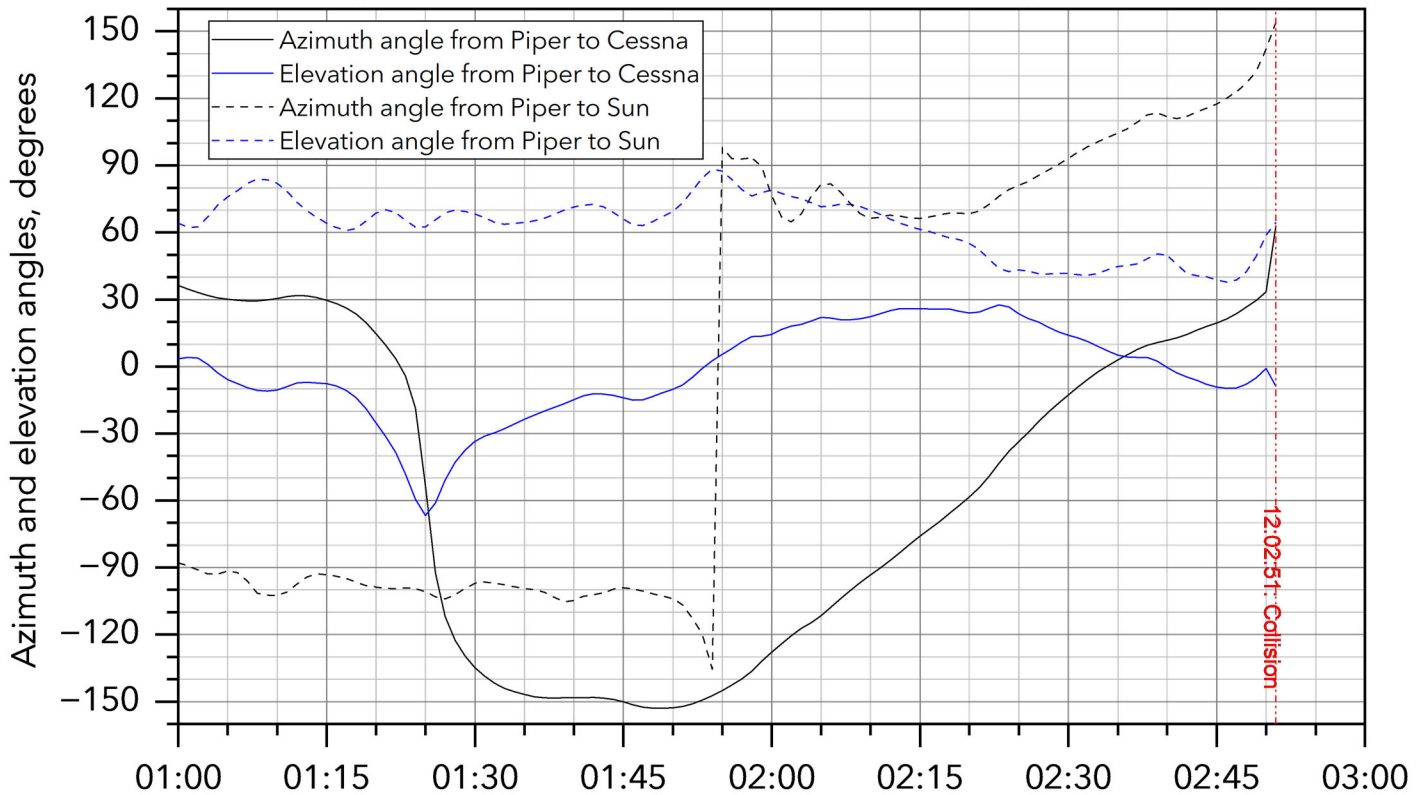
Figure 14.

Elevation vs. azimuth viewing angles from pilot seat of Piper to Cessna
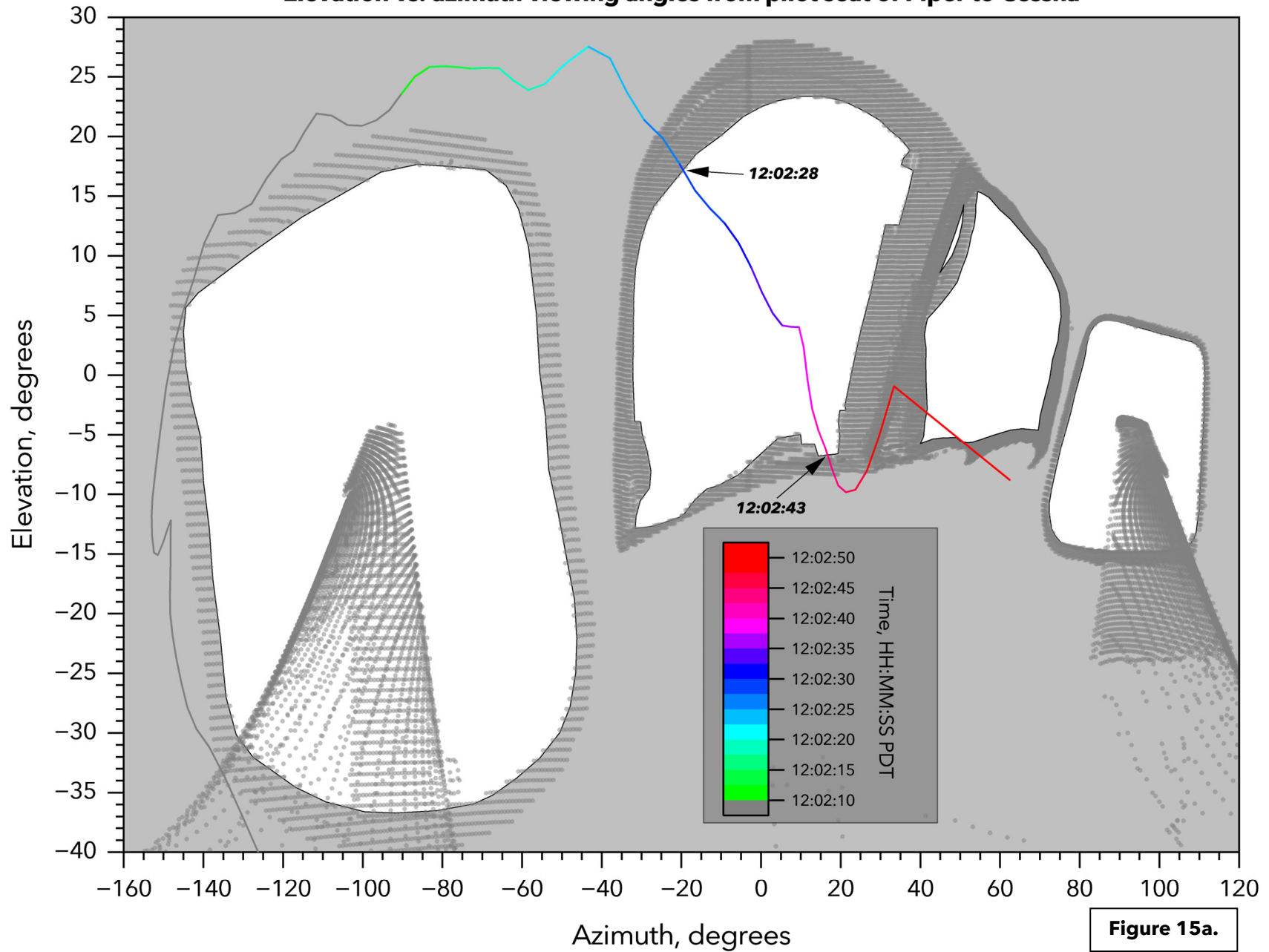
Figure 15a.

ERA22FA318: Midair collision, Piper PA46-350P N97CX / Cessna 172N N160RA
North Las Vegas, NV, 07/17/2022
Elevation vs. azimuth viewing angles from copilot seat of Piper to Cessna

12:02:26

12:02:49

Time, HH:MM:SS PDT

- 12:02:50
- 12:02:45
- 12:02:40
- 12:02:35
- 12:02:30
- 12:02:25
- 12:02:20
- 12:02:15
- 12:02:10

Elevation, degrees

Azimuth, degrees
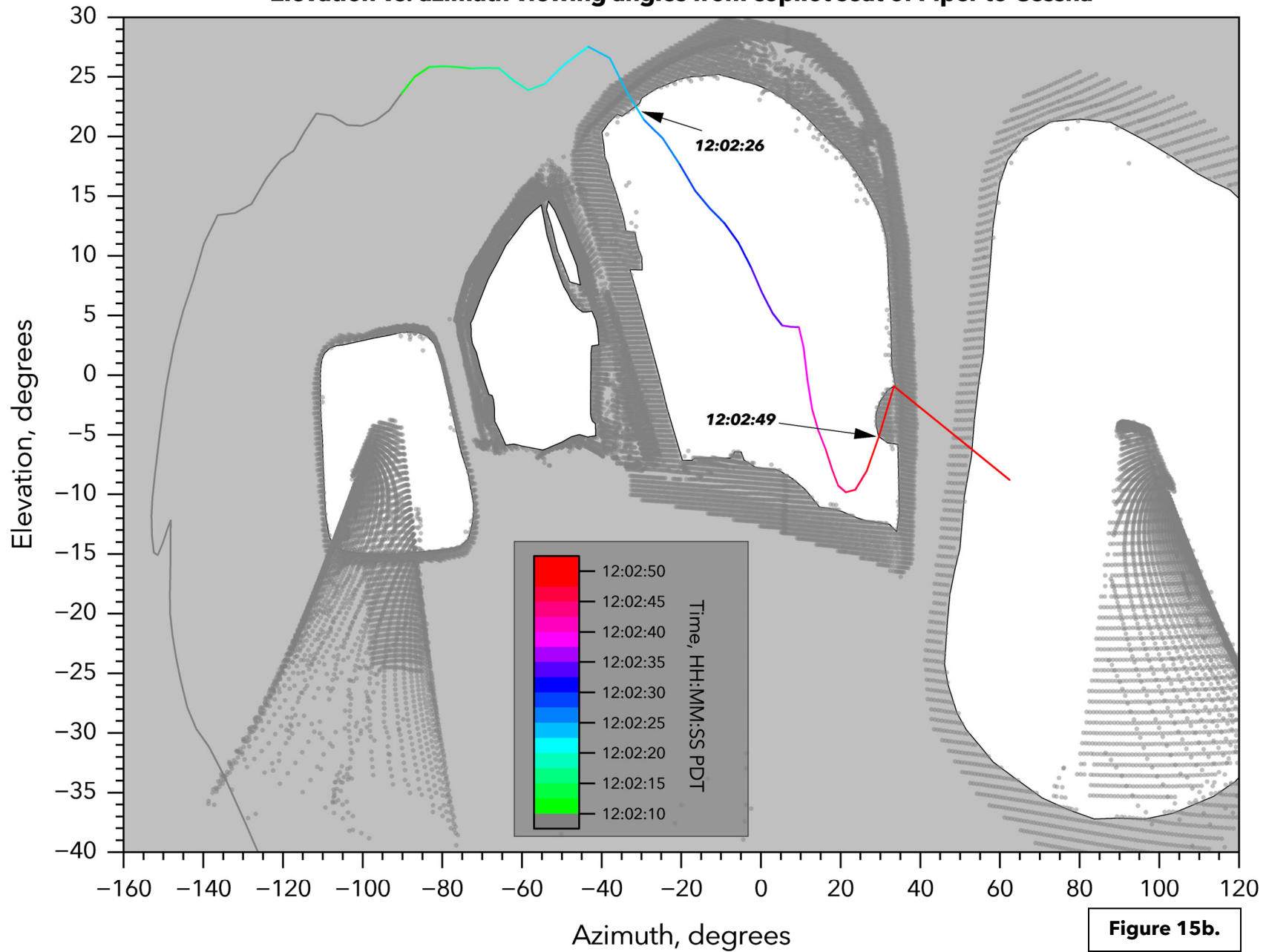
Figure 15b.

ERA22FA318: Midair collision, Piper PA46-350P N97CX / Cessna 172N N160RA
North Las Vegas, NV, 07/17/2022
Elevation vs. azimuth viewing angles from pilot seat of Cessna to Piper
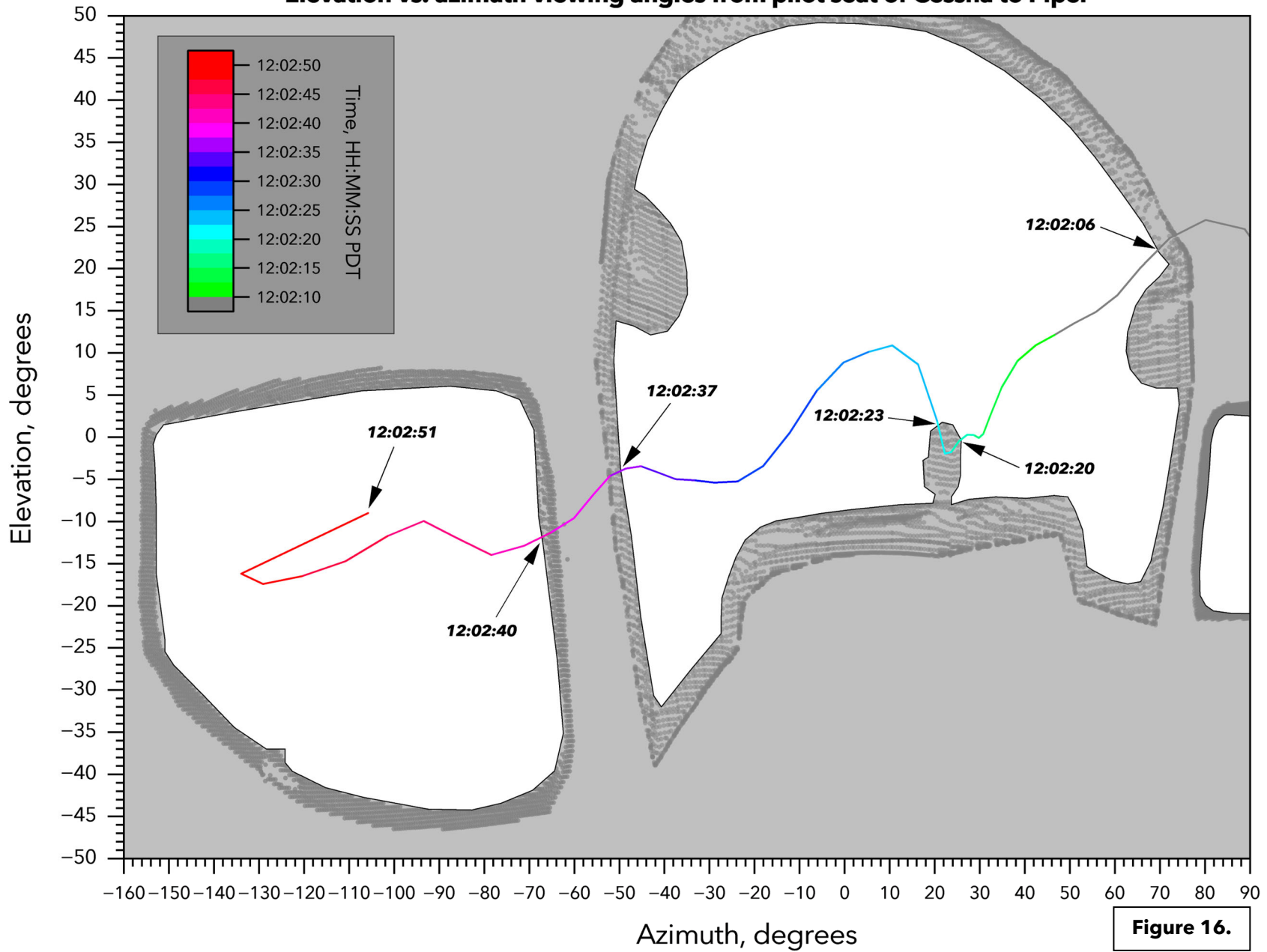
Figure 16.
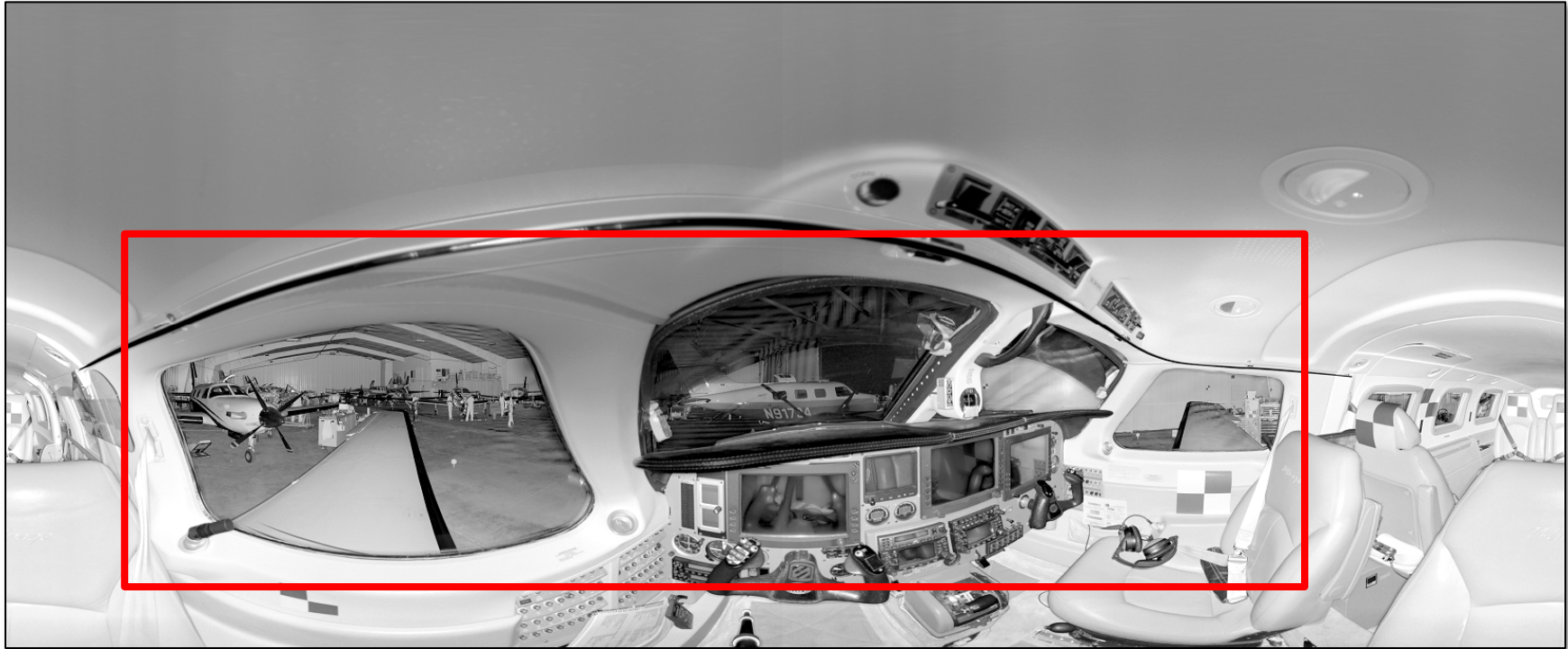
Figure 17a. Image of the 360° laser scan from the left seat of the exemplar Piper PA-46-350P JetProp DLX. The red box highlights the area depicted in Figure 15a.
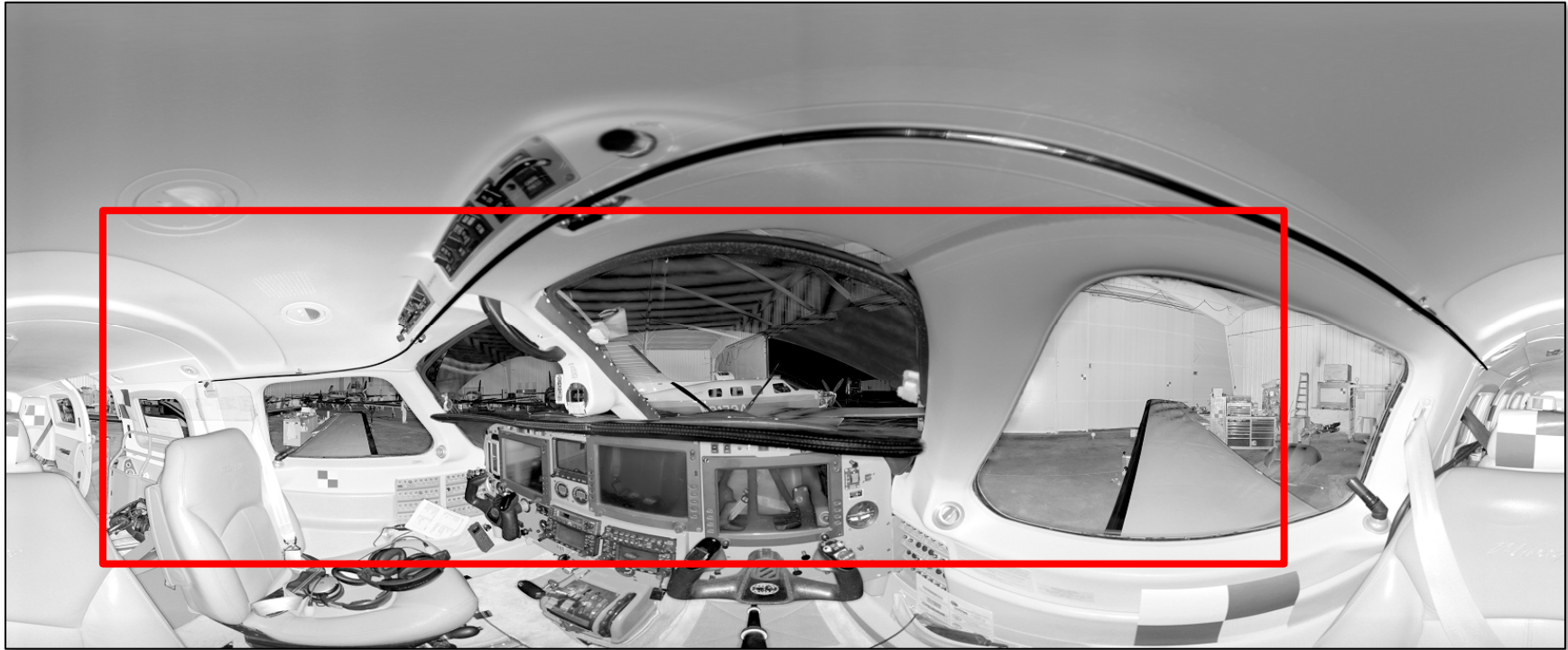
Figure 17b. Image of the 360° laser scan from the right seat of the exemplar Piper PA-46-350P JetProp DLX. The red box highlights the area depicted in Figure 15b.

Figure 18. Image of the 360° laser scan from the left seat of the exemplar Cessna 172. The red box highlights the area depicted in Figure 16.
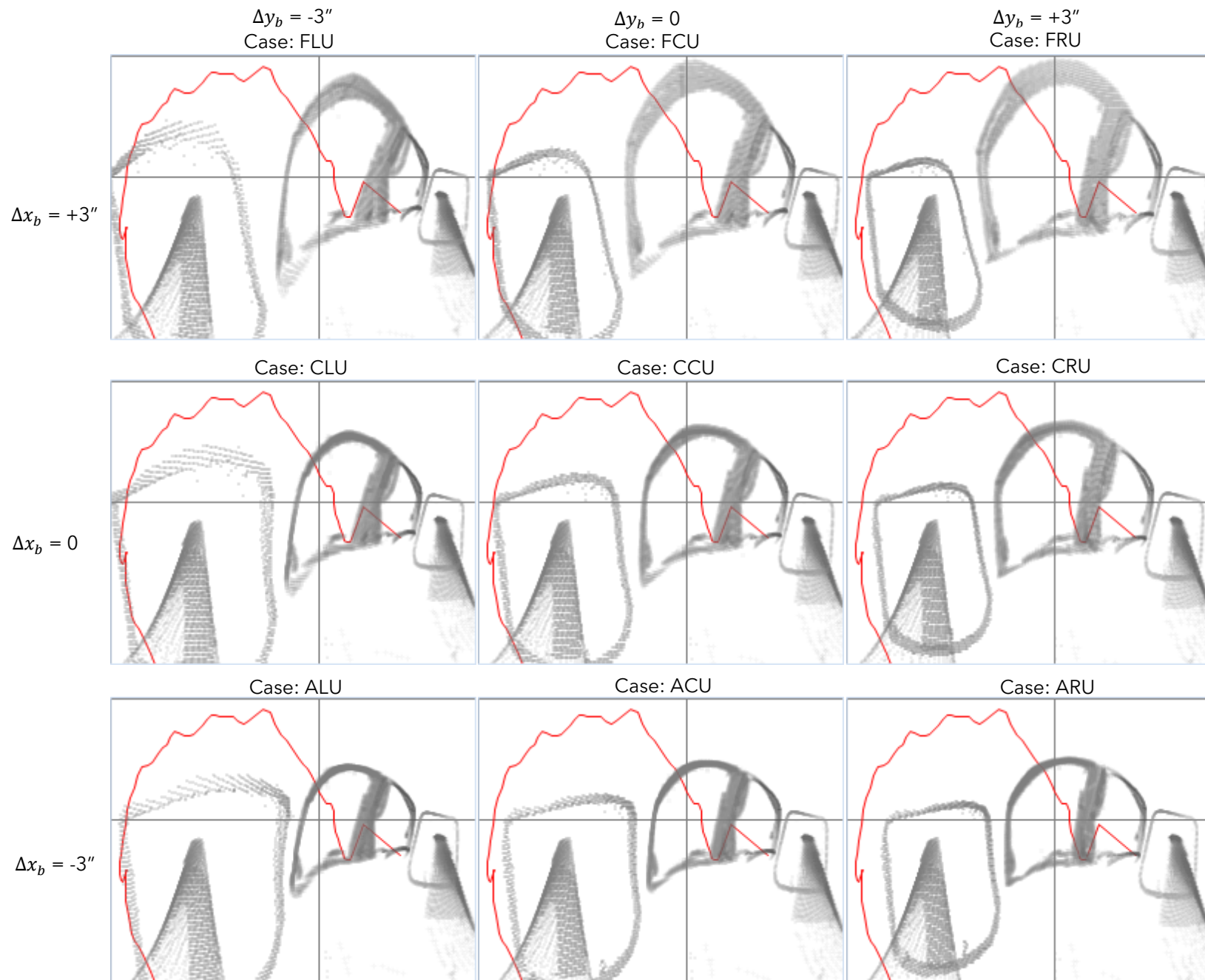
Figure 19a. Viewing angles for the Piper pilot seat at Δz_b = -1.5″ (i.e., up). Plots are elevation angle vs. azimuth angle.
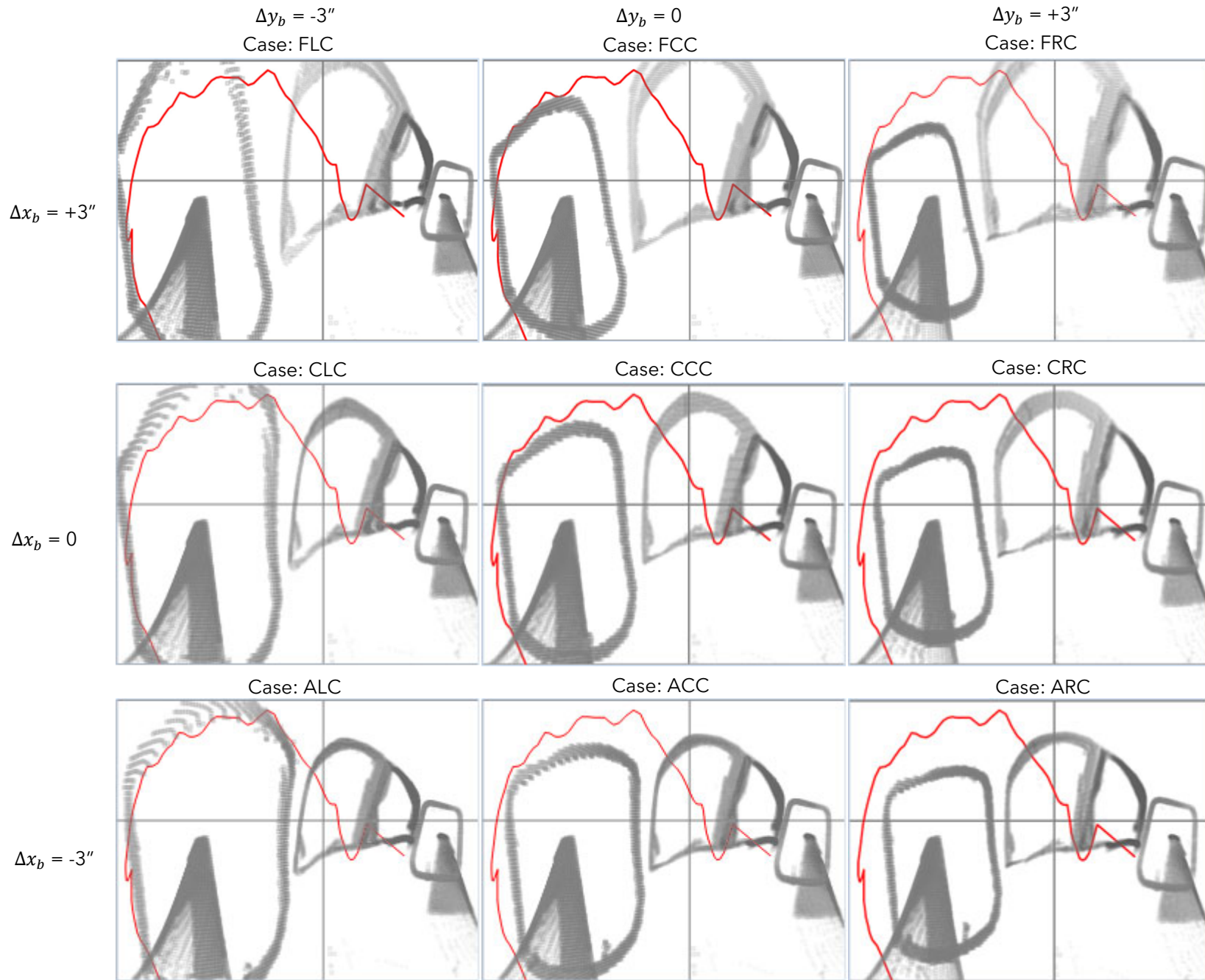
Figure 19b. Viewing angles for the Piper pilot seat at $\Delta z_b = 0$. Plots are elevation angle vs. azimuth angle.
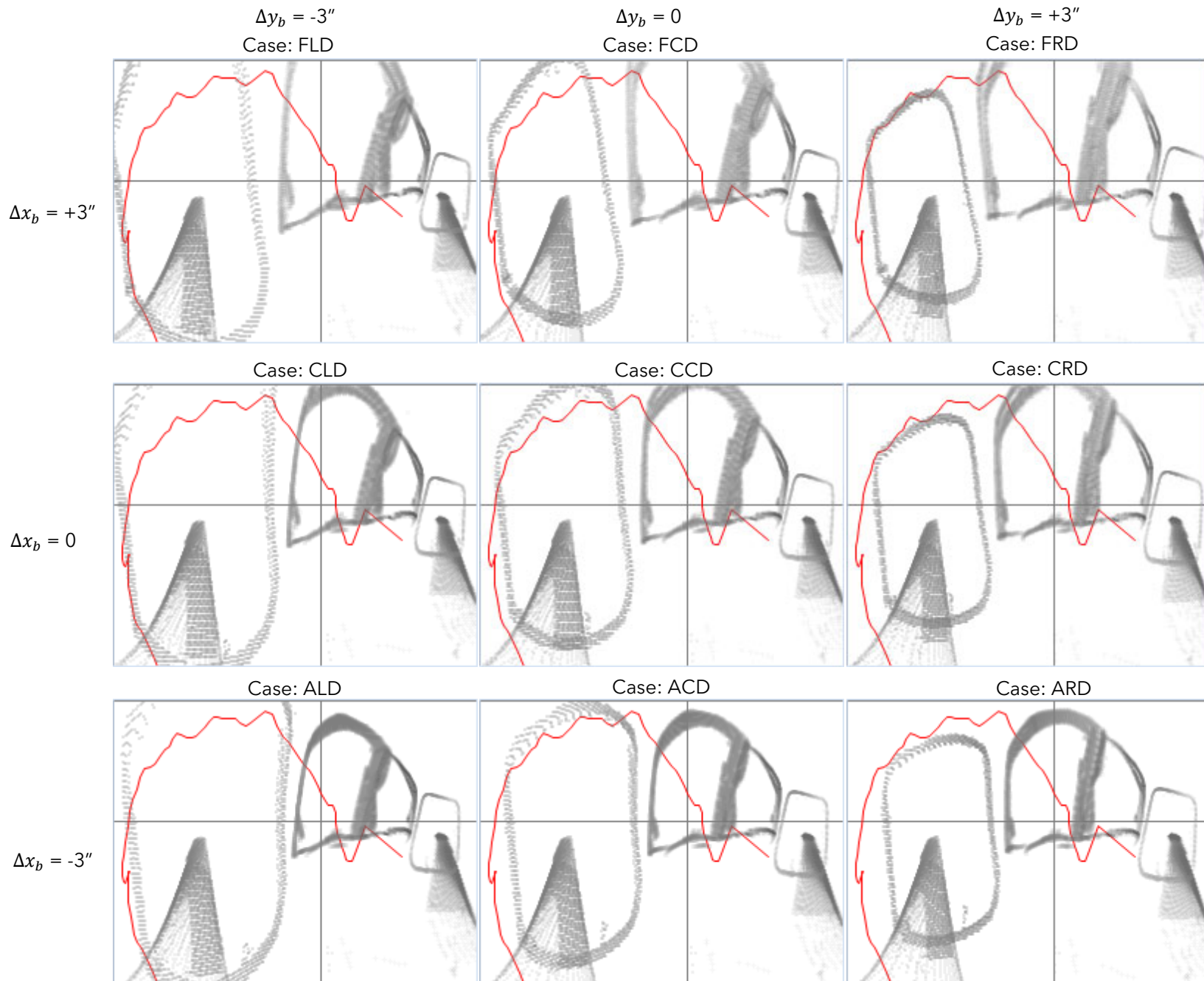
Figure 19c. Viewing angles for the Piper pilot seat at Δz_b = +1.5″ (i.e., down). Plots are elevation angle vs. azimuth angle.

AIRCRAFT PERFORMANCE & COCKPIT VISIBILITY STUDY

$\Delta y_b = -3''$
Case: FLU

$\Delta y_b = 0$
Case: FCU

$\Delta y_b = +3''$
Case: FRU

$\Delta x_b = +3''$

Case: CLU

Case: CCU

Case: CRU

$\Delta x_b = 0$

Case: ALU

Case: ACU

Case: ARU

$\Delta x_b = -3''$

Figure 20a. Viewing angles for the Piper copilot seat at $\Delta z_b = -1.5''$ (i.e., up). Plots are elevation angle vs. azimuth angle.

AIRCRAFT PERFORMANCE & COCKPIT VISIBILITY STUDY

$\Delta y_b = -3''$
Case: FLC

$\Delta y_b = 0$
Case: FCC

$\Delta y_b = +3''$
Case: FRC

$\Delta x_b = +3''$

Case: CLC

Case: CCC

Case: CRC

$\Delta x_b = 0$

Case: ALC

Case: ACC

Case: ARC

$\Delta x_b = -3''$
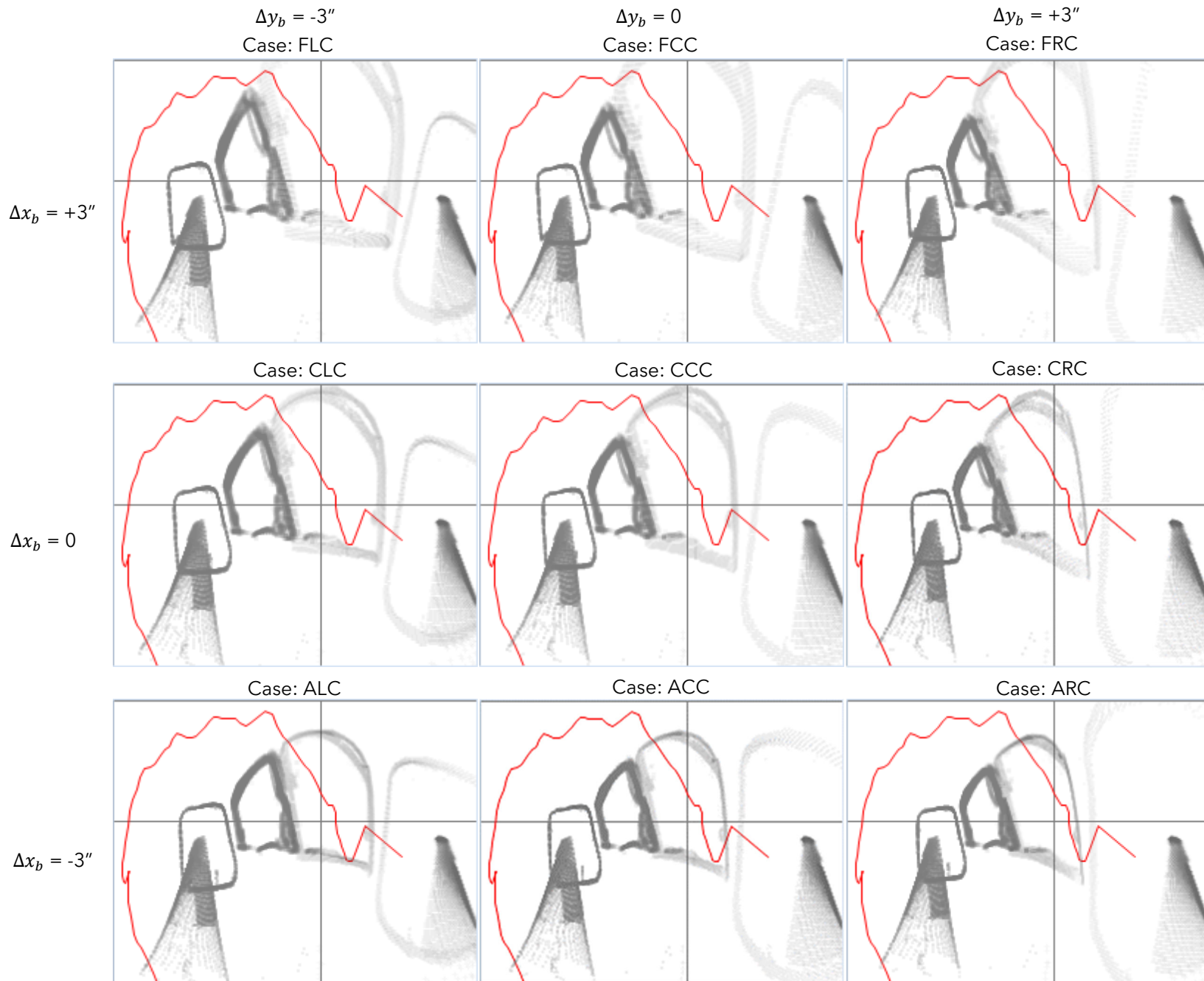
Figure 20b. Viewing angles for the Piper copilot seat at $\Delta z_b = 0$. Plots are elevation angle vs. azimuth angle.

$\Delta y_b = -3''$	$\Delta y_b = 0$	$\Delta y_b = +3''$
Case: FLD	Case: FCD	Case: FRD
Case: CLD	Case: CCD	Case: CRD
Case: ALD	Case: ACD	Case: ARD

$\Delta x_b = +3''$

$\Delta x_b = 0$

$\Delta x_b = -3''$
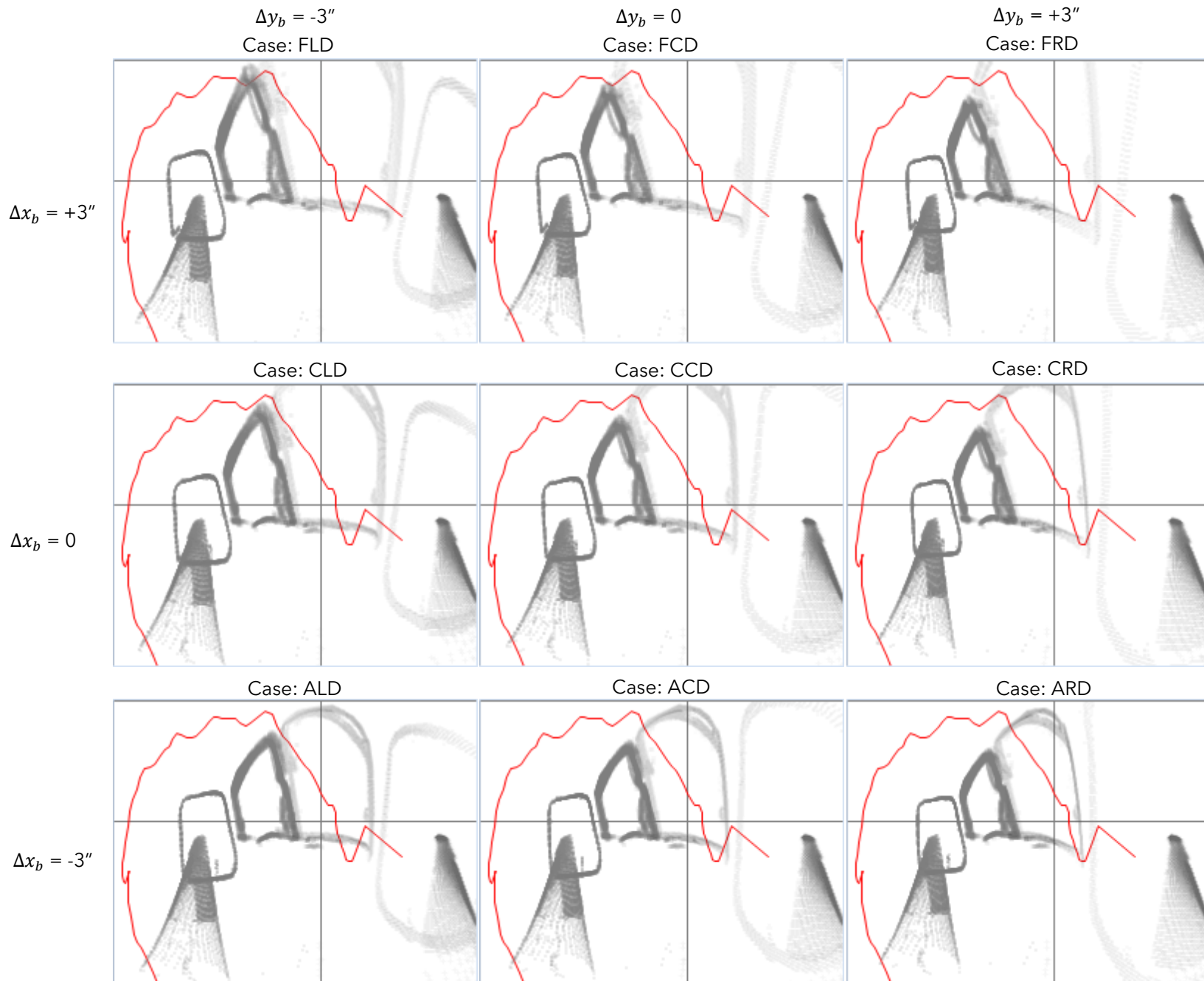
Figure 20c. Viewing angles for the Piper copilot seat at $\Delta z_b = +1.5''$ (i.e., down). Plots are elevation angle vs. azimuth angle.

AIRCRAFT PERFORMANCE & COCKPIT VISIBILITY STUDY

| $\Delta y_b = -3''$ | $\Delta y_b = 0$ | $\Delta y_b = +3''$ |
| Case: FLU | Case: FCU | Case: FRU |

$\Delta x_b = +3''$

| Case: CLU | Case: CCU | Case: CRU |

$\Delta x_b = 0$

| Case: ALU | Case: ACU | Case: ARU |

$\Delta x_b = -3''$
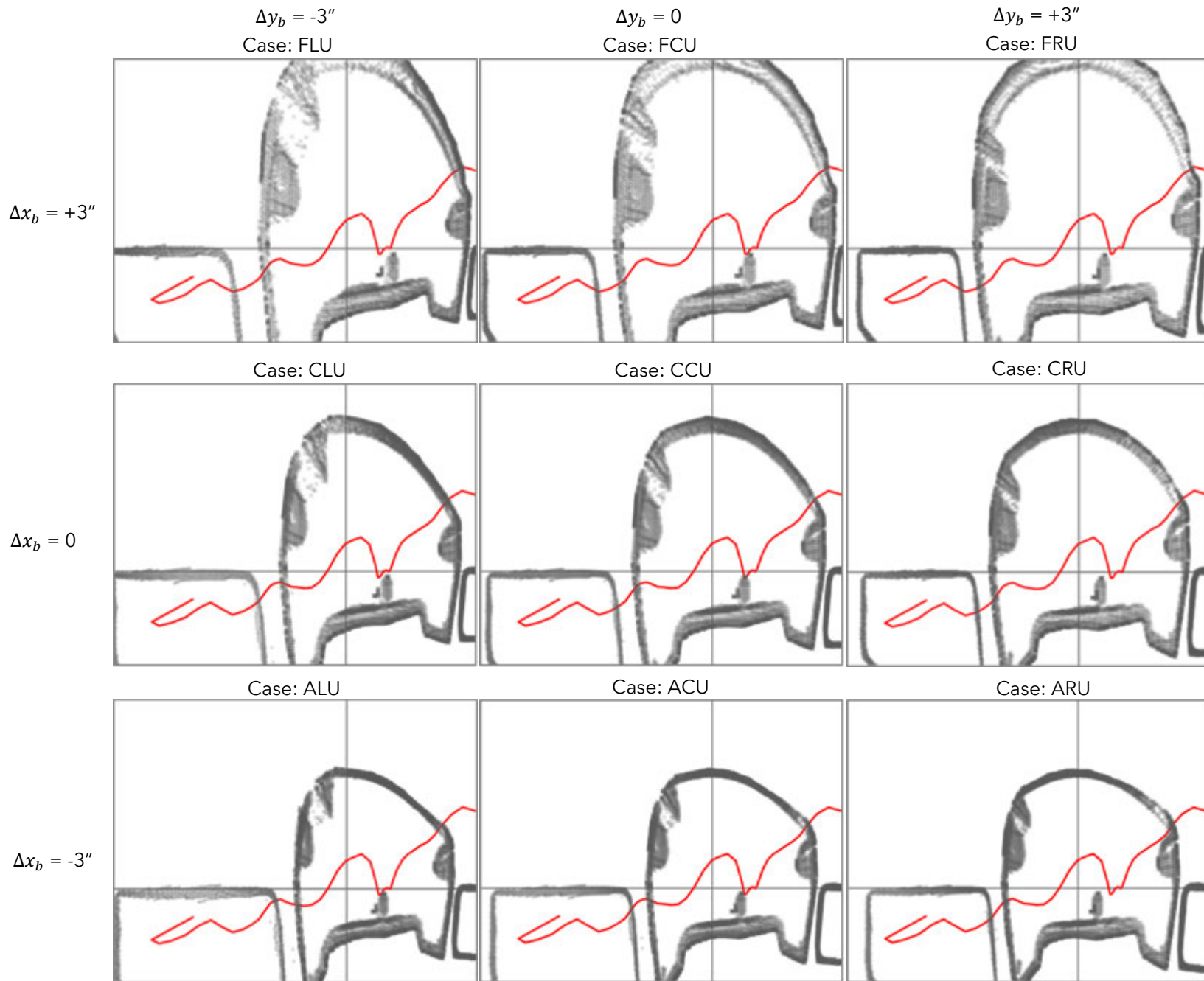
Figure 21a. Viewing angles for the Cessna pilot seat at $\Delta z_b = -1.5''$ (i.e., up). Plots are elevation angle vs. azimuth angle.
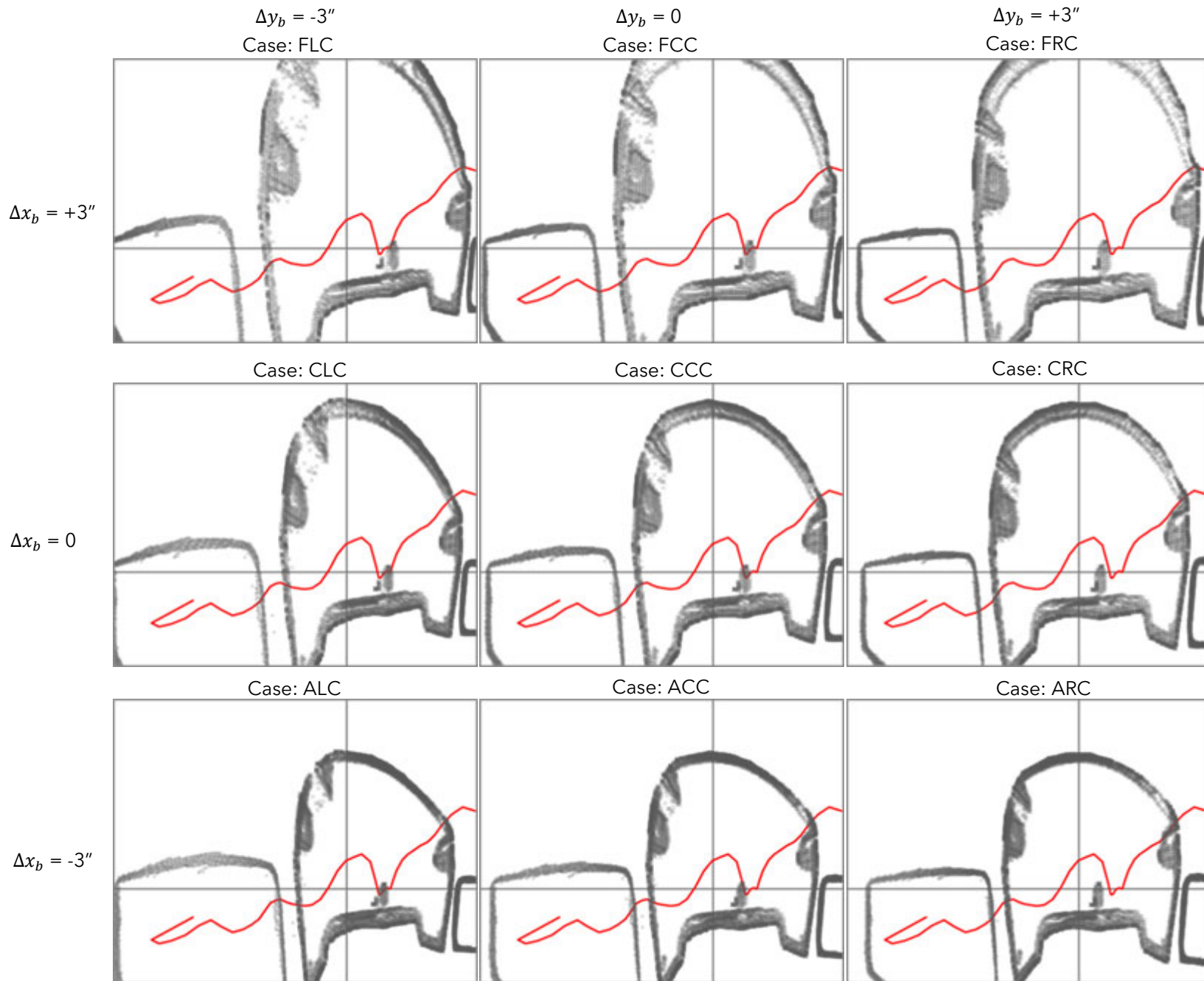
Figure 21b. Viewing angles for the Cessna pilot seat at Δz_b =0. Plots are elevation angle vs. azimuth angle.
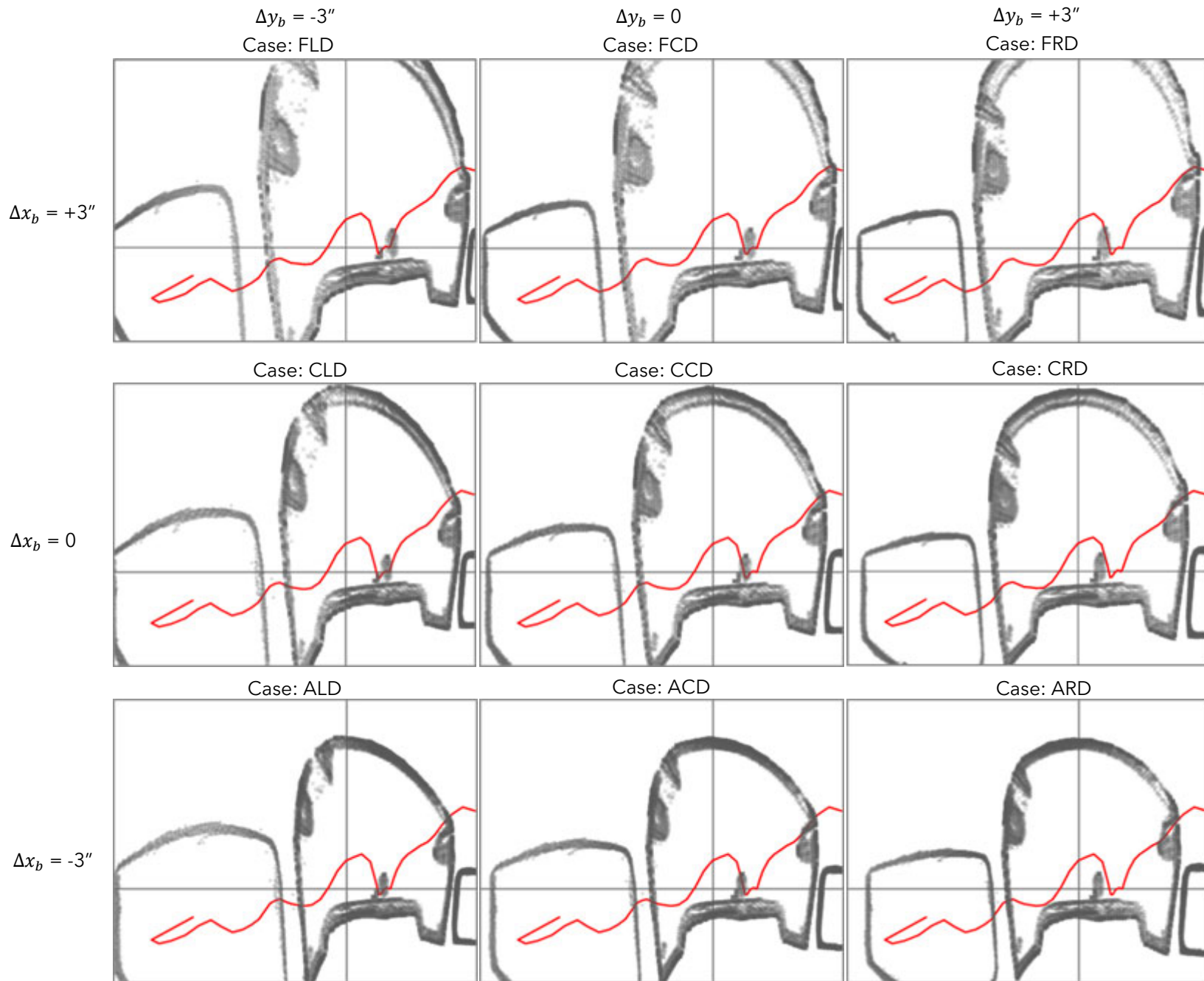
Figure 21c. Viewing angles for the Cessna pilot seat at Δz_b = +1.5″ (i.e., down). Plots are elevation angle vs. azimuth angle.
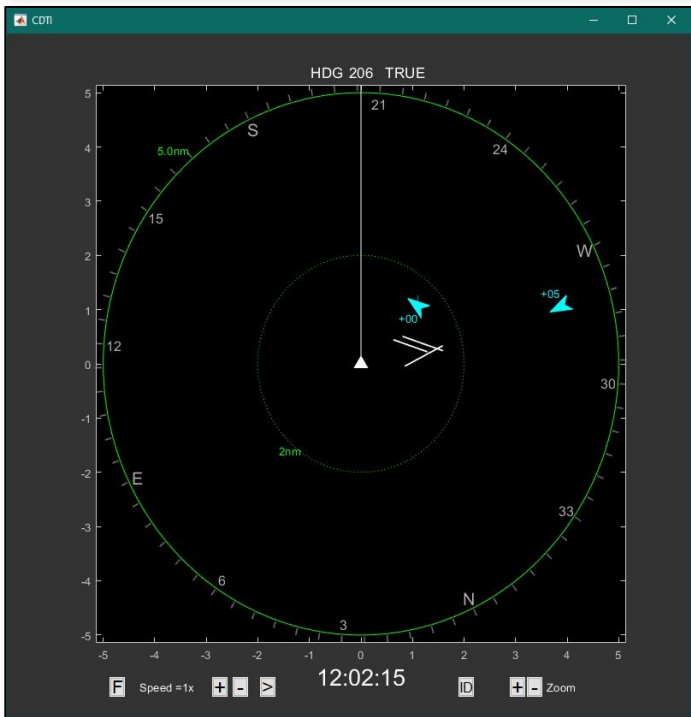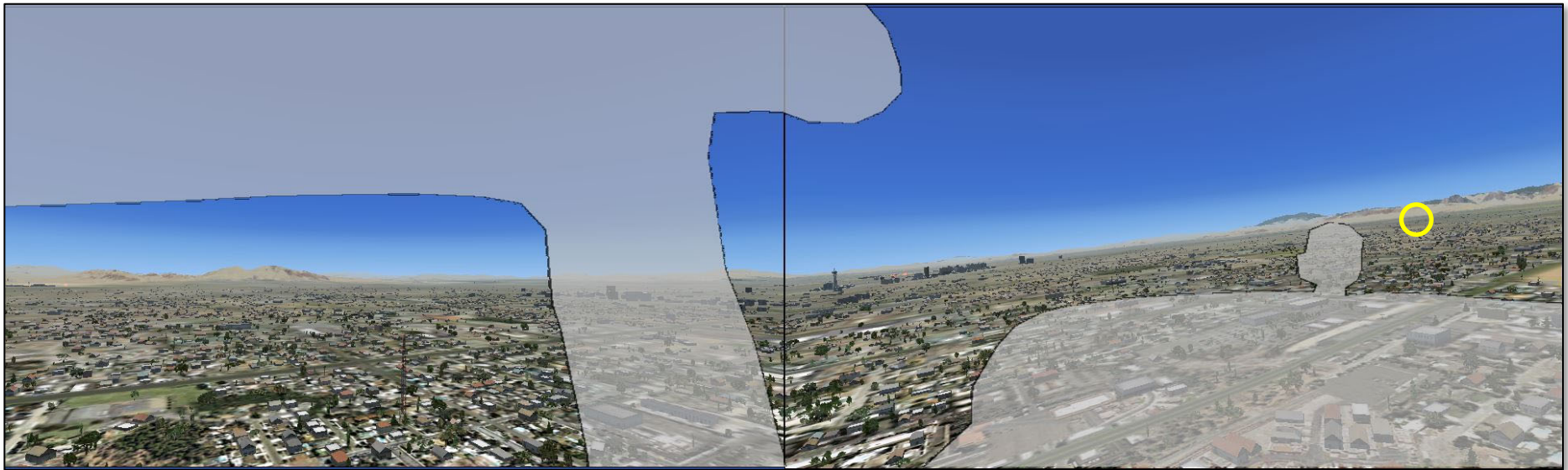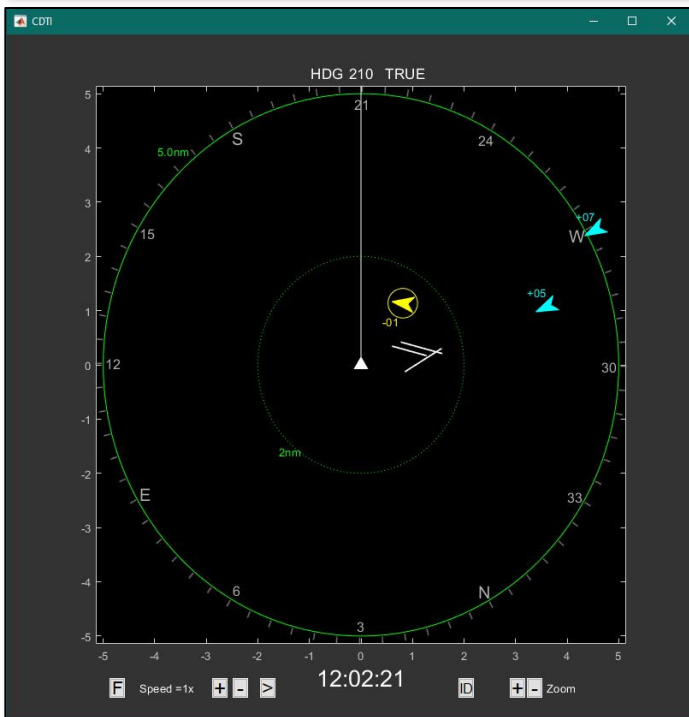
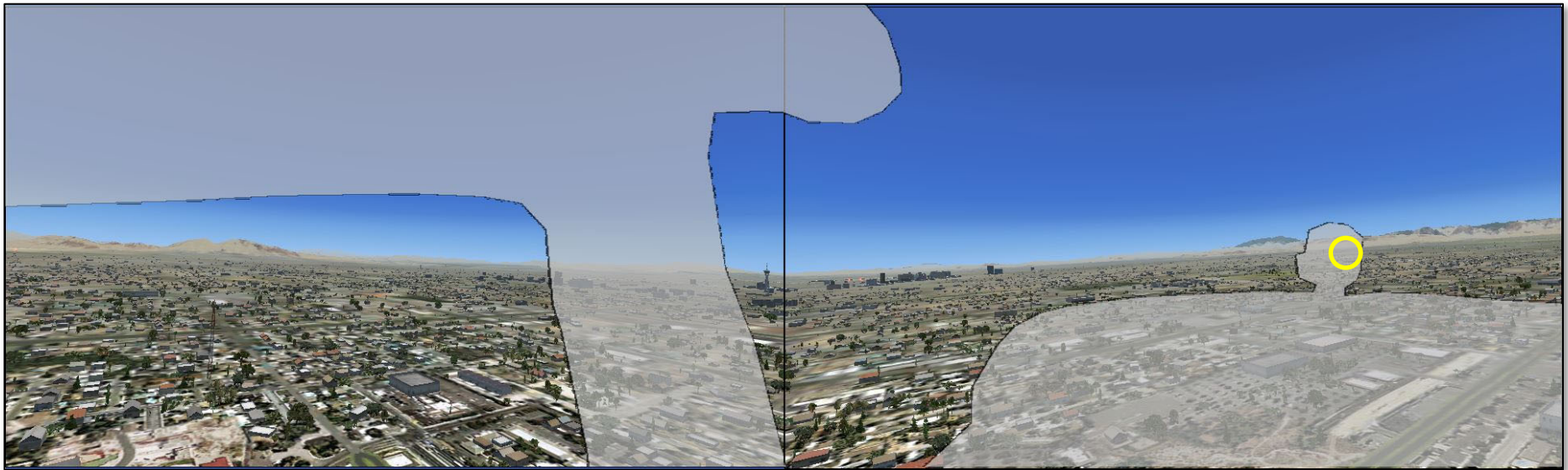**Figure 22a.** Simulated CDTI display and view from the Piper pilot seat at 12:02:15 (36 seconds before the collision). The Cessna is located in the yellow circle.
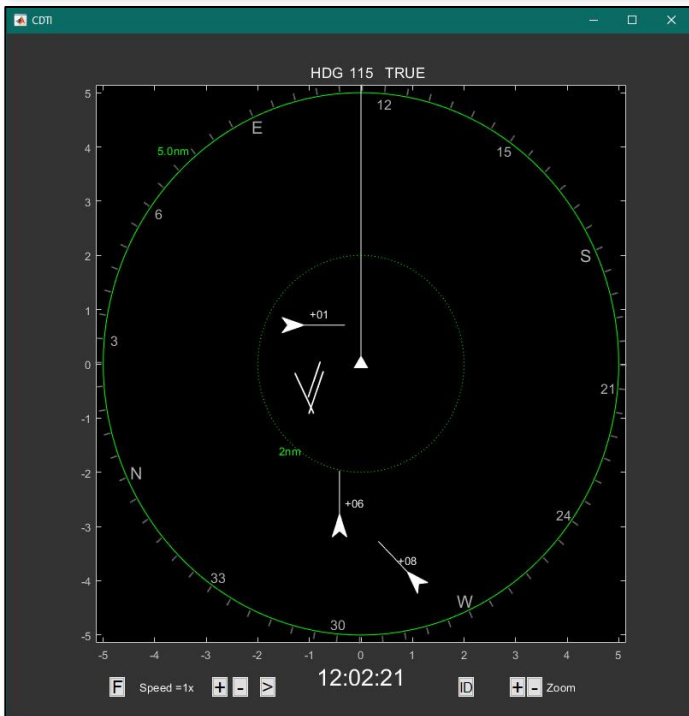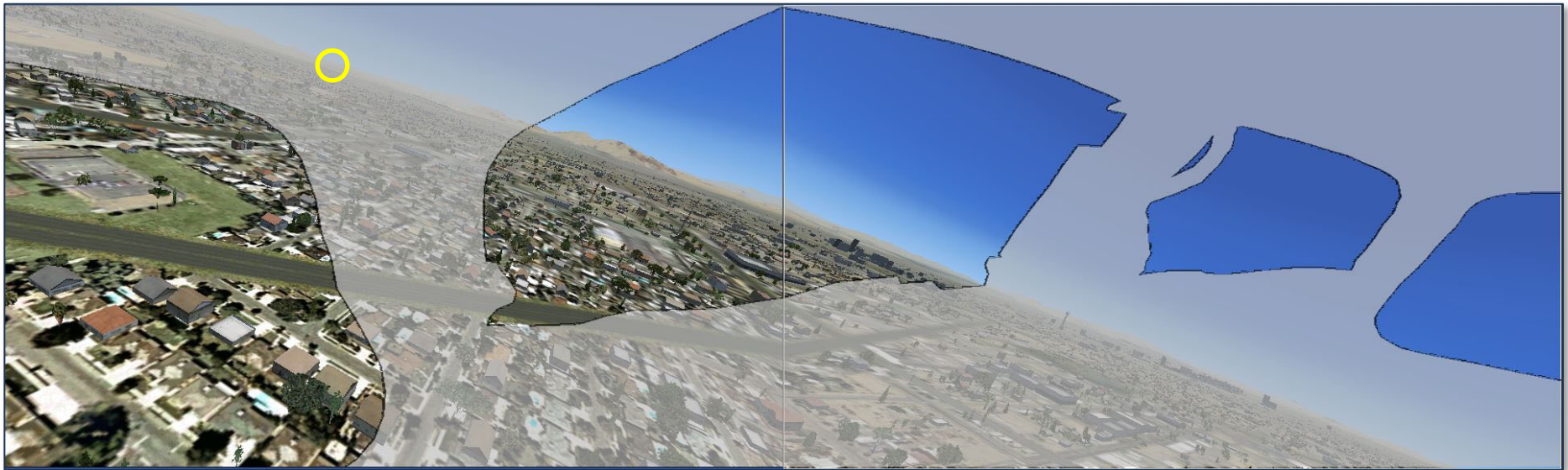
Figure 22b. Simulated CDTI display and view from the Piper pilot seat at 12:02:21 (30 seconds before the collision). The Cessna is located in the yellow circle.
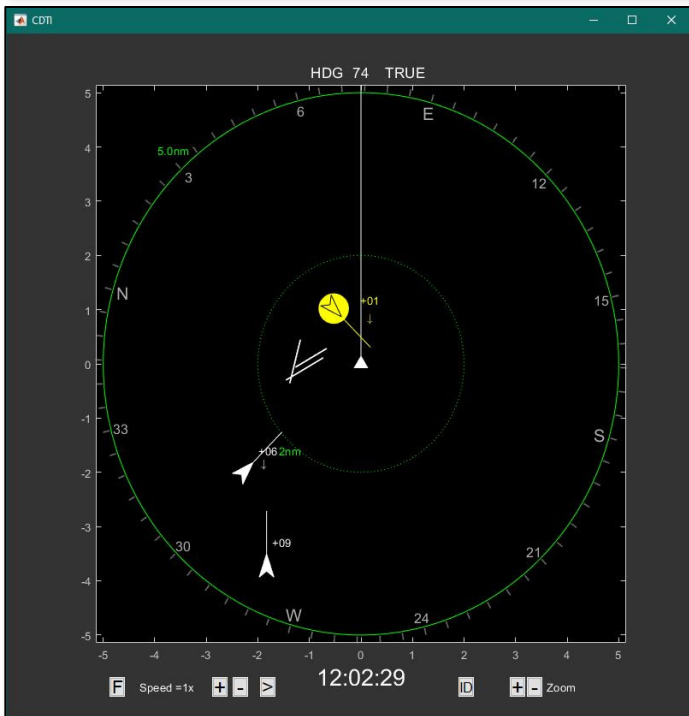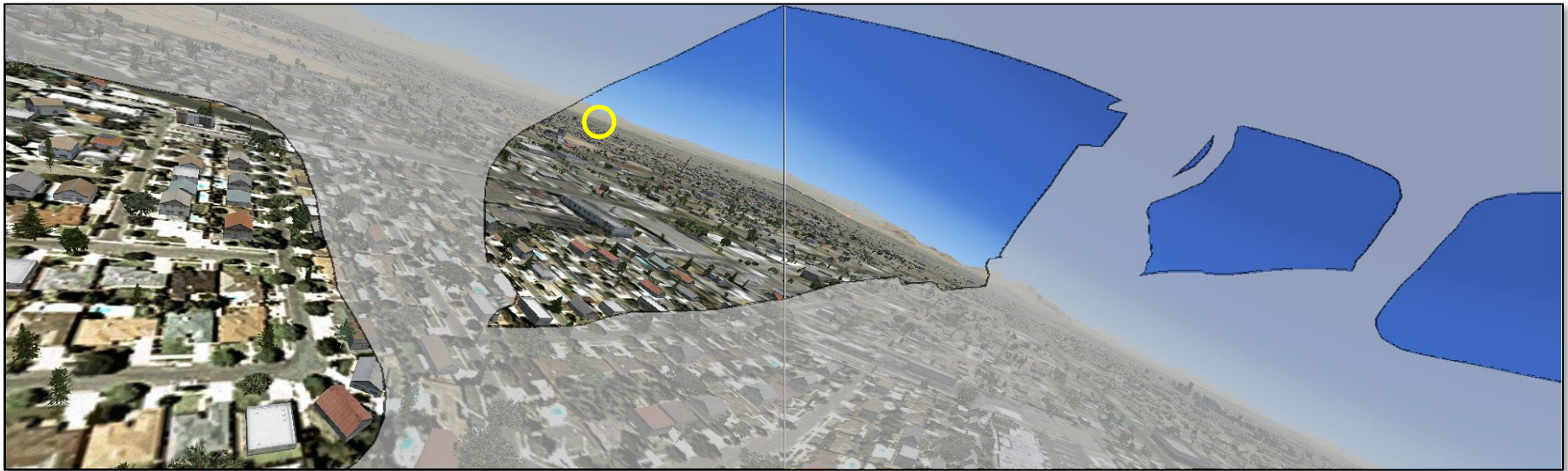
Traffic Alert:

"Traffic, 11 o'clock, same altitude, less than one mile."

Figure 22c. Simulated CDTI display and view from the Piper pilot seat at 12:02:29 (22 seconds before the collision). The Cessna is located in the yellow circle.
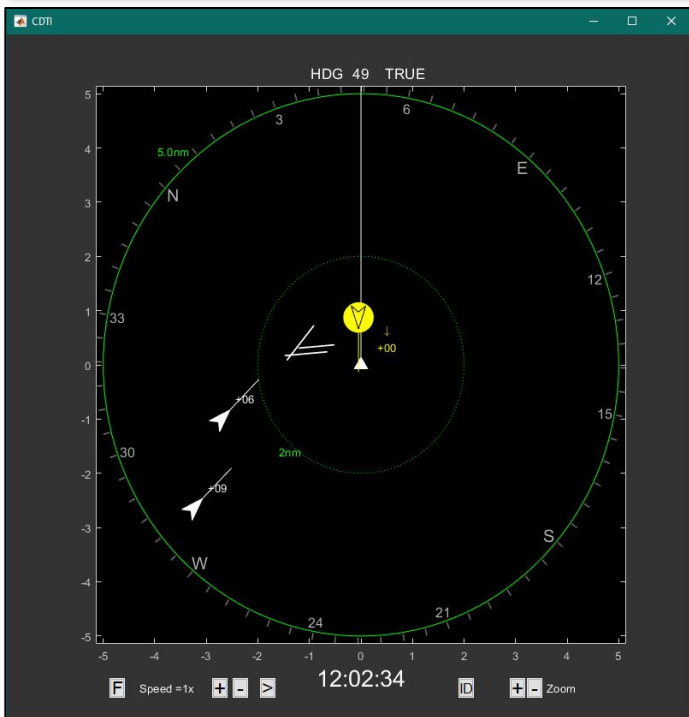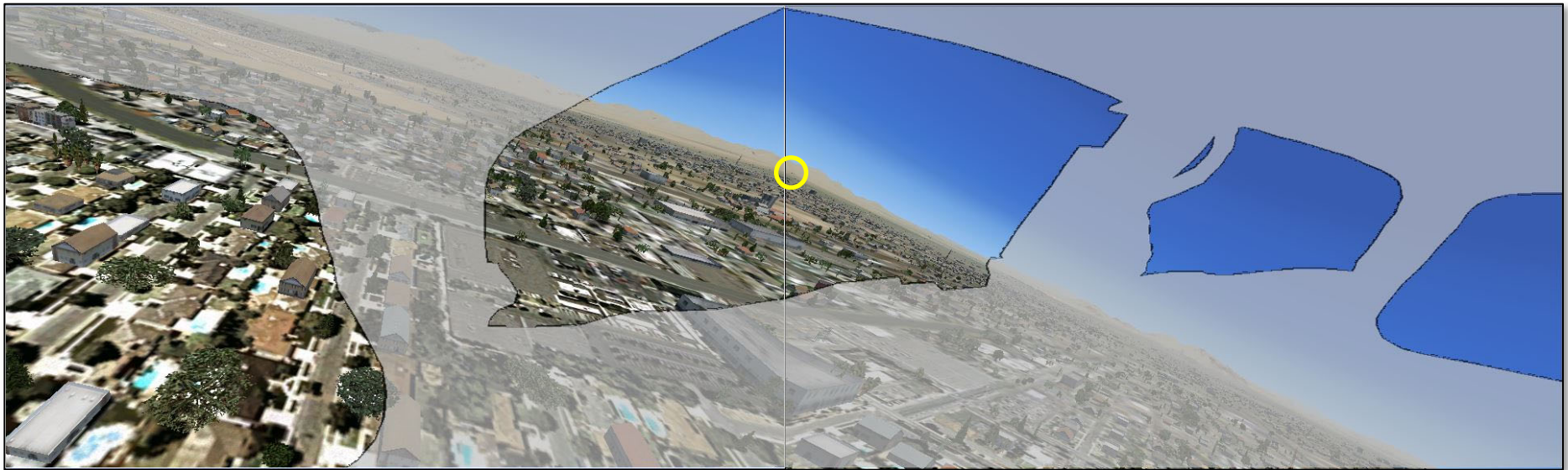
Figure 22d. Simulated CDTI display and view from the Piper pilot seat at 12:02:34 (17 seconds before the collision). The Cessna is located in the yellow circle.

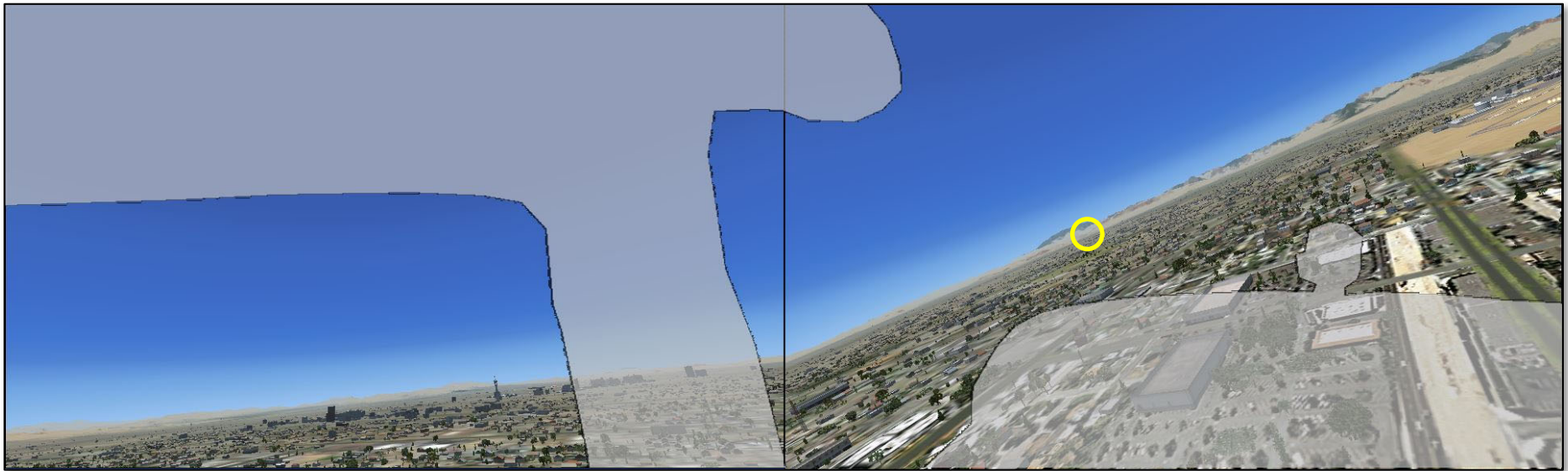AIRCRAFT PERFORMANCE & COCKPIT VISIBILITY STUDY
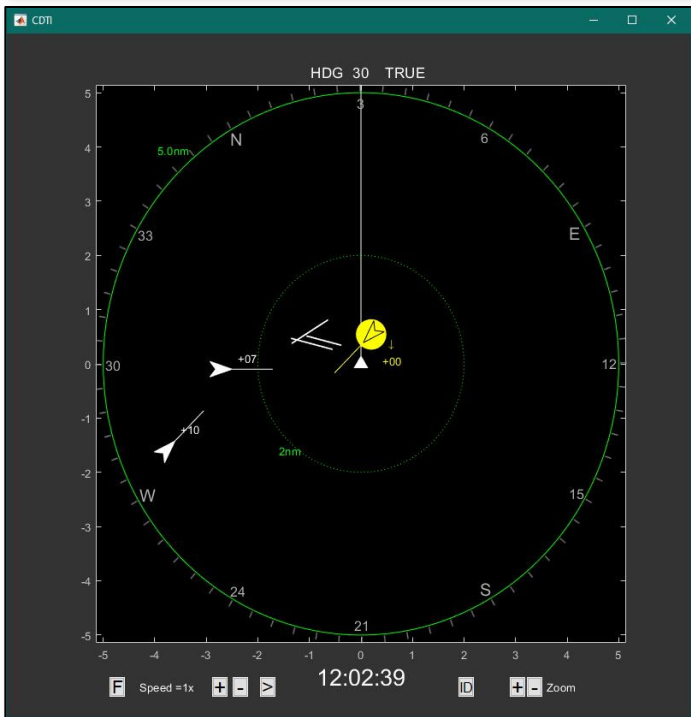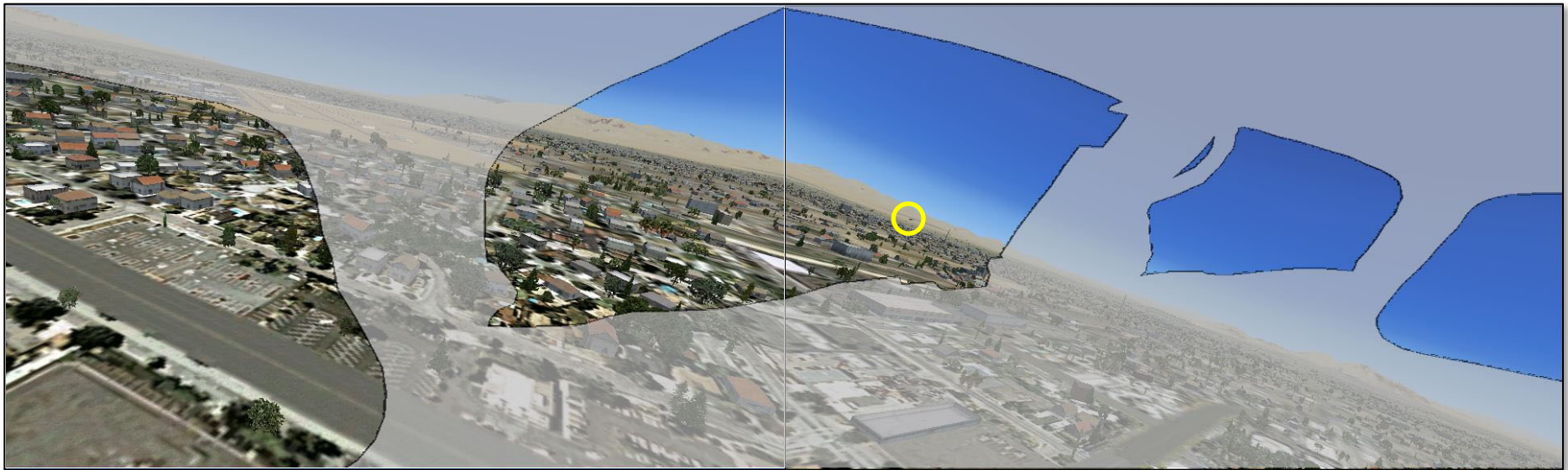
Figure 22e. Simulated CDTI display and view from the Piper pilot seat at 12:02:39 (12 seconds before the collision). The Cessna is located in the yellow circle.

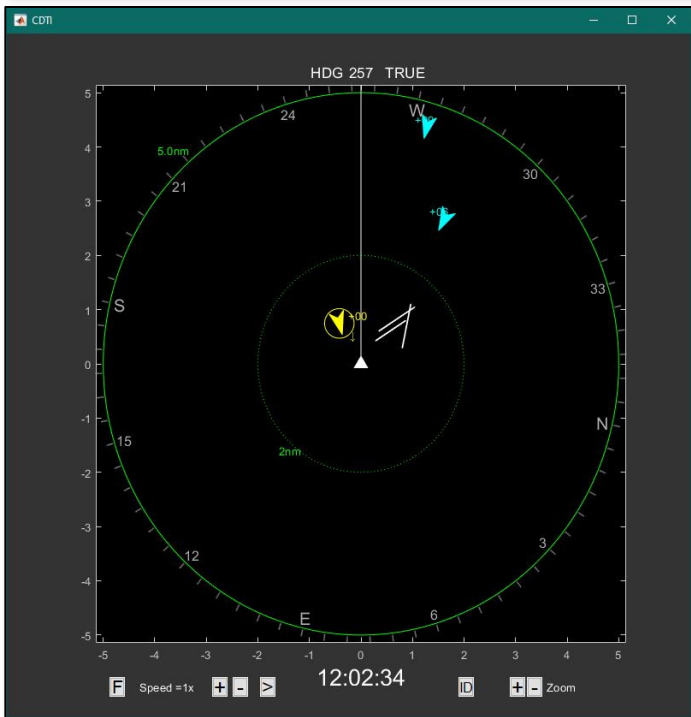AIRCRAFT PERFORMANCE & COCKPIT VISIBILITY STUDY
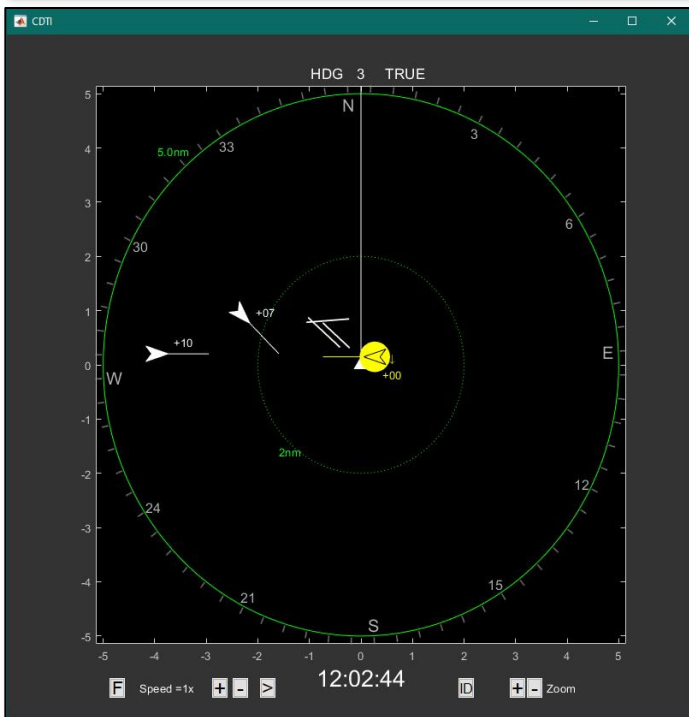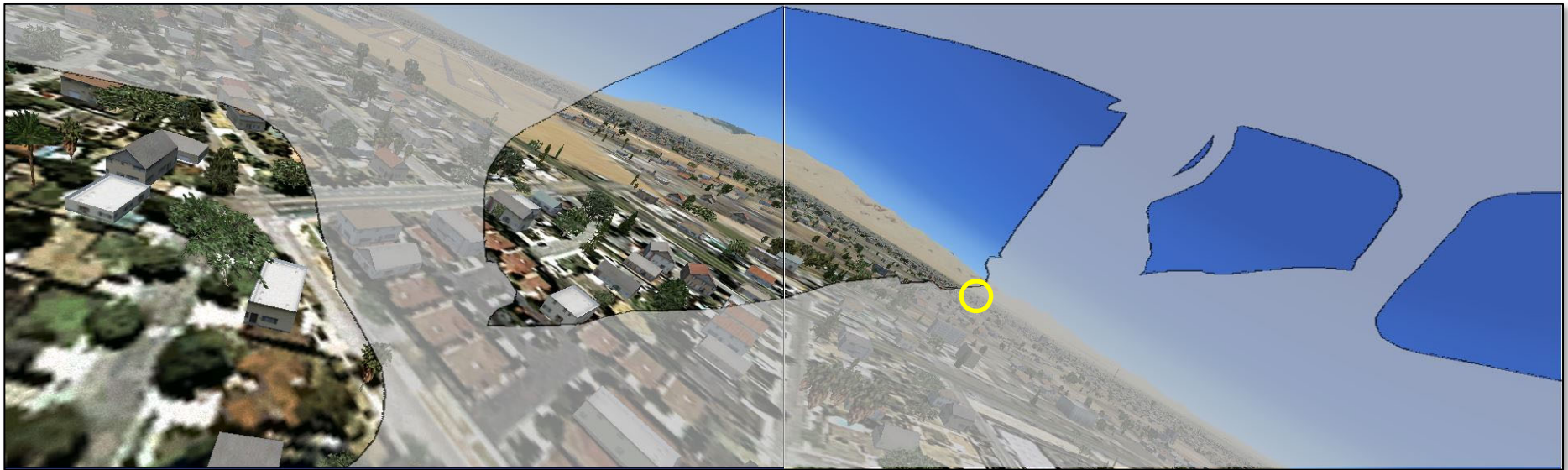
Figure 22f. Simulated CDTI display and view from the Piper pilot seat at 12:02:44 (7 seconds before the collision). The Cessna is located in the yellow circle.

AIRCRAFT PERFORMANCE & COCKPIT VISIBILITY STUDY
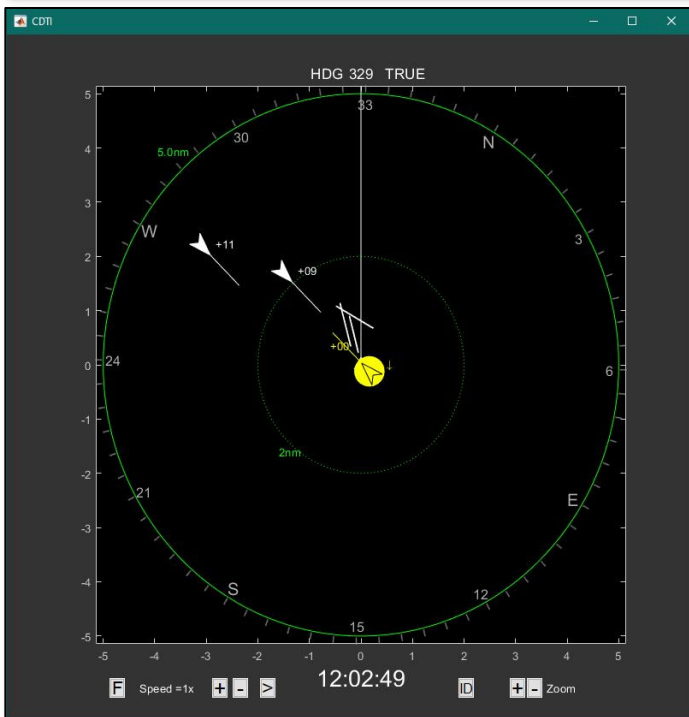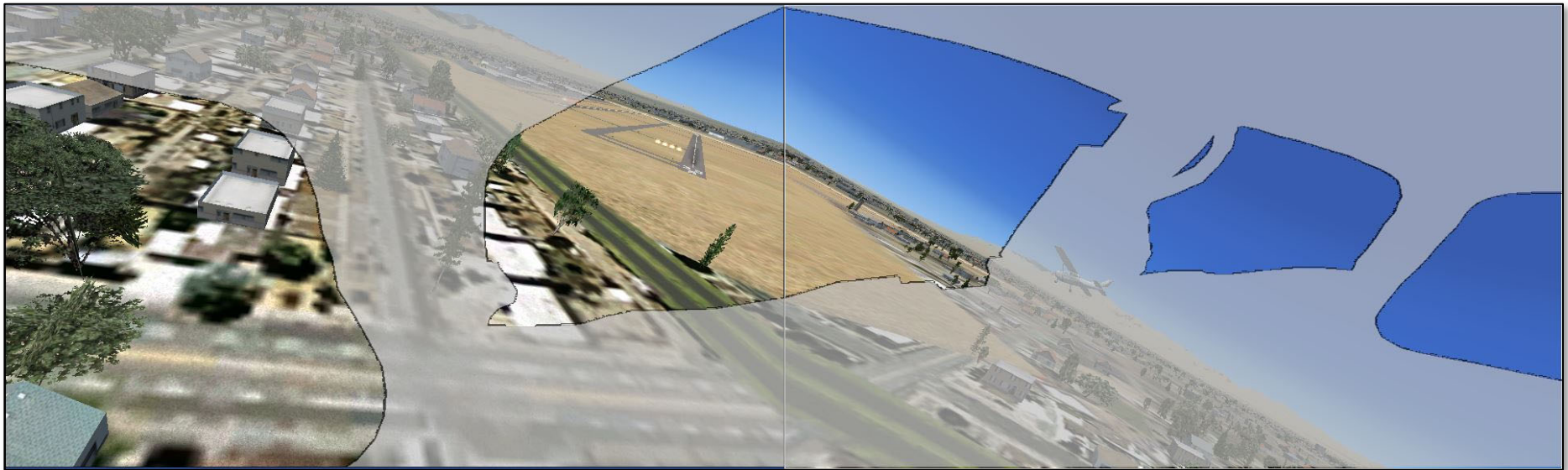
Figure 22g. Simulated CDTI display and view from the Piper pilot seat at 12:02:49 (2 seconds before the collision).

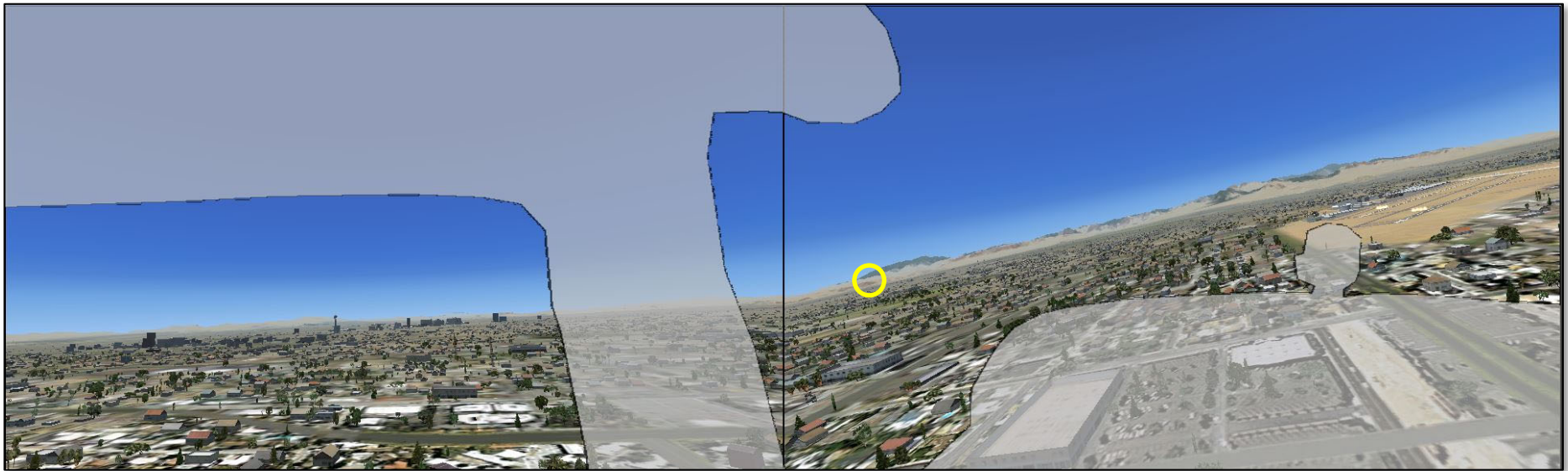AIRCRAFT PERFORMANCE & COCKPIT VISIBILITY STUDY

Figure 23a. Simulated CDTI display and view from the Cessna pilot seat at 12:02:15 (36 seconds before the collision). The Piper is located in the yellow circle.

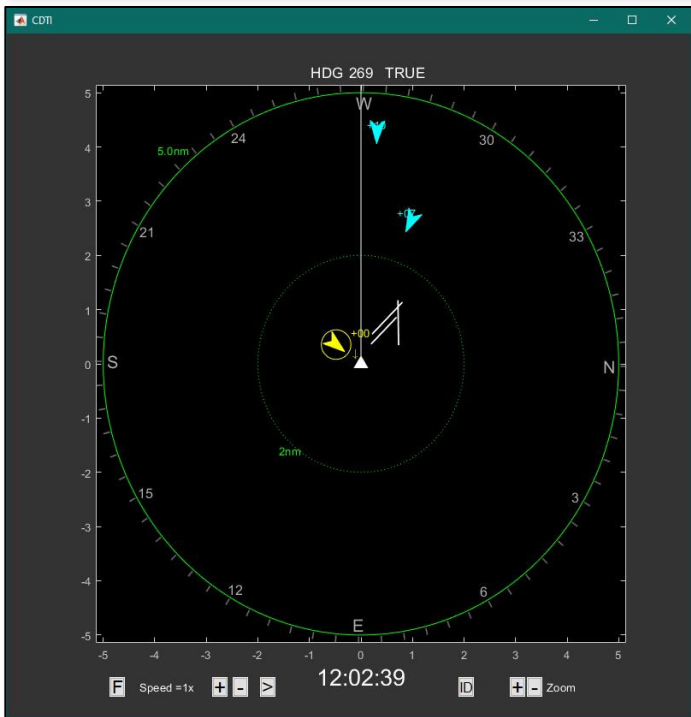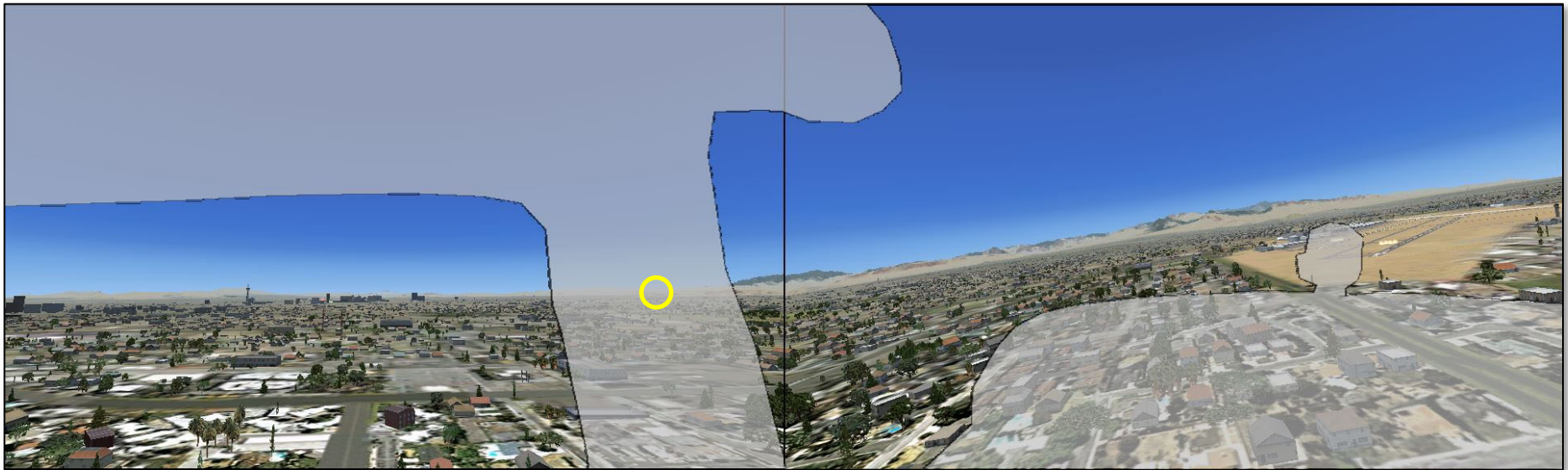AIRCRAFT PERFORMANCE & COCKPIT VISIBILITY STUDY

PAZ Alert:

"Traffic, 1 o'clock, same altitude, one mile."

Figure 23b. Simulated CDTI display and view from the Cessna pilot seat at 12:02:21 (30 seconds before the collision). The Piper is located in the yellow circle.

Figure 23c. Simulated CDTI display and view from the Cessna pilot seat at 12:02:29 (22 seconds before the collision). The Piper is located in the yellow circle.

Figure 23d. Simulated CDTI display and view from the Cessna pilot seat at 12:02:34 (17 seconds before the collision). The Piper is located in the yellow circle.
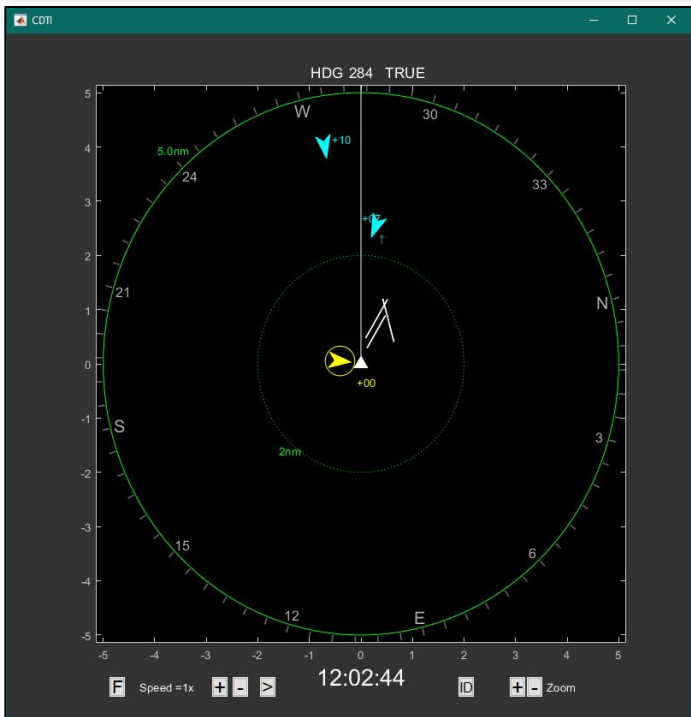
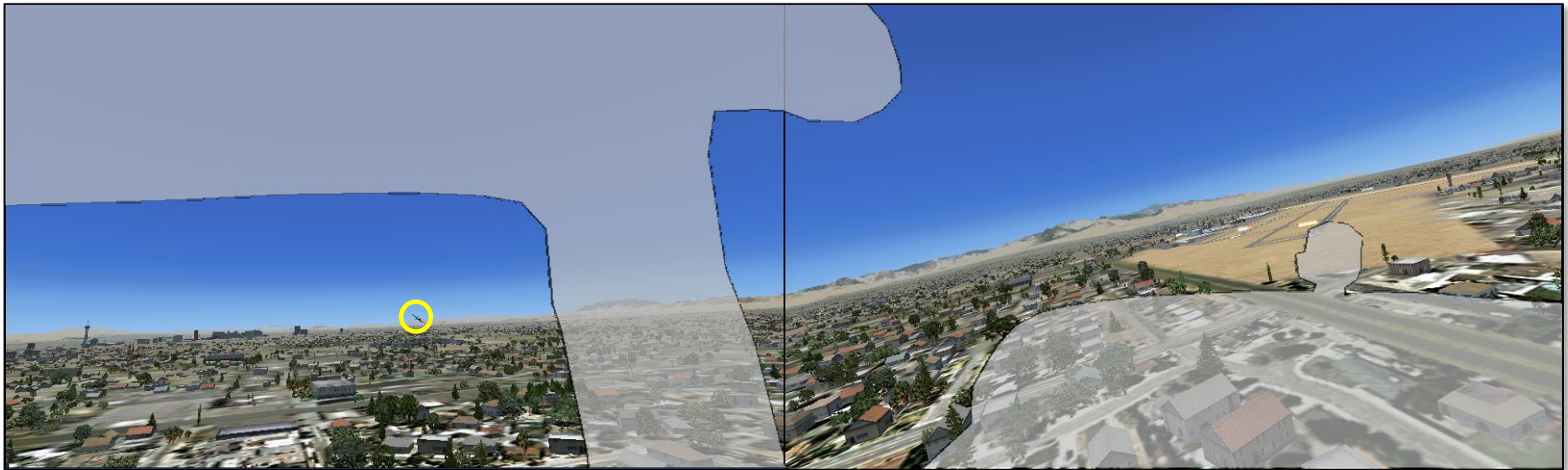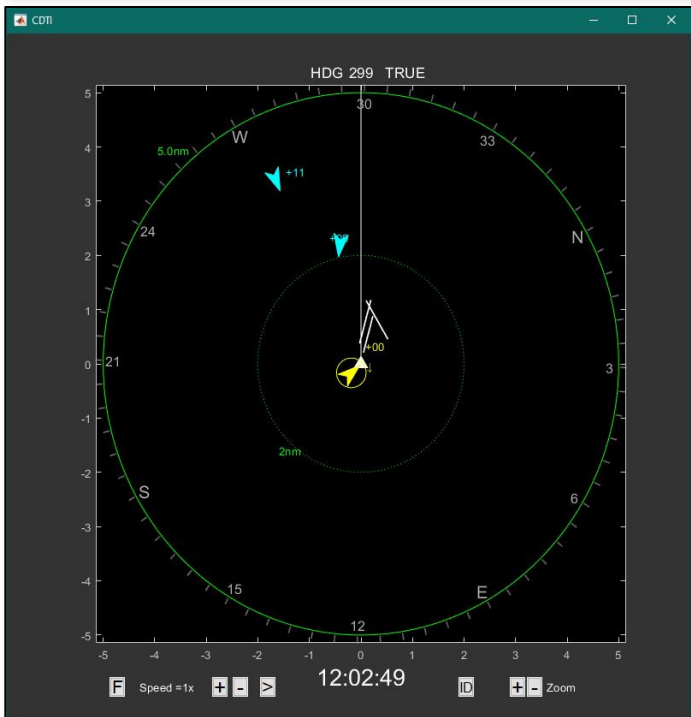AIRCRAFT PERFORMANCE & COCKPIT VISIBILITY STUDY

Figure 23e. Simulated CDTI display and view from the Cessna pilot seat at 12:02:39 (12 seconds before the collision). The Piper is located in the yellow circle.

Figure 23f. Simulated CDTI display and view from the Cessna pilot seat at 12:02:44 (7 seconds before the collision). The Piper is located in the yellow circle.
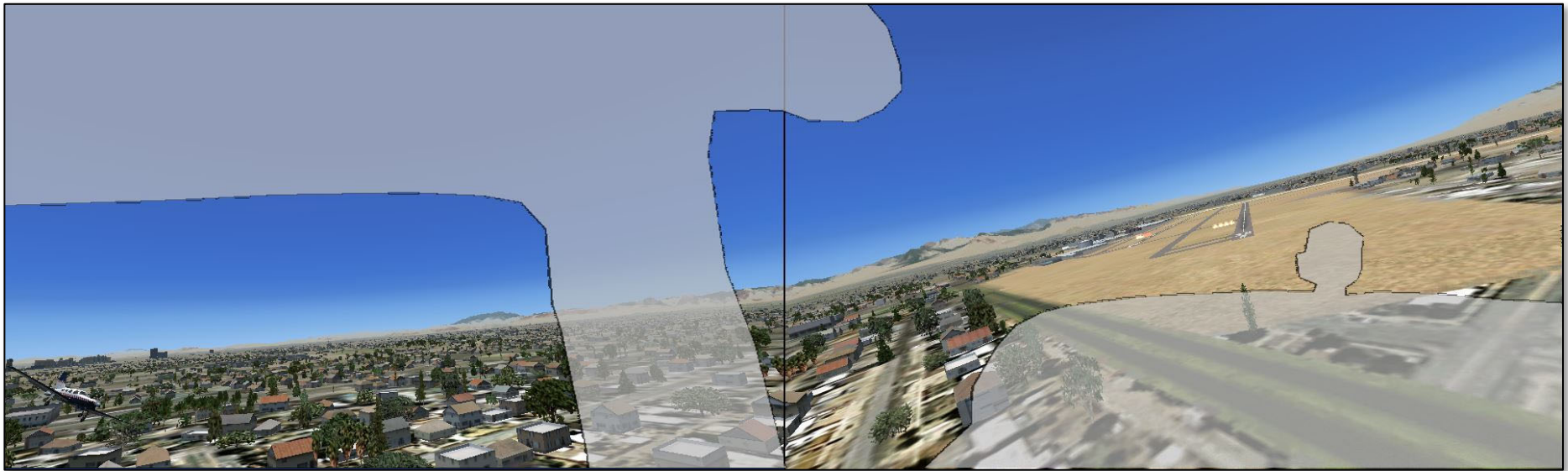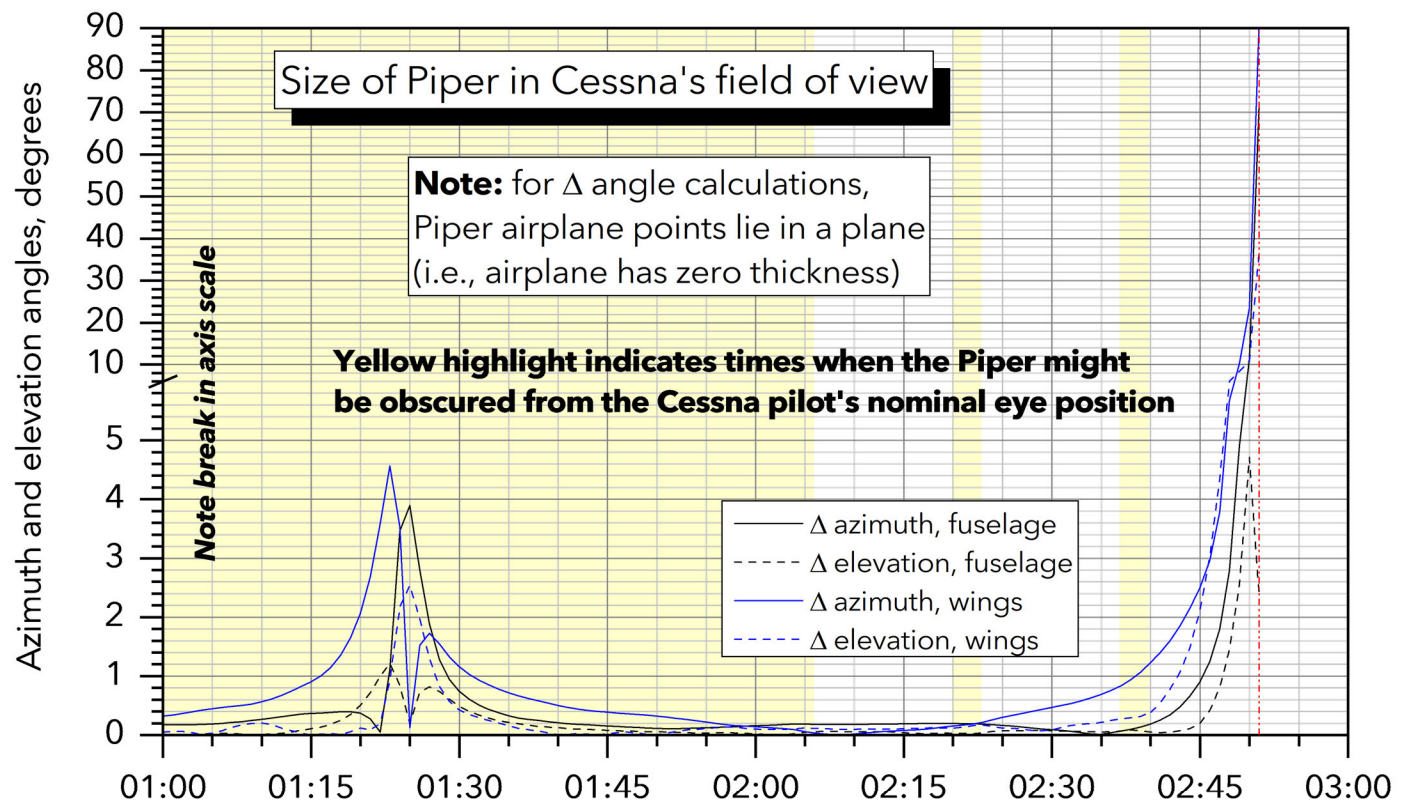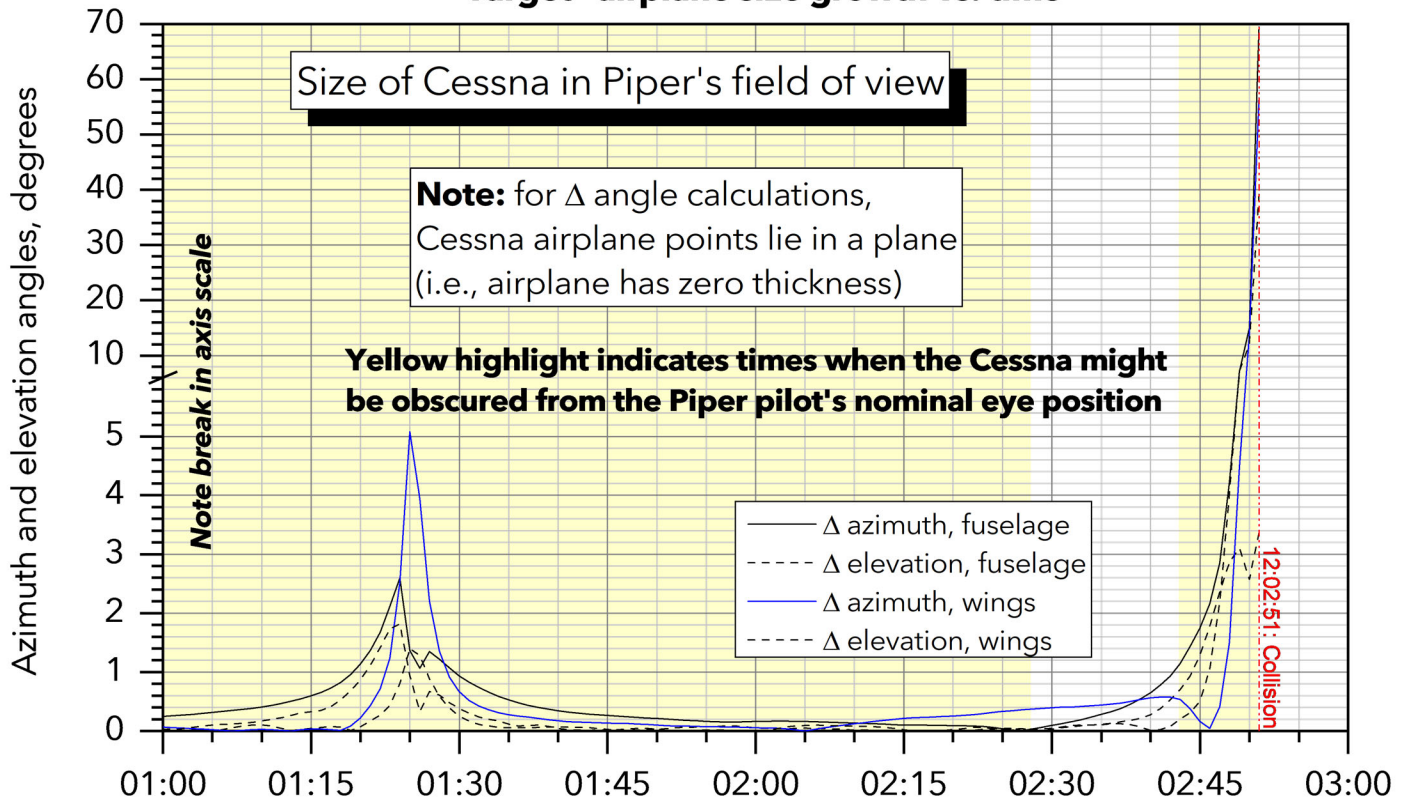
Figure 23g. Simulated CDTI display and view from the Cessna pilot seat at 12:02:49 (2 seconds before the collision).

AIRCRAFT PERFORMANCE & COCKPIT VISIBILITY STUDY

**ERA22FA318: Midair collision, Piper PA46-350P N97CX / Cessna 172N N160RA
North Las Vegas, NV, 07/17/2022
"Target" airplane size growth vs. time**

Size of Cessna in Piper's field of view

Note: for Δ angle calculations,
Cessna airplane points lie in a plane
(i.e., airplane has zero thickness)

**Yellow highlight indicates times when the Cessna might
be obscured from the Piper pilot's nominal eye position**

Note break in axis scale

— Δ azimuth, fuselage
- - Δ elevation, fuselage
— Δ azimuth, wings
- - Δ elevation, wings

12:02:51: Collision

Size of Piper in Cessna's field of view

Note: for Δ angle calculations,
Piper airplane points lie in a plane
(i.e., airplane has zero thickness)

**Yellow highlight indicates times when the Piper might
be obscured from the Cessna pilot's nominal eye position**

Note break in axis scale

— Δ azimuth, fuselage
- - Δ elevation, fuselage
— Δ azimuth, wings
- - Δ elevation, wings

Azimuth and elevation angles, degrees

ADS-B time, MM:SS after 12:00:00 PDT

Figure 24.

AIRCRAFT PERFORMANCE & COCKPIT VISIBILITY STUDY

ERA22FA318
PG 75 OF 77

Figure 25a. G500 ADS-B traffic display, from Reference 9.

Symbol	Description
◇ ◇	Basic Non-Directional Traffic (White in Air, Brown on Ground)
⬧ ⬧	Basic Directional Traffic (White in Air, Brown on Ground)
▽	Basic Off-scale Selected Traffic
◆	Proximate Non-Directional Traffic
▲	Proximate Directional Traffic
▼	Proximate Off-scale Selected Traffic
●	Non-Directional Alerted Traffic
◓	Off-Scale Non-Directional Alerted Traffic
◉	Directional Alerted Traffic
◉	Off-Scale Directional Alerted Traffic
▣	Non-Directional Surface Vehicle
⬠	Directional Surface Vehicle

ADS-B Traffic Symbols

Figure 25b. G500 ADS-B traffic symbols, from Reference 9.

APPENDIX A:

**Computing the Azimuth and Elevation Angles of
Airplane Cockpit Windows and other Structures from Laser Scans**

APPENDIX A: Computing the Azimuth and Elevation Angles of Airplane Cockpit Windows and other Structures from Laser Scans

Azimuth and elevations of "target" aircraft relative to "viewer" aircraft

The "visibility angles" from the "viewer" airplane to the "target" airplane correspond to the angular coordinates of the line of sight between the airplanes, measured in a coordinate system fixed to the viewer airplane (the viewer's "body axis" system), and consist of the azimuth angle and elevation angle (see Figure A1). The azimuth angle is the angle between the x-axis and the projection of the line of sight onto the x-y plane. The elevation angle is the angle between the line of sight itself, and its projection onto the x-y plane. At 0° elevation, 0° azimuth is straight ahead, and positive azimuth angles are to the right. 90° azimuth would be out the right window parallel to the y axis of the airplane. At 0° azimuth, 0° elevation is straight ahead, and positive elevation angles are up. 90° elevation would be straight up parallel to the z axis. The azimuth and elevation angles depend on both the position of the viewer and target airplanes, and the orientation (yaw, pitch, and bank angles) of the viewer.
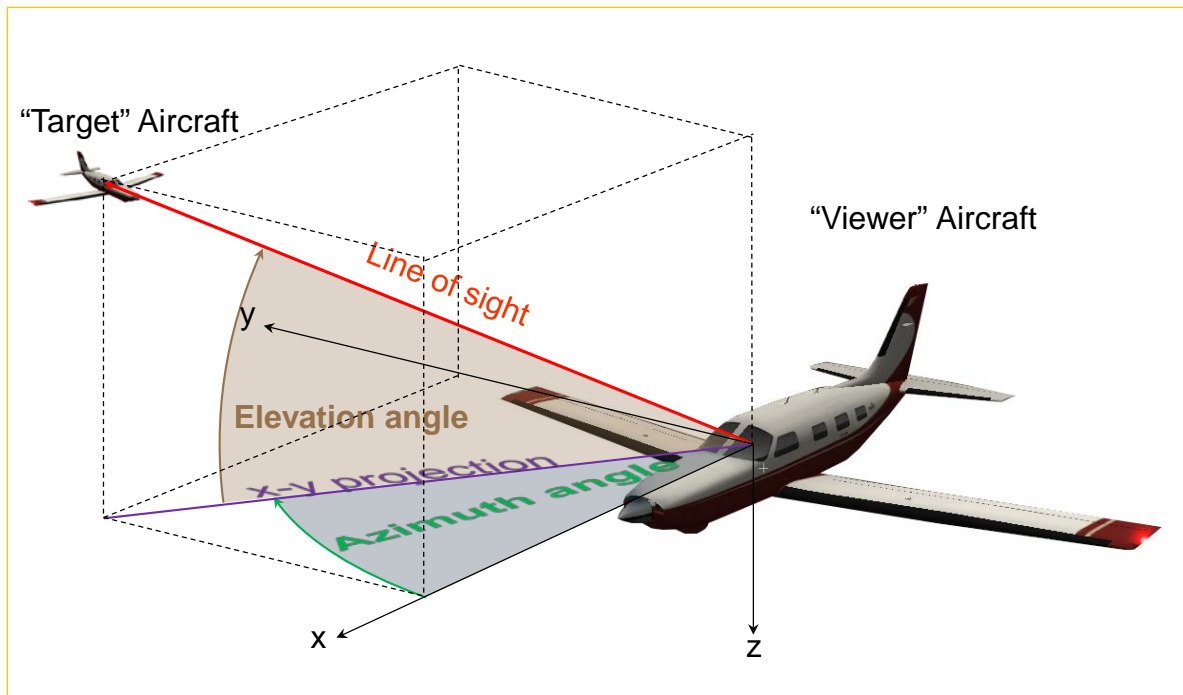
Figure A1. Azimuth and elevation angles from "viewer" airplane to "target" airplane.

The target airplane will be visible from the viewer airplane unless a non-transparent part of the viewer's structure lies in the line of sight between the two airplanes. To determine if this is the case, the azimuth and elevation coordinates of the boundaries of the viewer's transparent structures (windows) must be known, as well as the coordinates of the viewer's structure visible from the cockpit (such as the wings). If the line of sight passes through a non-transparent structure (such as the instrument panel, a window post, or a wing), then the target airplane will be obscured from the viewer.

Azimuth and elevation angles of airplane structures from laser scans

The azimuth and elevation angles of the window boundaries and other structures of the airplane of interest can be determined from the interior and exterior dimensions of the airplane, as measured using a FARO laser scanner.[1] The laser scanner produces a "point cloud" generated by the reflection of laser light off of objects in the laser's path, as the scanner sweeps through 360° of azimuth and approximately 150° of elevation. The 3-dimensional coordinates of each point in the cloud are known, and the coordinates of points from multiple scans (resulting from placing the scanner in different positions) are "merged" by the scanner software[2] into a common coordinate system. By placing the scanner in a sufficient number of locations so that the scanner can "see" every part of the airplane, the complete exterior and interior geometry of the airplane can be defined.

Coordinate transformations: scanner axes to body axes

The scanner software merges the point clouds from multiple scans into a single, "global" coordinate system. By default, this coordinate system is centered at the first scan location, which in general will not be coincident or aligned with the airplane body axis system. Hence, to compute azimuth and elevation angles of the scanned points relative to the pilot's eyes, the following transformations must be accomplished:

1. Translate the scanner global coordinates to the origin of the airplane body axis system.

2. Transform the translated scanner global coordinates into the airplane body axis system using a transformation matrix defined by the three rotations required to align the scanner axis system with the body axis system.

3. Determine the location of the pilot's eyes in the body axis system.

4. Determine the positions of the scanned points relative to the pilot's eyes in the body axis system.

5. Compute the azimuth and elevation angles from the pilot's eyes to the scanned points.

---

[1] Specifically, the FARO "Focus 3D" scanner; see http://www.faro.com/focus/us.
[2] FARO SCENE software: see http://www.faro.com/focus/us/software.

Note that to accomplish these steps, the following must also be known:

- The scanner global coordinates of the origin of the body axis system

- The three rotation angles between the scanner global coordinates and the body axis system

As will be shown below, these items can be determined from the scanned geometry of the airplane and the following known points:

- The scanner global coordinates at which the body x axis passes through the front and back of the airplane
- The body x coordinates of these points
- The scanner global coordinates of the left and right wingtips
- The body (x,y,z) coordinates of the wingtips

The body coordinates of the points listed above can be determined from technical or scaled drawings of the airplane.

The transformation equations and details of the steps outlined above can be derived starting from the sketch shown in Figure A2, where:

$\vec{R}_{sb}$ = Vector from the origin of the scanner global axis system to the origin of the airplane body axis system

$\vec{R}_s$ = Vector from the origin of the scanner global axis system to point P

$\vec{R}_b$ = Vector from the origin of the airplane body axis system to point P
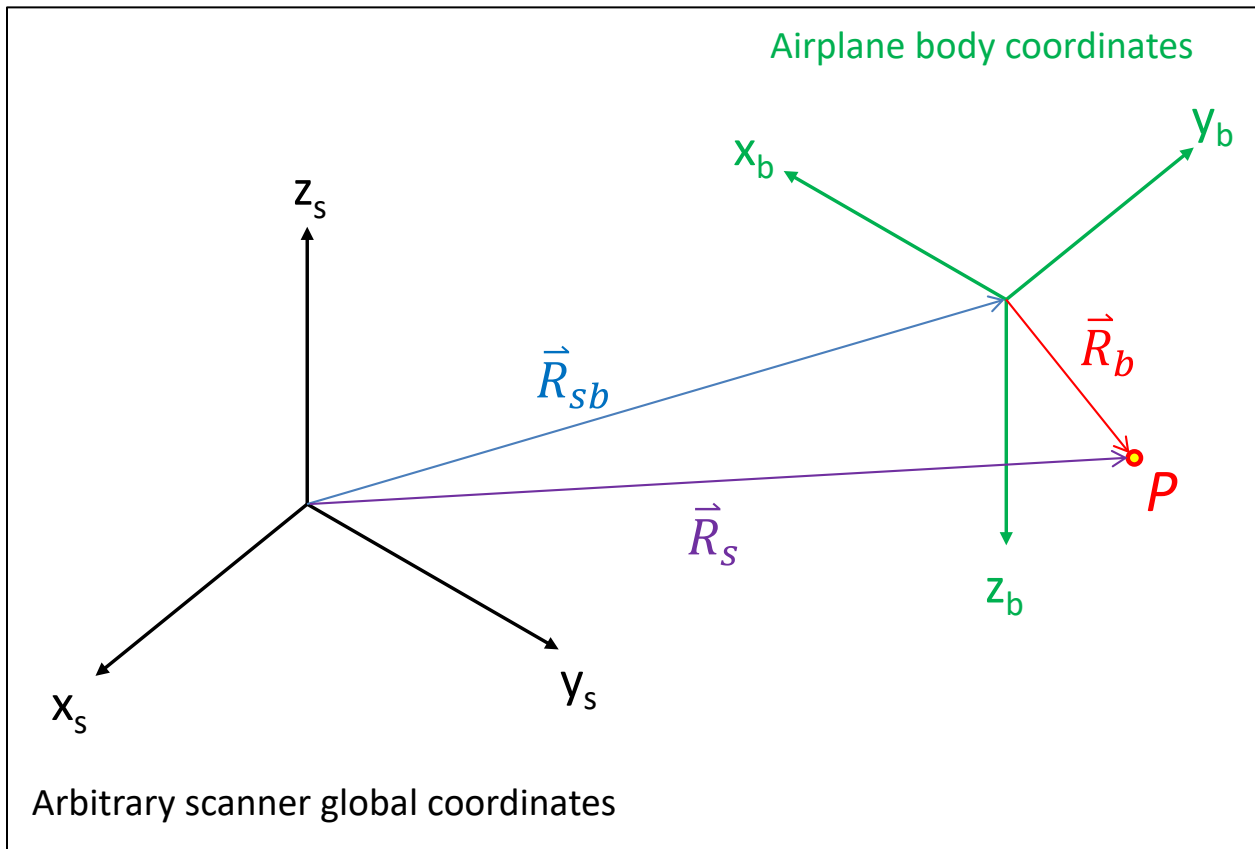
Figure A2. Vectors used to determine coordinates of point P in body axes coordinates.

The vectors $\vec{R}_{sb}$, $\vec{R}_s$, and $\vec{R}_b$ are expressed in the scanner global coordinates. We would like to know the coordinates of point *P* in body axis coordinates; let $\vec{r}_b$ be the vector from the origin of the body axis system to point *P*, expressed in body coordinates. Then, $\vec{r}_b$ is simply $\vec{R}_b$ transformed from scanner global coordinates to body axis coordinates. This transformation can be computed as follows. First, note that:

$$\vec{r}_b = \begin{Bmatrix} x \\ y \\ z \end{Bmatrix}_b = \text{coordinates of point } P \text{ from body axis origin, in body axes}$$

$$\vec{R}_b = \begin{Bmatrix} x \\ y \\ z \end{Bmatrix}_s = \text{coordinates of point } P \text{ from body axis origin, in scanner axes}$$

$$\vec{R}_s = \begin{Bmatrix} x_s \\ y_s \\ z_s \end{Bmatrix}_s = \text{coordinates of point } P \text{ from scanner axis origin, in scanner axes}$$

$$\vec{R}_{sb} = \begin{Bmatrix} x_{sb} \\ y_{sb} \\ z_{sb} \end{Bmatrix}_s = \text{coordinates of body axis origin from scanner axis origin, in scanner axes}$$

From Figure A2,

$$\vec{R}_b = \vec{R}_s - \vec{R}_{sb} = \begin{Bmatrix} x_s \\ y_s \\ z_s \end{Bmatrix}_s - \begin{Bmatrix} x_{sb} \\ y_{sb} \\ z_{sb} \end{Bmatrix}_s = \begin{Bmatrix} x \\ y \\ z \end{Bmatrix}_s \qquad [A1]$$

Equation [A1] translates the coordinates of point P from the origin of the scanner axis system to the origin of the body axis system, which is step 1 in the procedure outlined above. The coordinates are transformed into the body axis system (step 2 in the procedure) using a transformation matrix:

$$\vec{r}_b = [T_{sb}]\vec{R}_b \qquad [A2a]$$

Or, equivalently,

$$\begin{Bmatrix} x \\ y \\ z \end{Bmatrix}_b = [T_{sb}] \begin{Bmatrix} x \\ y \\ z \end{Bmatrix}_s \qquad [A2b]$$

Where $[T_{sb}]$ is the transformation matrix from the scanner axis system to the body axis system. This transformation matrix is defined by a series of three rotations of the scanner axis system, in the following order:

1. A rotation about the z_s axis through the angle ψ, yielding axes $(x'_s, y'_s, z'_s = z_s)$.
2. A rotation about the y'_s axis through the angle θ, yielding axes $(x''_s, y''_s = y'_s, z''_s)$.
3. A rotation about the x''_s axis through the angle ϕ, yielding axes $(x_b = x''_s, y_b, z_b)$.

There is a transformation matrix associated with each of these rotations; the elements of the matrices are sines or cosines of the rotation angles involved. Combining these transformations through matrix multiplication yields the final transformation matrix $[T_{sb}]$:

$$[T_{sb}] = \begin{bmatrix} \cos\theta\cos\psi & \cos\theta\sin\psi & -\sin\theta \\ \sin\phi\sin\theta\cos\psi - \cos\phi\sin\psi & \sin\phi\sin\theta\sin\psi + \cos\phi\cos\psi & \sin\phi\cos\theta \\ \cos\phi\sin\theta\cos\psi + \sin\phi\sin\psi & \cos\phi\sin\theta\sin\psi - \sin\phi\cos\psi & \cos\phi\cos\theta \end{bmatrix} \qquad [A3]$$

The details of these operations can be found in textbooks about airplane dynamics (or other subjects associated with rigid body dynamics and coordinate transformations).[3]

---

[3] See, for example, Roskam, Jan: <u>Airplane Flight Dynamics and Automatic Flight Controls, Part I</u> (Roskam Aviation and Engineering Corporation, 1979), pp. 24-27.

The reverse transformation (from airplane body axes to scanner axes) follows from Equations [A2a] and [A2b]:

$$\vec{R}_b = [T_{sb}]^{-1}\vec{r}_b = [T_{sb}]^T \vec{r}_b \tag{A4a}$$

$$\begin{Bmatrix} x \\ y \\ z \end{Bmatrix}_s = [T_{sb}]^{-1} \begin{Bmatrix} x \\ y \\ z \end{Bmatrix}_b = [T_{sb}]^T \begin{Bmatrix} x \\ y \\ z \end{Bmatrix}_b \tag{A4b}$$

Because the transformation matrix $[T_{sb}]$ is orthogonal, its inverse is equal to its transpose.

Note that Equations [A1], [A2b] and [A3] involve the coordinates of the origin of the body axis system in scanner axes $\{x_{sb}, y_{sb}, z_{sb}\}_s$, and the three rotation angles ψ, θ, and ϕ, which are all unknown and must be determined.

The coordinates $\{x_{sb}, y_{sb}, z_{sb}\}_s$ can be determined from the body axis coordinates of the points where the body x axis intersects the front and back of the airplane. It is assumed that these points are known from technical drawings of the airplane. It is also assumed that the location of these points can also be identified in the scanned point cloud by comparing the scan results to the technical drawings of the airplane, and that therefore the scanner coordinates $\{x_s, y_s, z_s\}_s$ of the points, measured from the scanner axis origin, can be determined using the scanner software.

Let $\{x_{sn}, y_{sn}, z_{sn}\}_s$ be the coordinates of the intersection of the body x axis with the front (nose) of the airplane, measured from the scanner axis origin, in scanner axes, as determined from the examination of the scanned point cloud using the scanner software.

Let $\{x_{st}, y_{st}, z_{st}\}_s$ be the coordinates of the intersection of the body x axis with the back (tail) of the airplane, measured from the scanner axis origin, in scanner axes, as determined from the examination of the scanned point cloud using the canner software.

The distance along the body x axis from nose to tail is then

$$l_{nt} = \sqrt{(x_{sn} - x_{st})_s^2 + (y_{sn} - y_{st})_s^2 + (z_{sn} - z_{st})_s^2} \tag{A5}$$

Since the ratio of the distance between the body axis origin and the nose (i.e., $(x_n)_b$) to l_{nt} is the same in both the scanner and body axis coordinate systems, the scanner coordinates of the body axis origin, measured from the scanner axis origin, are given by

$$\begin{Bmatrix} x_{sb} \\ y_{sb} \\ z_{sb} \end{Bmatrix}_S = \begin{Bmatrix} x_{sn} \\ y_{sn} \\ z_{sn} \end{Bmatrix}_S + \left[\begin{Bmatrix} x_{st} \\ y_{st} \\ z_{st} \end{Bmatrix}_S - \begin{Bmatrix} x_{sn} \\ y_{sn} \\ z_{sn} \end{Bmatrix}_S \right] \frac{(x_n)_b}{l_{nt}} \qquad [\text{A6}]$$

There remains to determine the rotation angles ψ, θ, and ϕ. From Equation [A4b],

$$\begin{Bmatrix} x_n \\ y_n \\ z_n \end{Bmatrix}_S = \begin{Bmatrix} x_{sn} \\ y_{sn} \\ z_{sn} \end{Bmatrix}_S - \begin{Bmatrix} x_{sb} \\ y_{sb} \\ z_{sb} \end{Bmatrix}_S = [T_{sb}]^T \begin{Bmatrix} x_n \\ y_n \\ z_n \end{Bmatrix}_b \qquad [\text{A7}]$$

Where $\{x_n, y_n, z_n\}_s$ are the coordinates of the nose measured from the body origin in scanner axes, and $\{x_n, y_n, z_n\}_b$ are the coordinates of the nose measured from the body origin in body axes. From Equations [A7] and [A3],

$$\{z_{sn} - z_{sb}\}_s = (-\sin\theta)\{x_n\}_b + (\sin\phi\cos\theta)\{y_n\}_b + (\cos\phi\cos\theta)\{z_n\}_b \qquad [\text{A8}]$$

Since by definition the "nose" lies on the x body axis, $(y_n)_b = (z_n)_b = 0$, and Equation [A8] gives

$$\theta = \sin^{-1}\left(\frac{-\{z_{sn}-z_{sb}\}_s}{\{x_n\}_b}\right) \qquad [\text{A9}]$$

Similarly, Equations [A7] and [A3] with $(y_n)_b = (z_n)_b = 0$ give

$$\{x_{sn} - x_{sb}\}_s = (\cos\theta\cos\psi)\{x_n\}_b \qquad [\text{A10}]$$

$$\{y_{sn} - y_{sb}\}_s = (\cos\theta\sin\psi)\{x_n\}_b \qquad [\text{A11}]$$

And therefore

$$\psi = \cos^{-1}\left(\frac{\{x_{sn}-x_{sb}\}_s}{\{x_n\}_b \cos\theta}\right) \qquad [\text{A12}]$$

$$\psi = \sin^{-1}\left(\frac{\{y_{sn}-y_{sb}\}_s}{\{x_n\}_b \cos\theta}\right) \qquad [\text{A13}]$$

These two equations for ψ allow the proper quadrant for ψ to be determined.

To solve for the remaining rotation angle (ϕ), the coordinates of the wingtips can be used. Let $\{x_{sl}, y_{sl}, z_{sl}\}_s$ be the coordinates of the left wingtip, measured from the scanner axis origin, in scanner axes, as determined from the examination of the scanned point cloud

using the scanner software. Similarly, let $\{x_{sr}, y_{sr}, z_{sr}\}_s$ be the corresponding coordinates for the right wing. The coordinates of the wingtips in body coordinates, measured from the body axis origin, are

$$\begin{Bmatrix} x_r \\ y_r \\ z_r \end{Bmatrix}_b = \begin{Bmatrix} x_w \\ y_w \\ z_w \end{Bmatrix}_b \quad \text{for the right wing, and}$$

$$\begin{Bmatrix} x_l \\ y_l \\ z_l \end{Bmatrix}_b = \begin{Bmatrix} x_w \\ -y_w \\ z_w \end{Bmatrix}_b \quad \text{for the left wing.}$$

From Equation [A4b],

$$\begin{Bmatrix} x_r \\ y_r \\ z_r \end{Bmatrix}_s = \begin{Bmatrix} x_{sr} \\ y_{sr} \\ z_{sr} \end{Bmatrix}_s - \begin{Bmatrix} x_{sb} \\ y_{sb} \\ z_{sb} \end{Bmatrix}_s = [T_{sb}]^T \begin{Bmatrix} x_w \\ y_w \\ z_w \end{Bmatrix}_b \tag{A14}$$

$$\begin{Bmatrix} x_l \\ y_l \\ z_l \end{Bmatrix}_s = \begin{Bmatrix} x_{sl} \\ y_{sl} \\ z_{sl} \end{Bmatrix}_s - \begin{Bmatrix} x_{sb} \\ y_{sb} \\ z_{sb} \end{Bmatrix}_s = [T_{sb}]^T \begin{Bmatrix} x_w \\ -y_w \\ z_w \end{Bmatrix}_b \tag{A15}$$

Then, from Equations [A14], [A15], and [A3],

$$\{z_{sr} - z_{sb}\}_s = (-\sin\theta)\{x_w\}_b + (\sin\phi\cos\theta)\{y_w\}_b + (\cos\phi\cos\theta)\{z_w\}_b \tag{A16}$$

$$\{z_{sl} - z_{sb}\}_s = (-\sin\theta)\{x_w\}_b + (\sin\phi\cos\theta)\{-y_w\}_b + (\cos\phi\cos\theta)\{z_w\}_b \tag{A17}$$

Solving Equations [A16] and [A17] for $\cos\phi$ gives

$$\cos\phi = \frac{\{z_{sl}-z_{sb}\}_s + \{z_{sr}-z_{sb}\}_s + 2(\sin\theta)\{x_w\}_b}{2(\cos\theta)\{z_w\}_b} \tag{A18}$$

Solving Equations [A16] and [A17] for $\sin\phi$ gives

$$\sin\phi = \frac{\{z_{sr}-z_{sl}\}_s}{2(\cos\theta)\{y_w\}_b} \tag{A19}$$

$\cos\phi$ and $\sin\phi$ then define the proper quadrant for ϕ, and ϕ itself. Now, Equations [A1], [A2b] and [A3] can be used to compute the body axis coordinates of any scanned point, starting from the scanner coordinates of that point.

Azimuth and elevation angles from body axis coordinates

Once the coordinates of the scanned points are available in the body axis system, the azimuth and elevation angles of these points relative to the pilot's eye position can be computed. In keeping with the previous notation, let $\{x_e, y_e, z_e\}_b$ be the body-axis coordinates of one of the pilot's eyes,[4] and $\{x_P, y_P, z_P\}_b$ be the body-axis coordinates of a point P. Then the distance from the eye to point P is

$$l_{eP} = \sqrt{(x_P - x_e)_b^2 + (y_P - y_e)_b^2 + (z_P - z_e)_b^2} \qquad \text{[A20]}$$

The azimuth angle from the eye to the point P is

$$\Psi = \tan^{-1}\left[\frac{(y_P - y_e)}{(x_P - x_e)}\right] \qquad \text{[A21]}$$

The elevation angle from the eye to the point P is

$$\Theta = -\sin^{-1}\left[\frac{(z_P - z_e)}{l_{eP}}\right] \qquad \text{[A22]}$$

---

[4] Note that the pilot's left and right eyes are in slightly different positions, so these calculations should be made for each eye.

APPENDIX B:

**Creating Geometrically Correct Cockpit Window "Masks"
in Microsoft Flight Simulator X (*FSX*)**

**APPENDIX B: Creating Geometrically Correct Cockpit Window "Masks"
in Microsoft Flight Simulator X (*FSX*)**

Field of view vs. FSX screen display coordinates

The geometry of an airplane's cockpit windows and other structures can be defined in terms of their azimuth and elevation angles (Ψ and Θ, respectively) from the pilot's eyes. The visual systems of flight simulation programs, such as *FSX*, include a "cockpit view" that similarly displays the cockpit and other airplane structures from the "pilot's point of view." The *FSX* "virtual cockpit," in particular, depicts a 3-dimensional model of the airplane interior from the pilot's seat (or any other point at which a "camera" is placed). The 3D model can be explored by rotating and / or translating the camera from the pilot's eye position.

While many airplane models for *FSX* include "virtual cockpits" that are very convincing and satisfactory for gaming or flight training purposes, the geometrical accuracy of these models is unknown, and so they are not suitable for determining whether outside objects would be visible or obscured in the real airplane in any particular scenario. *FSX* also includes a simple "2D cockpit" view, which presents a forward-looking scene of the outside world, overlaid with an instrument panel that is a compromise between realism, and the desire to have all the necessary flight instruments (and a sufficiently large out-the-window view) visible to the user at the same time, given limited screen real estate. These "2D cockpits" are necessarily less representative of the real airplane than the "virtual cockpits." However, the default 2D cockpit instrument panel can be substituted with a user-created "panel" that correctly represents the pilot's view of the cockpit and airplane structures in the real airplane, as determined from the airplane geometry measured with a laser scanner (see Appendix A). This "geometrically correct" panel can be used to determine whether an object outside the airplane is obstructed from the pilot's view.

The custom panel created by the user is a whole-screen instrument panel that contains transparent and non-tranparent areas. The transparent areas correspond to areas of the windows that offer unobstructed views of the outside world; the non-transparent areas correspond to everything else (cockpit structure, and exterior structure visible from the cockpit that obstructs the outside view). The "panel" is simply a 1024 x 768 bitmap image file, in which transparent areas are defined by assigning pixels a particular color (e.g., black) that *FSX* interprets as "transparent." Hence, the coordinates and color of the pixels in the bitmap file define the shapes of the panel transparent and non-transparent areas.

However, while the scope of the scene of the outside world displayed on the screen is defined in terms of angular and vertical "fields of view," the screen coordinates of objects "seen" by the camera (including the cockpit windows) are not simply proportional to the angular Ψ and Θ coordinates of those objects from the camera positon. Instead, the screen coordinates of an object correspond to the points where the line of sight from the camera to the object intercepts a flat surface (the screen) placed some distance R between the camera and the object, as shown in Figure B1 (this Figure, and the discussion below, is adapted from Reference B1).
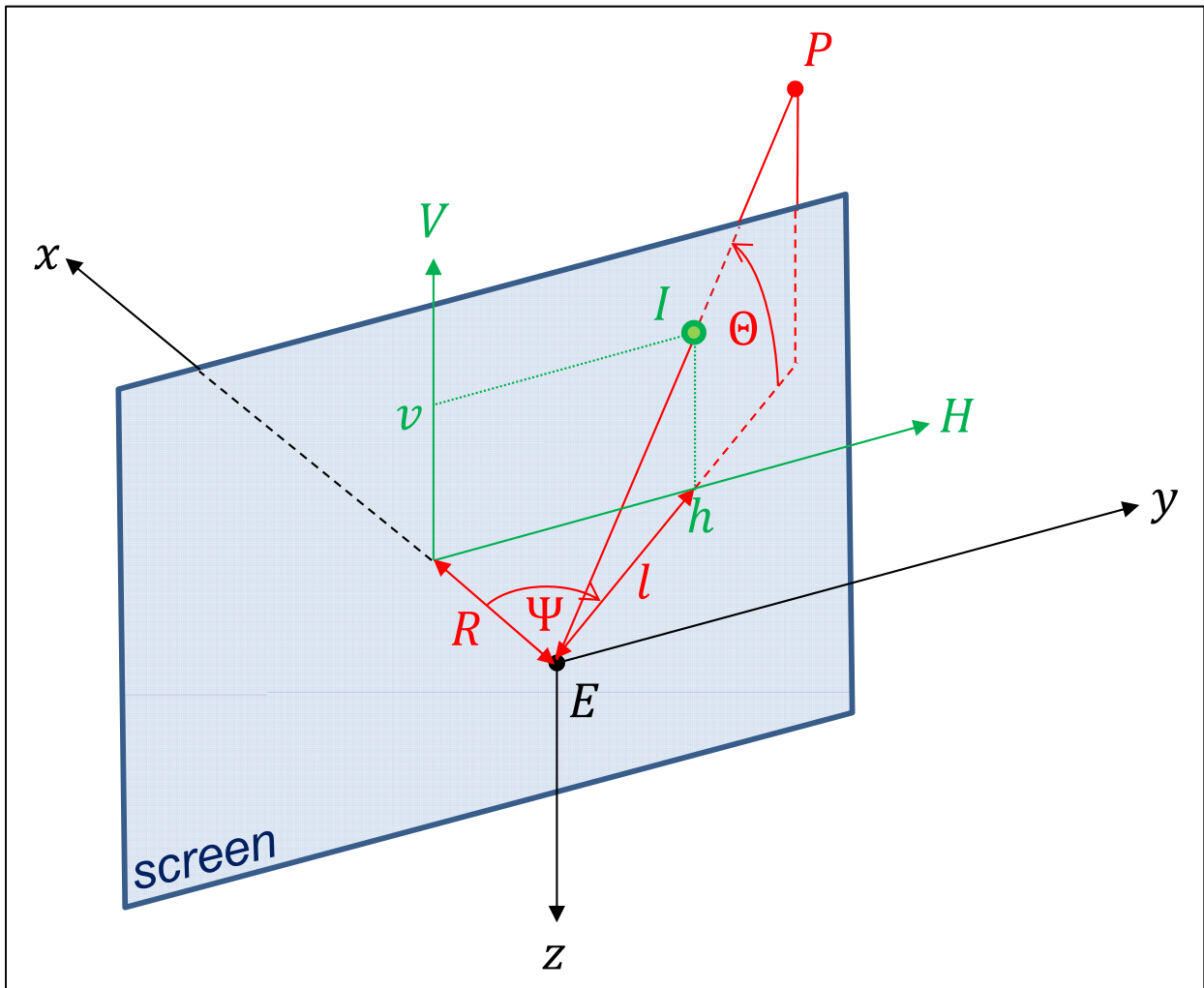

Figure B1. Relationships between the (Ψ, Θ) viewing angles of the line of sight from E to P (EP), and the (h, v) screen coordinates of the point I, where EP intersects the screen.

In Figure B1,

E = location of viewer's eye point (i.e., the camera location in *FSX*);
(x, y, z) = airplane body axis system with origin at E;
P = location of point or object to be drawn on the screen;
EP = line of sight from E to P;
Ψ = azimuth angle of EP;
Θ = elevation angle of EP;
I = point where EP intersects a flat screen placed in the yz plane between E and P;
R = x coordinate of I (i.e., the distance from E to the screen along x axis);
(H, V) = screen horizontal and vertical axis coordinate system, originating where the x body axis intersects the screen;
(h, v) = screen coordinates of I;
l = distance from E to the point defined by screen coordinates $(h, 0)$.

We seek to find the screen coordinates (h, v) at which a point P should be drawn, given the viewing angles (Ψ, Θ) from E to P.

From the geometry of Figure B1,

$$h = R \tan \Psi \qquad \text{[B1]}$$

$$l = \sqrt{R^2 + h^2} = \sqrt{R^2 + R^2 \tan^2 \Psi} = R\sqrt{1 + \tan^2 \Psi} \qquad \text{[B2]}$$

$$v = l \tan \Theta = R \tan \Theta \sqrt{1 + \tan^2 \Psi} \qquad \text{[B3]}$$

Consequently, (h, v) can be computed from (Ψ, Θ) once the distance R is known. R can be determined in *FSX* if the angular range of the horizontal field of view ($HFOV$) and the width of the screen in pixels (w) are known. For example, at the right edge of the screen, $h = w/2$, and $\Psi = HFOV/2$. Then, from Equation [B1],

$$R = \frac{(w/2)}{\tan(HFOV/2)} \qquad \text{[B4]}$$

Unfortunately, determining the exact $HFOV$ in *FSX* is not straightforward. $HFOV$ is modified by the *FSX* "zoom" level (smaller zoom yields greater $HFOV$), but the quantitative relationship between the zoom and $HFOV$ is not specified in any *FSX* documentation. However, both the $HFOV$ and vertical $VFOV$ in *FSX* can be determined by experiment, using a method presented in Reference 2 and described below.

Determining the field of view in FSX

Reference 2 describes how to modify *FSX* .FLT files to customize the geometry (size, shape, and screen location) of *FSX* windows (in which visual scenes are displayed), and to control the cameras used to view the world in each window. Significantly, the camera position, orientation, and zoom level can be defined in the .FLT files.

The field of view of a window of a given shape and zoom level can be determined by creating a second window of similar shape and zoom level adjacent to the first. The camera in the second window is then rotated until the scene at the edge where the two windows meet match. The rotation of the camera required to accomplish this is known. Furthermore, the azimuth angle from the second camera to the common edge is half of the $HFOV$, and since the two windows are the same size, it is also half of the camera rotation angle. Hence, the $HFOV$ is simply the rotation angle of the camera required to match the scene at the window edges (see Figure B2). This method can also be used to determine the $VFOV$.
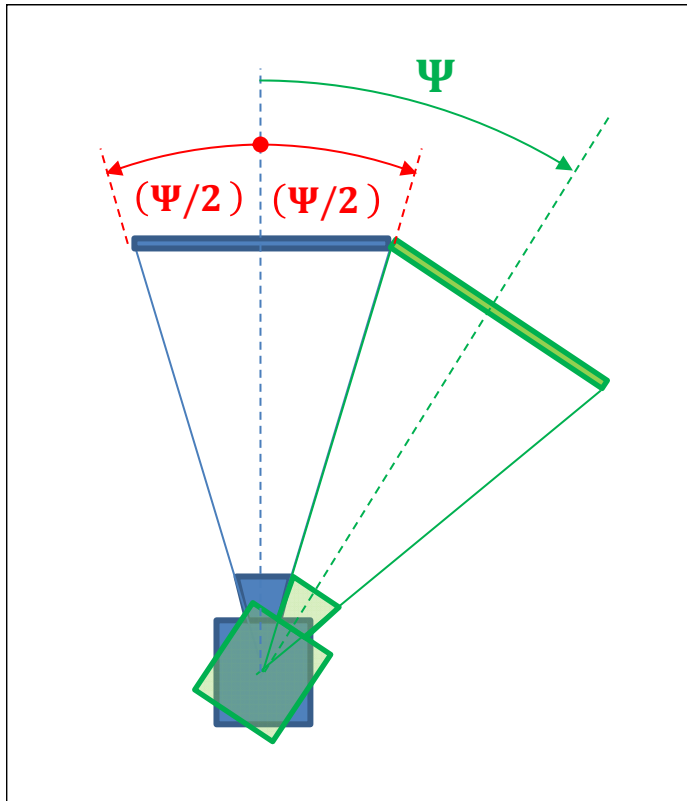

Figure B2. Determining the $HFOV$ by rotating a second (green) camera through angle Ψ to match the scene at the boundary of the view from the first (blue) camera.

Experiments with this method indicate that the $HFOV$ in *FSX* is a function of the window aspect ratio (width / height), as well as the *FSX* zoom level. Results using a window of aspect ratio of 1.6 and a zoom of 0.3 are shown in Figure B3. In this case, the $HFOV$ is 90° and the $VFOV$ is 61.8°. Per Equation [B4], R in this case would be equal to $w/2$.

Creating the FSX *instrument panel "mask" bitmap file*

With the value of R determined as described above, Equations [B1] and [B3] can be used to convert the (Ψ, Θ) viewing angles of the cockpit window structures into the (h, v) screen coordinates at which they should be drawn in order to be consistent with the outside scenery drawn by *FSX*. Once the (h, v) coordinates are in hand, the bitmap file defining the full-screen instrument panel "mask" can be created.

These bitmaps were created for this *Study* as follows.

1. First, the (h, v) coordinates of the windows were plotted into a graph with boundaries set equal to the horizontal and vertical resolution of the computer screen (i.e., the horizontal scale ranged from $-w/2$ to $+w/2$, and the vertical scale ranged from $-h/2$ to $+h/2$, where w is the screen width in pixels and h is the screen height in pixels); see Figure B4.

2. An image of the plot created in step 1 was pasted into Microsoft *PowerPoint*, and the graphical tools in *PowerPoint* were used to create a grey background covering the entire plot area, with black-filled polygons depicting the unobstructed areas of the window transparencies (see Figure B5).

3. The *PowerPoint* image was pasted into the *GIMP2* image-manipulation program, and resized to 1024 x 768, as required by *FSX.*

4. The *FastStone Photo Resizer 3.2* program was used to change the color depth of the bitmap to "4 (2 bit)." This step successfully compresses the bitmap into an "8 bit file," as required by *FSX*.

5. The bitmap is specified in the *FSX panel.cfg* file for the desired airplane model. In addition, the windows that are to use the panel (with camera rotations defined to be consistent with the view created in the bitmap file) are created in the *FSX .FLT* files for the "flight" corresponding to the project. Details concerning configuring the *panel.cfg* and .FLT files can be found in the *FSX* Software Development Kit (SDK) documentation, and in Reference 2.

The instrument panel mask constructed per the steps illustrated in Figures B4 and B5 is shown in its finished form within *FSX* in Figure B6.
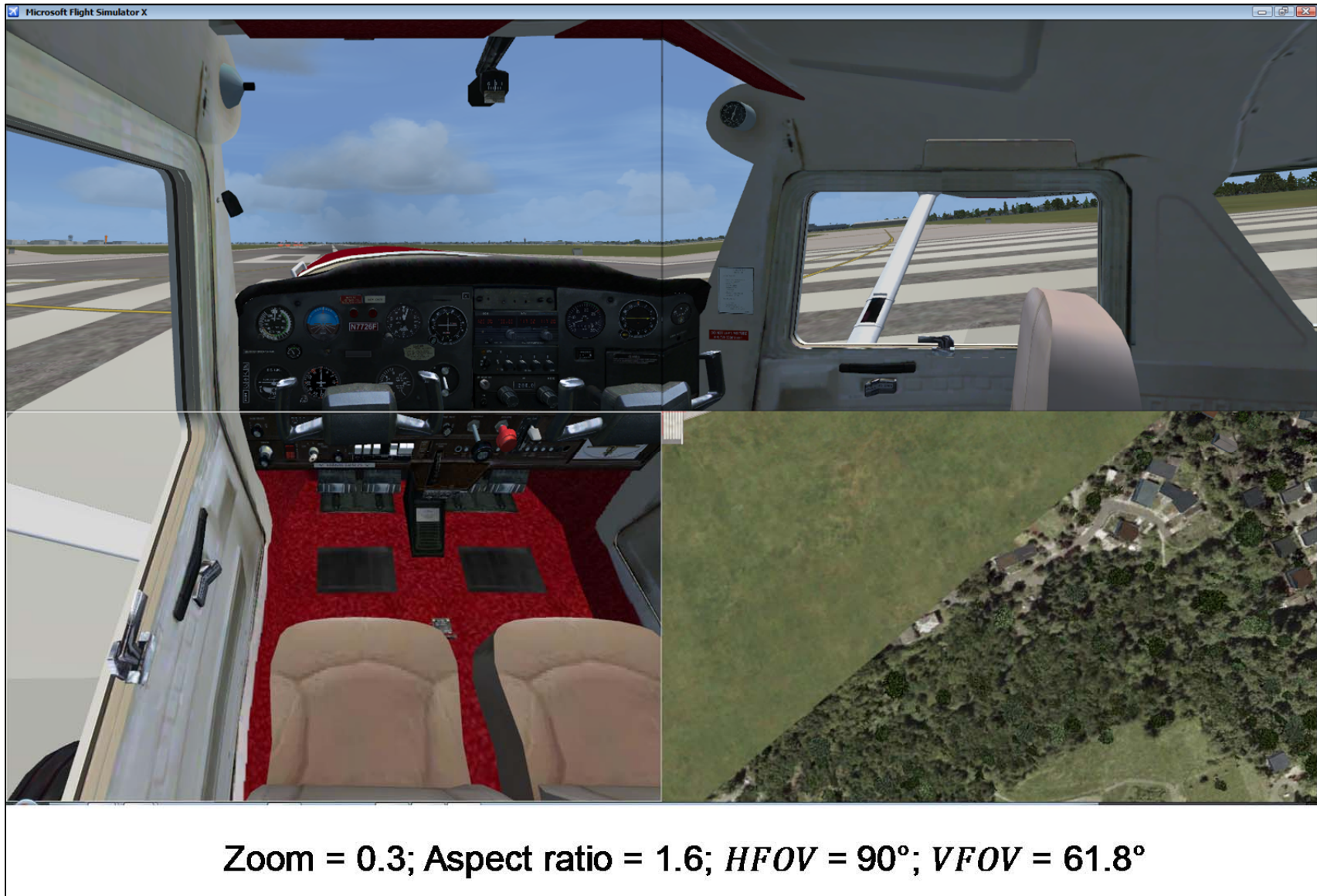
Zoom = 0.3; Aspect ratio = 1.6; $HFOV = 90°$; $VFOV = 61.8°$

Figure B3. Application of the method for determining the $HFOV$ illustrated in Figure B2.
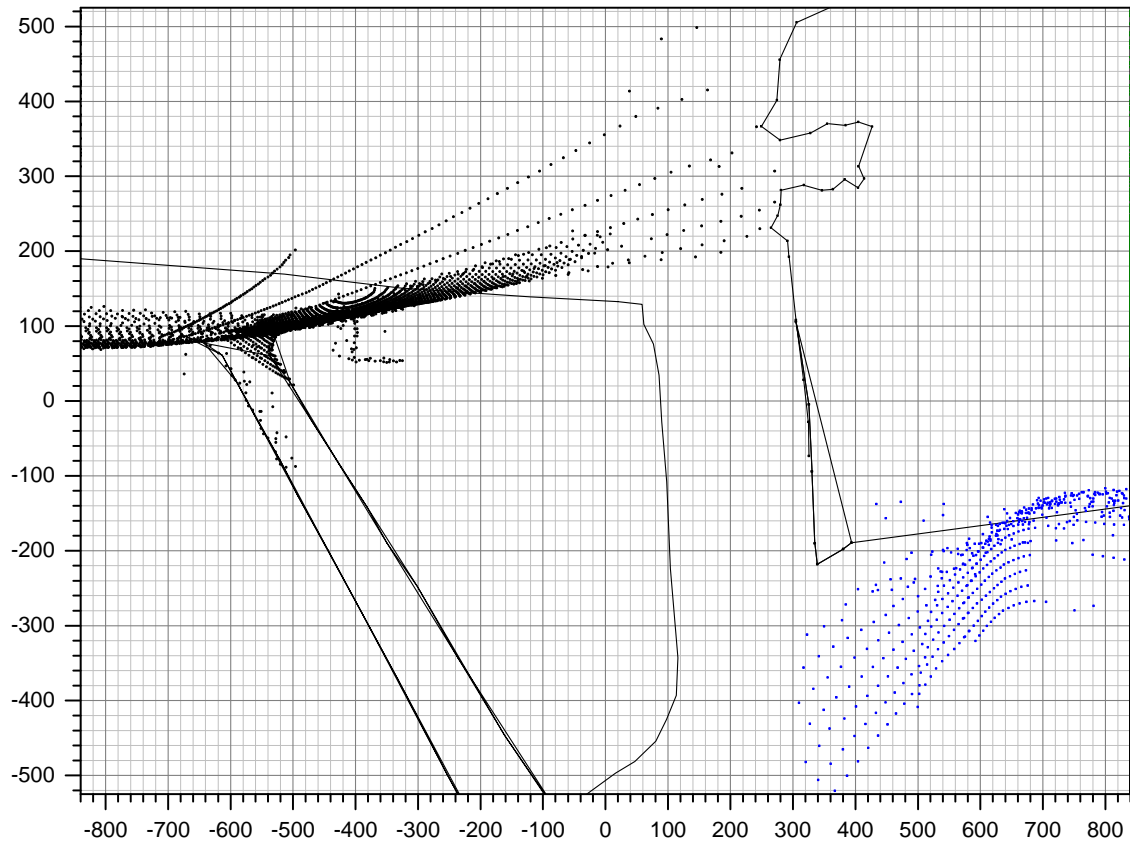
Figure B4. Plot of window v vs. h screen coordinates. The axis scales correspond to screen height and width.
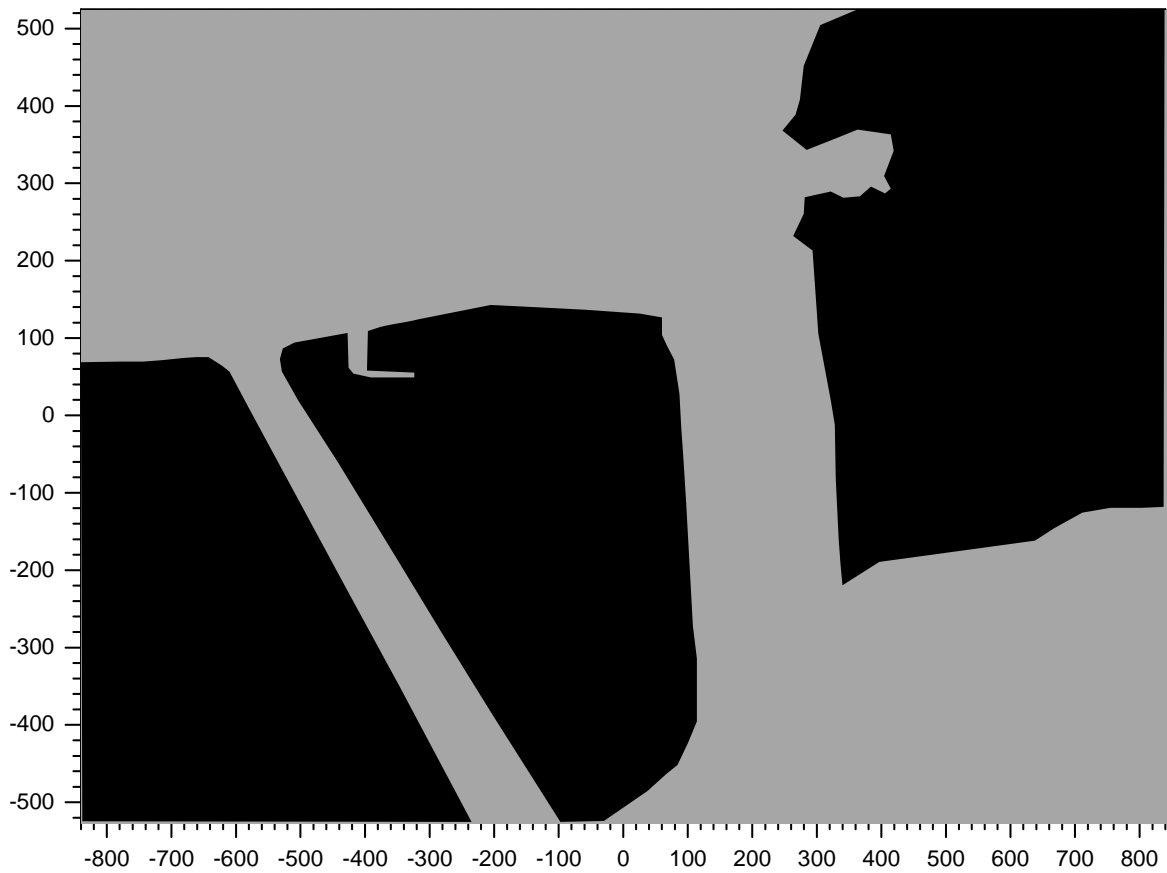

Figure B5. Black color applied to plot of Figure B4 to denote unobstructed window transparencies.
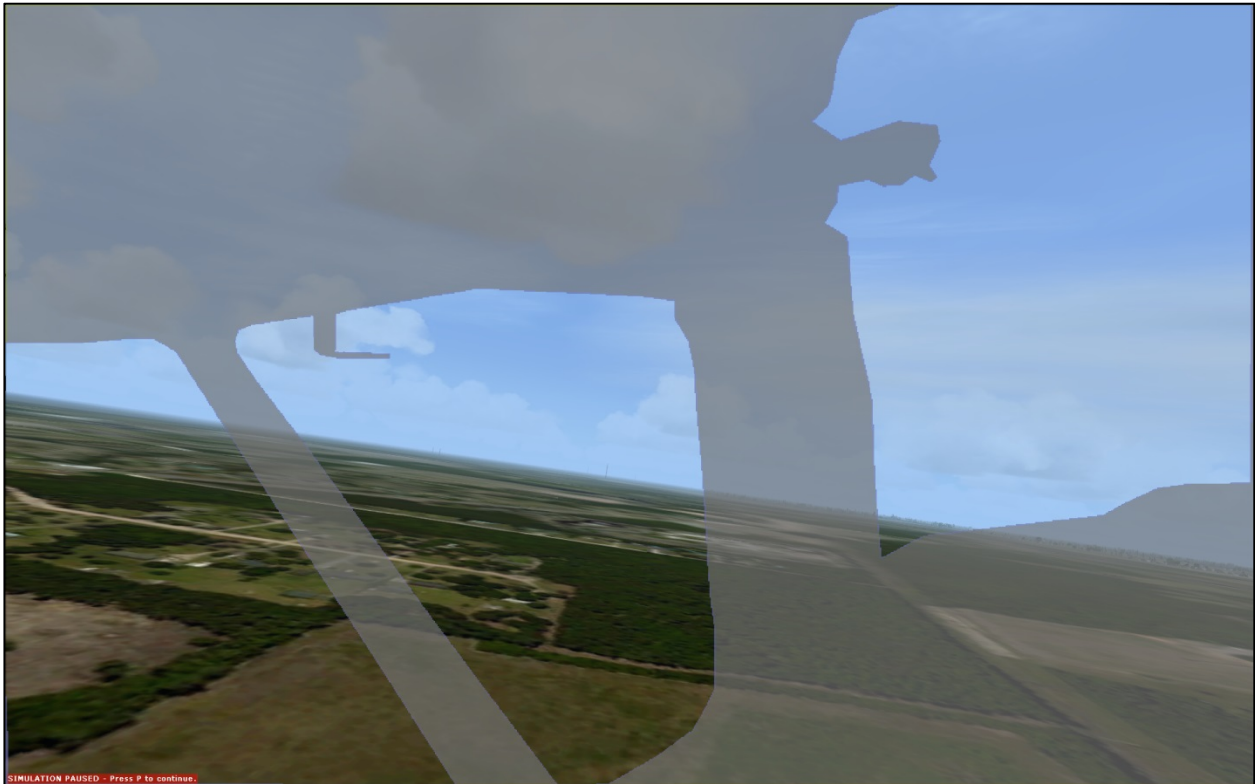
Figure B6. Finished instrument panel mask as it appears in *FSX*, with panel transparency set to 34%.

Joining windows in FSX to create larger field of view

As noted above, the maximum field of view available in a single *FSX* window is 90°, corresponding to the minimum available zoom level of 0.3. In this view, objects beyond an azimuth angle Ψ of ±45° (for a camera pointed straight ahead) will be outside the field of view and not visible.

To see objects beyond ±45° of azimuth while at the same time preserving a field of view of at least ±45° of azimuth about the direction of travel, the view from two co-located cameras can be joined side-by-side, with the second camera pointed in such a way that the boundaries of the fields of view of the cameras coincide at a particular azimuth angle. This method is illustrated in the top two images of Figure B3. In this Figure, the camera in the left image is pointed straight ahead (Ψ = 0°), and the right boundary of its field of view is at Ψ = +45°. The camera in the right image is rotated to Ψ = +90°, and its left boundary is at +90° - 45° = +45° (coinciding with the right boundary of the image on the left). By setting the views from the cameras side-by-side, a continuous field of view from -45° to +135° is obtained.

However, discontinuities (kinks) in straight lines may appear at the boundary of these views when they are viewed side-by-side on a flat surface (such as a computer screen), because the viewer will be viewing both from the same angle, whereas one of the views is intended to be viewed at an angle rotated relative to the other. The discontinuities can be removed if each view is presented on a separate surface (monitor), and then the surfaces are joined at an angle equal to the relative rotation between the cameras (though this may be impractical). The discontinuities are apparent in Figure B3.

To use this method to increase the total field of view, and also use the user-defined instrument panel masks described above, a separate mask must be created for each camera view. In addition, the airplane *model.cfg FSX* file must be modified to comment out the line specifying the airplane interior model, so that this model does not get drawn and the instrument panel masks appear over a scene that only depicts the outside world.

References

1. Diston, Dominic J., *Computational Modeling and Simulation of Aircraft and the Environment, Vol. 1: Platform Kinematics and Synthetic Environment,* p. 58. Copyright © 2009, John Wiley & Sons, Ltd.

2. Hestnes, Ivar, *Visual System Tutorial, Rev. 1.0.* Available at *http://www.google.com/url?sa=t&rct=j&q=&esrc=s&source=web&cd=1&cad=rja&uact=8&ved=0ahUKEwiFkpCX-PDOAhVG7B4KHfVCCtAQFggcMAA&url=http%3A%2F%2Fwww.flightdeck737.be%2Fwp-content%2Fuploads%2F2011%2F03%2FVisual-system-tutorial.pdf&usg=AFQjCNFHJq7T3TRTvT4yIwOAm1PpzJc-Eg*